1989

Coordination Chemistry Of A Coordinatively Unsaturated Trinuclear Platinum Cluster

Arleen Marie Bradford

NOTICE

The quality of this microform is heavily dependent upon the quality of the original thesis submitted for microfilming. Every effort has been made to ensure the highest quality of reproduction possible.

If pages are missing, contact the university which granted the degree.

Some pages may have indistinct print especially if the original pages were typed with a poor typewriter ribbon or if the university sent us an inferior photocopy.

Reproduction in full or in part of this microform is governed by the Canadian Copyright Act, R.S.C. 1970, c. C-30, and subsequent amendments.

AVIS

La qualité de cette microforme dépend grandement de la qualité de la thèse soumise au microfilmage. Nous avons tout fait pour assurer une qualité supérieure de reproduction.

S'il manque des pages, veuillez communiquer avec l'université qui a conféré le grade.

La qualité d'impression de certaines pages peut laisser à désirer, surtout si les pages originales ont été dactylographiées à l'aide d'un ruban usé ou si l'université nous a fait parvenir une photocopie de qualité inférieure.

La reproduction, même partielle, de cette microforme est soumise à la Loi canadienne sur le droit d'auteur, SRC 1970, c. C-30, et ses amendements subséquents.

COORDINATION CHEMISTRY OF A COORDINATIVELY UNSATURATED TRINUCLEAR PLATINUM CLUSTER

by

Arleen Marie Bradford

Department of Chemistry

Submitted in partial fulfillment
of the requirements for the degree of
Doctor of Philosophy

Faculty of Graduate Studies
The University of Western Ontario
London, Ontario

September 1989

ISBN 0-315-51713-1

ABSTRACT

This thesis examines the reactivity of the coordinatively unsaturated triplatinum cluster $[Pt_3(\mu_3\text{-}CO)(\mu\text{-}dppm)_3][PF_6]_2$, **1**. The complex can act as a model for a triangle of platinum atoms on a Pt(111) surface and this thesis describes studies of its reactivity towards various main group reagents.

The halide ions, Cl^-, Br^- and I^-, yielded the clusters $[Pt_3(\mu_3\text{-}CO)(\mu\text{-}_3\text{-}X)(\mu\text{-}dppm)_3]^{1+}$ which were characterized spectroscopically. In addition, attempts were made to investigate the bonding in these systems with respect to the degree of ionic, or covalent, character in the $Pt_2(\mu_3\text{-}X)$ bonds through ligand exchange studies.

Monodentate tertiary phosphines and phosphites yielded the clusters $[Pt_3(\mu\text{-}CO)(L)(\mu\text{-}dppm)_3]^{2+}$, L = phosphine or phosphite. The cluster complex $[Pt_3(\mu_3\text{-}CO)\{P(OPh)_3\}(\mu\text{-}dppm)_3]^{2+}$ was characterized by X-ray crystallography. These clusters contained an asymmetrically capping CO ligand for which the spectroscopic parameters were obtained. The phosphine and phosphite ligands displayed a unique fluxionality and this work demonstrated the feasibility of the synthesis of $M_3(\mu_3\text{-}PF_3)$ groups.

Complex 1 was reacted with a variety of phosphorus and sulphur-containing bidentate ligands including dppm, $PPh_2CH_2PPh_2$. The novel cluster $[Pt_3(\mu\text{-}CO)(\mu\text{-}dppm)_4]^{2+}$ was synthesized. This cluster was particularly interesting because the μ-dppm ligand beneath the plane of the platinum triangle displays a new form of fluxionality not previously observed for dppm.

The triplatinum cluster, complex 1, was reacted with various isocyanides to form the clusters $[Pt_3(\mu_3\text{-}CO)CNR(\mu\text{-}dppm)_3]^{2+}$. The mechanism of the reaction was followed by variable temperature NMR spectroscopy and a novel mechanism of ligand addition for metal-isocyanide complexes was observed.

The cluster $[Pt_3(2,6\text{-}Me_2C_6H_3NC)_2(\mu\text{-}dppm)_3]^{2+}$ was synthesized by adding two molar equivalents of $2,6\text{-}Me_2C_6H_3NC$ to $[Pt_3(\mu_3\text{-}CO)(\mu\text{-}dppm)_3]^{2+}$. This complex was characterized by X-ray crystallography and is the first $Pt_3(\mu\text{-}dppm)_3$ cluster with no capping ligand. The structure also appears to violate the theoretical results obtained for similar systems suggesting that a new theoretical treatment may be warranted.

Mechanistic studies using variable temperature NMR were done on the reaction of various isothiocyanate ligands with complex 1. The strong C=S bond of the isothiocyanate ligand is cleaved under mild conditions by Pt_3 clusters and the strongly bonded μ-dppm ligands were able to prevent

fragmentation of complex 1 to binuclear and mononuclear species.

Finally a tetraplatinum cluster was also examined. The fluxionality of this cluster, which differs from that of the usual tetraplatinum butterfly fluxionality, was proposed on the basis of variable temperature NMR data and the previously characterized cluster $[Pt_4(\mu\text{-}H)(CO)_2(\mu\text{-}dppm)_3(\eta_1\text{-}dppm)]^{1+}$.

ACKNOWLEDGEMENTS

I am deeply indebted to Dr. R.J. Puddephatt who has been a continual source of guidance in all aspects of the chemistry presented in this thesis. I would therefore like to express my deepest gratitude for the patience, guidance and encouragement he has continuously provided during the course of this work.

I would also like to thank Valerie Richardson and Susan Wilson who have provided NMR service which has been both excellent and entertaining.

Thanks to Drs. Lj. Manojlovic-Muir, K.W. Muir and N.C. Payne for the x-ray crystallographic structure determinations presented in this work.

I would like to express my gratitude for the friendships formed among the graduate students, postdocs, staff and faculty. Their warmth and encouragement have been invaluable and will be greatly missed.

Most of all, I would like to thank my family for their support, patience and understanding throughout the course of this work. I couldn't have done it without them.

You know with all your heart and soul that not one of all the good promises the Lord your God gave you has failed. Every promise has been fulfilled; not one has failed. **Joshua 23:14**

TABLE OF CONTENTS

LIST OF TABLES

LIST OF FIGURES

LIST OF APPENDICES

KEY ABBREVIATIONS

Anal. Calcd = analysis calculated

^{t}Bu = tertiary butyl

br = broad

Cy = cyclohexyl

dppm = bis(diphenylphosphino) methane

dppe = bis(diphenylphosphino) ethane

δ = chemical shift

d = doublet

Et = ethyl

HOMO = highest occupied molecular orbital

Hz = hertz

IR = infrared

J = coupling constant

L = phosphine, carbonyl or isocyanide

LUMO = lowest unoccupied molecular orbital

M = metal centre

Me = methyl

ν = frequency

NMR = nuclear magnetic resonance

Ph = phenyl

^{i}Pr = isopropyl

R = alkyl or aryl

UV = ultraviolet

CHAPTER 1

INTRODUCTION

1.1 INTRODUCTION

Considerable research effort has been directed towards the synthesis and structural characterization of cluster compounds of platinum. These studies have been stimulated by a desire to understand more clearly the electronic and steric factors which influence the stoichiometries, geometries and reactivities of metal cluster compounds. The long term aim of this research is an understanding, at the molecular level, of the catalytic processes that occur on metal surfaces and the possible synthesis of selective catalysts based on cluster compounds.

Although considerable progress has been made in the surface science of chemisorption and catalysis, the structural interpretation, at the molecular level, of the observed results represents a very difficult experimental and theoretical exercise and a wide range of surface analysis techniques is now available.[1] Clusters in which each metal atom is coordinatively unsaturated should be able to mimic the reactions that occur on metal surfaces[2] and it is this potential that has motivated the studies reported in the later chapters of this thesis.

1.2 COMPARISON OF SURFACES AND CLUSTERS

It was originally observed by Muetterties that many correlations exist between metal surfaces and clusters.[3-10] Metal core structures of clusters can be viewed as fragments of hexagonal close-packed, or body-centred cubic metal bulk structures. The geometry of ligands bound to clusters and to metal surfaces are similar in many instances and the average bond energies for ligand-metal and metal-metal bonds are comparable for specific metals in both the cluster and the transition metal surface. In addition, ligand mobility has been observed for both ligands bound to transition metal clusters and molecules bound to surfaces.

There are, however, important differences between surfaces and clusters. The average coordination numbers for metal-metal interactions are larger for surfaces, while the coordination numbers for metal-ligand interactions are larger for clusters. The surface state is also differentiated from the cluster state by the degree of coordinative saturation of the metal atoms. The metal atoms of surfaces are less coordinatively saturated, even for states in which molecules or molecular fragments are chemisorbed at the surface, than the metal atoms at the periphery of a molecular metal cluster. Metal surfaces tend to be more reactive than metal clusters. This is due, in part, to the high degree of coordinative unsaturation of

the surface which results in surfaces exhibiting a wide range and high level of catalytic activity.

1.3 HOMONUCLEAR CLUSTER COMPOUNDS OF PLATINUM

The earliest reported synthesis of platinum cluster compounds was by the reduction of alkali metal tetrachloroplatinates under CO atmospheres in the presence of tertiary phosphines.[11]

$$Na_2PtCl_4 \xrightarrow[NH_2NH_2/KOH/CO]{2\ PPh_3/EtOH} [Pt_3(\mu\text{-}CO)_3(PPh_3)_4] \qquad (1.1)$$

$$Na_2PtCl_4 \xrightarrow[NH_2NH_2/KOH/CO]{2\ PMe_2Ph/MeOH} [Pt_4(\mu\text{-}CO)_5(PMe_2Ph)_4] \qquad (1.2)$$

Reduction of hexachloroplatinates by CO in the absence of tertiary phosphine ligands leads to the formation of a series of platinum carbonyl dianions.[12]

$$Na_2PtCl_6 \xrightarrow[NaOH/MeOH]{CO} (XR_4)_2[Pt_3(\mu\text{-}CO)_3(CO)_3]_n \qquad (1.3)$$

$$(X = N, P \text{ or } As;\ n = 2\text{-}5)$$

These oligomers result from the stacking of two to five $[Pt_3(\mu\text{-}CO)_3(CO)_3]$ triangular units along the pseudo-threefold axis. The nuclearity of the cluster formed is critically dependent on the stoichiometry and

conditions of the reaction and great skill is necessary to isolate and purify the compounds.

Syntheses have also been developed using mononuclear platinum phosphine compounds as starting materials.

$$3\ [PtH_2(PCy_3)_2] \xrightarrow[C_6H_6]{CO} [Pt_3(\mu\text{-}CO)_3(PCy_3)_3] + 3\ H_2 + PCy_3 \qquad (1.4)$$

$$[Pt(PPh_3)_2Cl_2 \xrightarrow[THF]{NaMn(CO)_5} [Pt_5(\mu\text{-}CO)_5(CO)(PPh_3)_4] + [Mn_2(CO)_{10-x}(PPh_3)_x] \quad (X = 0\text{-}2) \qquad (1.5)$$

Reaction 1.3 is limited to complexes of bulky phosphines[13,14] for which the dihydride complex is known while the platinum cluster in reaction 1.4 must be separated from phosphine substituted metal carbonyls.[15]

Mingos et al have reported more recently that the reduction of cis-$[PtCl_2(CO)(PR_3)]$ under mild conditions gives homonuclear platinum clusters in good yields (60-80%).[16]

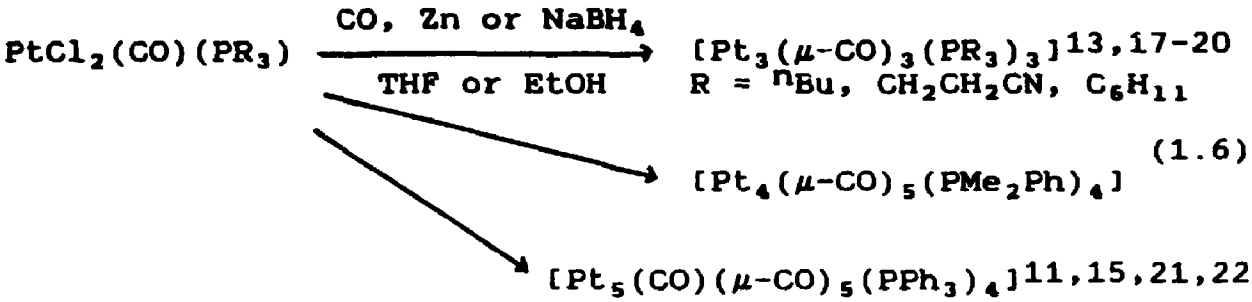

(1.6)

The nuclearity of the cluster obtained in this case is sensitive to the steric and/or electronic requirements of the tertiary phosphine in addition to the mode of synthesis employed.

The tertiary phosphine carbonyl clusters described have been used for a wide range of ligand exchange, cluster degradation and aggregation reactions. The 42 electron triangular-clusters $[Pt_3(\mu\text{-}X)_3(PCy_3)_3]$, (X = CO or SO_2), react with chelating tertiary phosphines such as dppp, [1,3-bis(diphenylphosphino)propane], to give the 44 electron clusters $[Pt_3(\mu\text{-}X)_3(PCy_3)_2(dppp)]$.[23] The chelating effect of the bidentate tertiary phosphines stabilizes the 44 electron species relative to the 42 electron cluster.

The reactions of $[Pt_3(\mu\text{-}CO)_3(PCy_3)_3]$ with 2,6-dimethylphenyl isocyanide give substitution products where both bridging and terminal ligands have been replaced.[24]

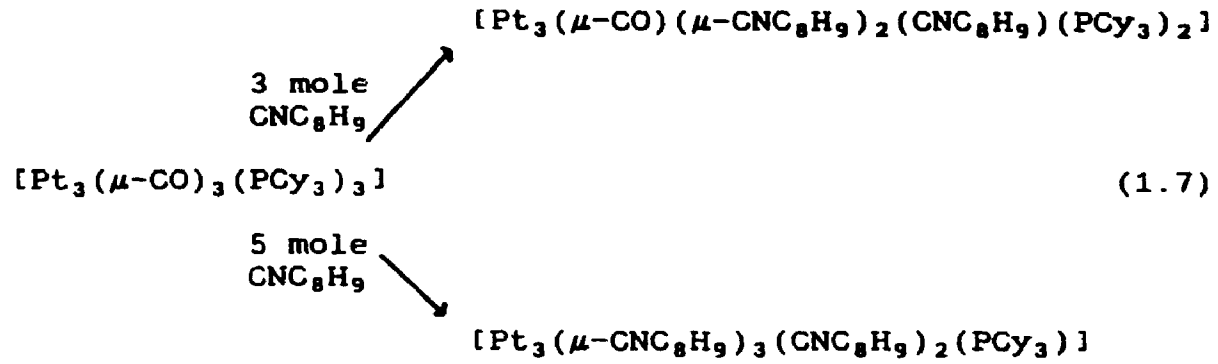

(1.7)

Aggregation and degradation reactions of platinum carbonyl clusters lead to dramatic changes in cluster nuclearity and occur with relative ease as a result of either oxidation with platinum (IV), or reduction with lithium metal or Na/K alloy.[12]

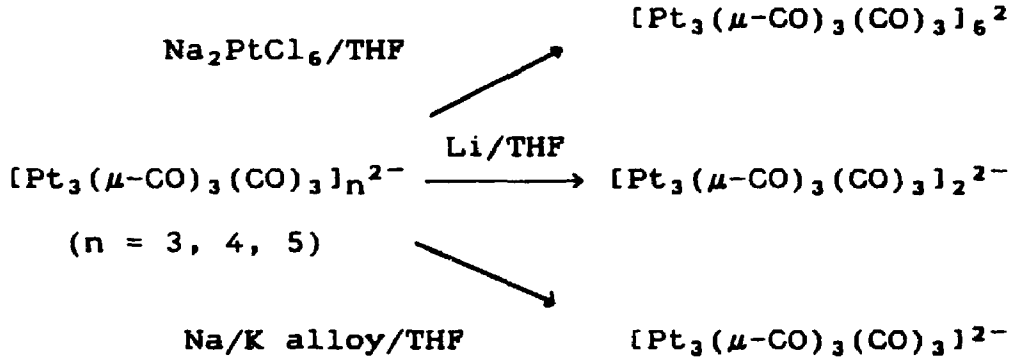

(1.8)

An interesting example of oxidation accompanied by aggregation occurs when a toluene solution of $[Pt_3(\mu\text{-}H)_3H_3(P^tBu_3)_3]$ is treated with ethylene,[25]

$$[Pt_3(\mu\text{-}H)_3H_3(P^tBu_3)_3] + CH_2CH_2 \xrightarrow[1\ atm/24\ h]{PhMe} [Pt_4(\mu\text{-}H)_2(P^tBu_3)_4] + MeMe \quad . \tag{1.9}$$

Some striking aggregation reactions occur as a result of redox reactions of the following type.[26]

$$[Pt_3(\mu\text{-}CO)_3(CO)_3]_3^{2-} + [Pt_3(\mu\text{-}CO)_3(CO)_3]_4^{2-}$$

$$\text{Ratio 5:1} \quad \downarrow \quad \text{MeCN/Reflux} \qquad (1.10)$$

$$[Pt_{19}(\mu\text{-}CO)_{10}(CO)_{12}]^{4-}$$

This compound contains a pseudo-fivefold principal axis and is based on stacked pentagonal pyramids.

A widely used diphosphine ligand in platinum chemistry is bis(diphenylphosphino)methane, dppm, and its chemistry has been reviewed.[27,28] A triplatinum cluster with three bridging dppm ligands has been prepared in this laboratory: $[Pt_3(\mu\text{-dppm})_3(\mu_3\text{-}CO)]^{2+}$, 1.[29] This cluster is coordinatively unsaturated since it only has 42 valence electrons. Platinum trinuclear clusters with 42, 44 and 46 valence electron counts have all been prepared and it has been found that the reactions of these clusters with main group ligands often mimic the behaviour of Pt(111) surfaces.[30-33] The molecular orbital theory which predicts the geometry and the number of valence electrons for stabilized triplatinum clusters is discussed in section 1.4

1.4 MOLECULAR ORBITAL THEORY

It has been proposed that D_{3h} trinuclear metal clusters are the inorganic equivalent of cyclopropane.[34]

The bonding network of cyclopropane can be constructed by means of two localized hybrids at each carbon atom. One σ and one π orbital at each centre combine to form three radial and three tangential combinations resulting in the formation of three C-C single bonds since the bonding combinations are fully occupied as shown in Figure 1.1.

Similar schemes may be constructed for trinuclear metal clusters provided that each metal fragment has suitable σ and π orbitals.

The isolobal analogy which explains the isolobal connection between d^8-ML_4, d^{10}-ML_2 and CH_2 fragments predicts the assembly of three ML_2 fragments to form, using Mingos' terminology, a latitudinal trimer, M_3L_6. This means that the ligands are in the plane of the platinum triangle. The three bridging and three terminal ligands found in such species have the effect of stabilizing these clusters by increasing the HOMO-LUMO gap.[35] Since the CH_2 fragment is derived from tetrahedral geometry while the PtL_2 fragment is derived from square planar geometry, a difference in the relative energies of the b_2 and a_1 orbitals will occur.

Mealli has examined the interaction of CO^{2+} with Pt_3L_6.[35] The $Pt_3(CO)_6$ levels are characterized by the high energy of the radial $2a_1'$ molecular orbital (Figure 1.2b). The capping ligand removes the $2a_1'$ molecular orbital from the LUMO area and allows it to be populated.

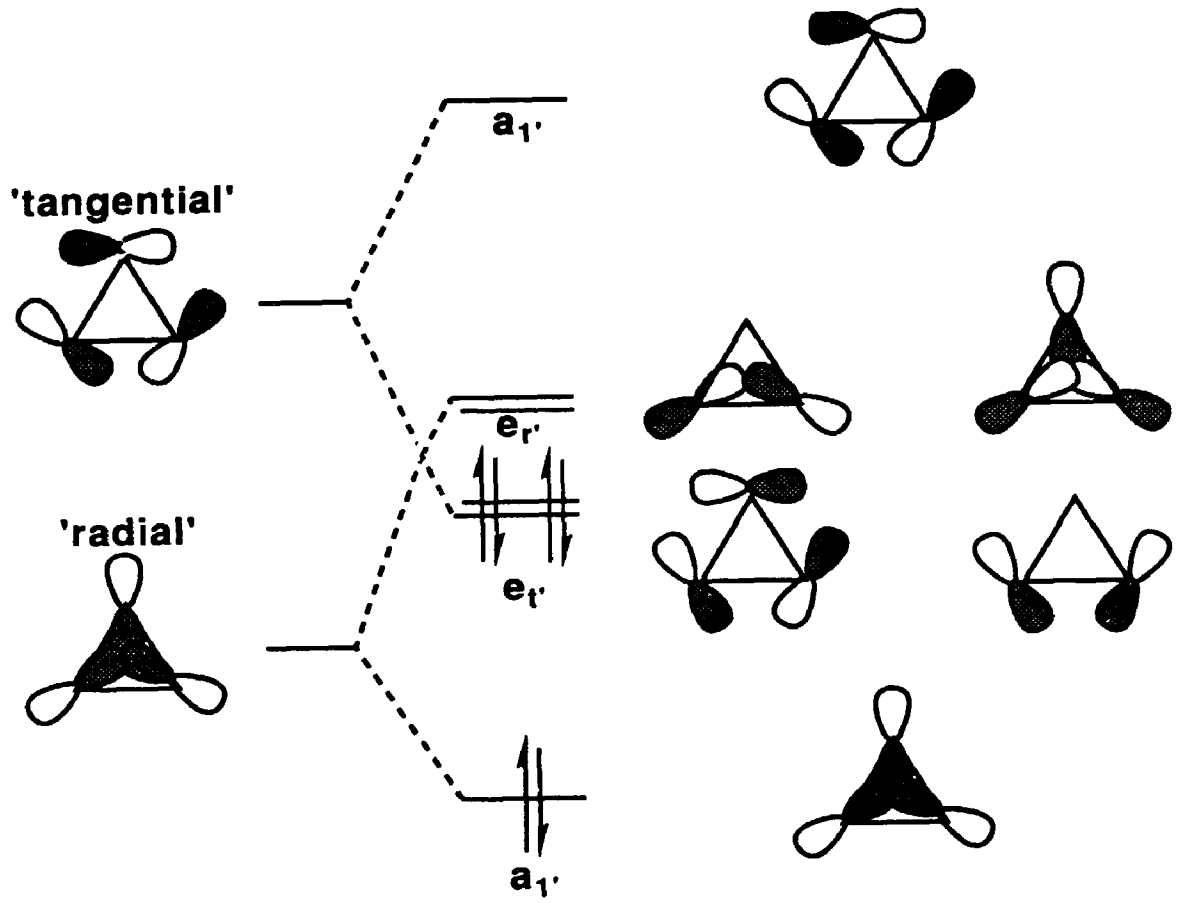

Figure 1.1: MO Treatment for Pt_3L_6

FIGURE 1.2: Molecular Orbitals for Pt_3L_6 Systems and Their Interaction with a Capping CO Ligand

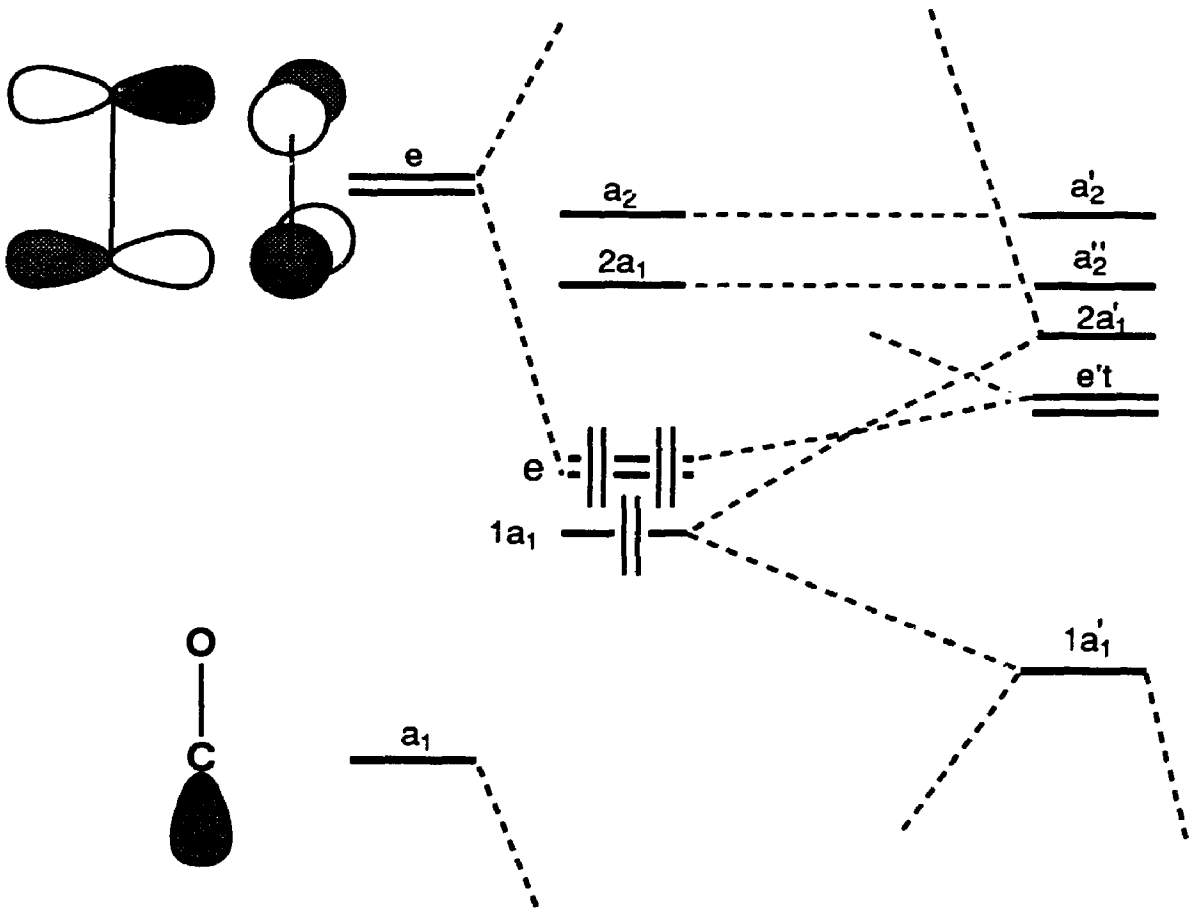

CO
a

$[Pt_3(CO)_6(\mu^3\text{-}CO)]^{2+}$
b

$Pt_3(CO)_6$
c

If two or more electrons are added to the valence shells of these clusters the electrons can enter the nonbonding platinum orbital on any of the platinum atoms, or the antibonding M-M orbitals. The addition of 4 electrons to the molecular orbitals of Pt_3L_6 gives a valence electron count of 46 and results in the filling of antibonding or nonbonding orbitals.

The clusters Pt_3L_6 closely represent the cationic 42 electron cluster, **1**. Since **1** has bridging dppm ligands while Mealli's clusters have carbonyl ligands, the molecular orbitals obtained will be similar in that they will have the correct ordering although the actual energies may be different. Examples of 42, 44 and 46 electron clusters can be found throughout this thesis.

1.5 THE PLATINUM-CARBONYL INTERACTION

It is apparent from the preceding discussion that platinum has a tendency to form complexes with CO. The metal-carbonyl bond possesses two essential components. The first is a σ component in which the filled 5σ orbital of the carbonyl ligand donates its electron density to an empty σ orbital of the metal atom. The second involves a π bond interaction via electron donation from the filled d-orbitals of the metal atom to the empty π antibonding orbitals of the carbonyl ligand.

The stabilization of platinum-carbonyls is generally enhanced through the use of ligands, such as

tertiary phosphines, which possess strong σ-donation and poor π-acceptor character, thus inducing stronger π-donation from the metal.[36]

1.6 OVERVIEW OF THE THESIS

This thesis is concerned with the reactions which occur between the 42 electron cationic cluster, 1, and various main group reagents. The impetus for this study was the similarity of 1 to the Pt(111) surface.[30-33] Various compounds were reacted with the cluster and, where possible, the reactions were compared to the analogous surface reactions. Thus, it is hoped that we will gain some insight into the sorts of species formed on a platinum surface. The homonuclear platinum clusters, however, have proven themselves to have a novel chemistry in their own right.

The reagents used were mono and bidentate tertiary phosphines and phosphites, various isocyanides and ligands with the bridging CS_2 moiety. The products were fully characterized using spectroscopic techniques and in several cases X-ray crystallographic studies were carried out. In addition, the characterization of a novel tetranuclear platinum cluster was carried out.

1.7 REFERENCES.

1. G.A. Somorjai, "Chemistry in Two Dimensions: Surfaces", Cornell University Press, USA, (1981).
2. E.L. Muetterties, Catal. Rev. - Sci. Eng., (1981), **23**, 69.
3. E.L. Muetterties, Bull. Soc. Chim. Belg., (1975), **84**, 959; (1976), **85**, 451.
4. E.L. Muetterties, Angew. Chem., Int. Ed. Eng., (1978), **17**, 545.
5. E.L. Muetterties, Science, (1977), **196**, 839.
6. E.L. Muetterties, J.N. Rhodin, E. Band, C.F. Brucker and W.R. Pretzer, Chem. Rev., (1979), **79**, 91.
7. E. Band and E.L. Muetterties, Chem. Rev., (1978), **78**, 639.
8. E.L. Muetterties and J. Stein, Chem. Rev., (1979), **79**, 479.
9. E.L. Muetterties, J. Organomet. Chem., (1980), **200**, 177.
10. E.L. Muetterties, Isr. J. Chem., (1980), **20**, 84.
11. J. Chatt and P. Chini, J. Am. Chem. Soc. (A), (1970), 1538.
12. G. Longoni and P. Chini, J. Am. Chem. Soc., (1976), **98**, 7225.
13. M.C. Clark, A.B. Goel and C.S. Wong, Inorg. Chim. Acta, (1979), **34**, 159.
14. R.G. Goel, W.O. Ogini and R.C. Srivastava, Organometallics, (1982), **1**, 819.

15. J.P. Barbier, R. Bender, P. Braunstein, J. Fischer and L. Ricard, *J. Chem. Res. (S)*, (1978), 230; J. Chem. Res. (M), (1978), 2913.

16. D.G. Evans, M.F. Hallam, D.M.P. Mingos and R.W.M. Wardle, *J. Chem. Soc., Dalton Trans.*, (1978), 1889.

17. I. Yoshida and S. Otsuka, *J. Am. Chem. Soc.*, (1977), **99**, 1022.

18. C.A. Johman, *Chem. Rev.*, (1977), **77**, 313.

19. D.M.P. Mingos, *Inorg. Chem.*, (1982), **21**, 464.

20. L.S. Meriwether, E.C. Colthup, M.L. Fiene and F.A. Cotton, *J. Inorg. Nucl. Chem.*, (1959), **11**, 181.

21. A. Moor, P.S. Pregosin, L.M. Venanzi and A.J. Welch, *Inorg. Chim. Acta*, (1984), **85**, 103.

22. R. Bender, P. Braunstein, J. Fischer, L. Ricard and A. Mitschler, *Nouv. J. Chem.*, (1981), **5**, 81.

23. M.F. Hallam, N.D. Howells, D.M.P. Mingos and R.W.M. Wardle, *J. Chem. Soc., Dalton Trans.*, (1985), 845.

24. C.E. Briant, D.I. Gilmour, D.M.P. Mingos and R.W.M. Wardle, *J. Chem. Soc., Dalton Trans.*, (1985), 1693.

25. P.W. Frost, J.A.K. Howard, J.L. Spencer, D.G. Turner and D. Gregsen, *J. Chem. Soc., Chem. Commun.*, (1981), 1104.

26. D.M. Washecheck, R.J. Wucherer, L.F. Dahl, A. Ceriotti, G. Longoni, M. Munassera, M. Sansoni and P. Chui, *J. Am. Chem. Soc.*, (1979), **101**, 6110.

27. R.J. Puddephatt, *Chem. Soc. Rev.*, (1983), **12**, 99.

28. B. Chaudret, B. Delavaux and R. Poilblanc, *Coord. Chem. Rev.*, (1988), **86**, 191.

29. G. Ferguson, B.R. Lloyd and R.J. Puddephatt, *Organometallics*, (1986), **5**, 344.

30. B.R. Lloyd, A.M. Bradford and R.J. Puddephatt, *Organometallics*, (1987), **6**, 424.

31. G. Ferguson, B.R. Lloyd, Lj. Manojlovic-Muir, K.W. Muir and R.J. Puddephatt, *Inorg. Chem.*, (1986), **25**, 4190.

32. Lj. Manojlovic-Muir, K.W. Muir, B.R. Lloyd and R.J. Puddephatt, *J. Chem. Soc., Chem. Commun.*, (1985), 536.

33. M.C. Jennings, N.C. Payne and R.J. Puddephatt, *Inorganic Chem.*, (1987), **26**, 3776.

34. R. Hoffmann, *Angew. Chem., Int. Ed. Engl.*, (1982), **21**, 711.

35. C. Mealli, *J. Am. Chem. Soc.*, (1985), **107**, 2245.

36. F.R. Hartley, *Comp. Organomet. Chem.*: The Synthesis, Reactions and Structures of Organometallic Compounds, (Eds. G. Wilkinson, F.G.A. Stone and E.W. Abel), Pergamon Press, Toronto, (1982), 6, 39, 471.

CHAPTER 2

COORDINATION AT THE μ_3-TRIPLY BRIDGING SITE: THE REACTION OF $[Pt_3(\mu_3\text{-}CO)(\mu\text{-}dppm)_3]^{2+}$ WITH HALIDE IONS

2.1 INTRODUCTION

It is well known that trinuclear clusters can be stabilized via the use of μ_3-capping ligands and there are a number of clusters characterized in which the μ_3 ligand is a halide.[1,2] Examples of both symmetrically and asymmetrically capping halides are known. In the cluster

$P\frown P = PPh_2CH_2PPh_2$

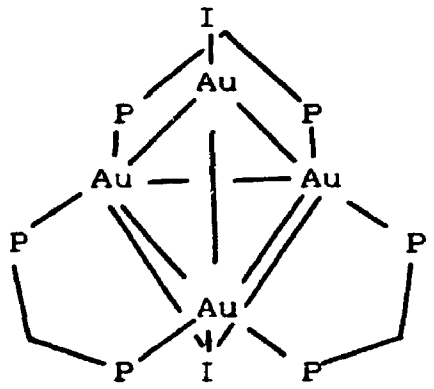

I

the capping iodide on the bottom face of the gold triangle is asymmetrically coordinated with long Au-I distances of 3.13 to 3.67 Å.[3] Similarly, the iodine atoms in the silver tetramer asymmetrically cap the silver triangles with two

short Ag-I bonds of 2.898(4) and 2.941(4) Å and one long Ag-I distance of 3.126(4) Å.[4]

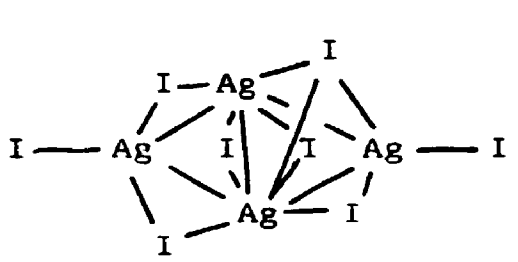

II

The halide cap is much more symmetrical in the copper cluster,[5,6]

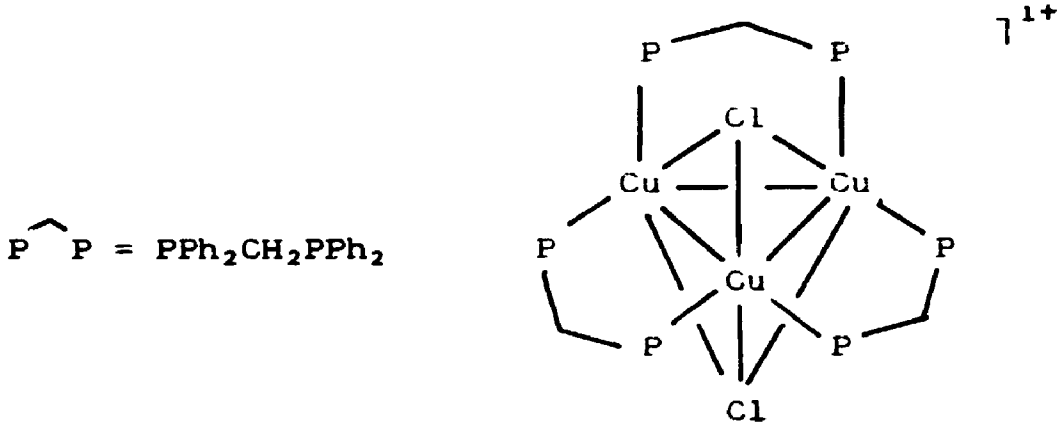

III

in the nickel trimer,[7]

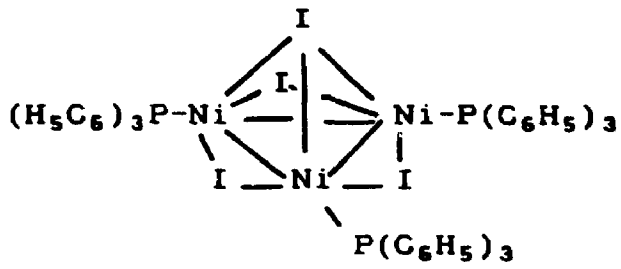

IV

and in the palladium cluster,[8]

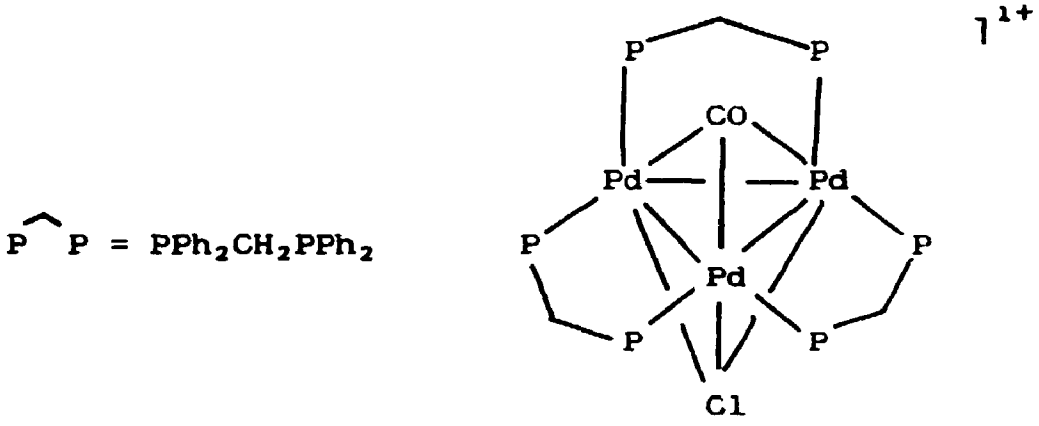

V

A general trend for halide capped clusters is an increase in the metal-halide bond lengths in going from terminal, via bridging, to capping coordination modes. This is consistent with the fact that bond weakening is expected in this order. Another interesting feature is that metal-metal bonds tend to be shorter and metal-halide-metal angles smaller when the halide is iodine as opposed to chlorine or bromine. The shortening of the metal-metal distances in these clusters is attributed to

the ability of iodine to act as a bridging ligand forming narrow M-I-M angles.[6,9]

The long metal-halide bond lengths associated with the μ_3-capping coordinative mode are usually considered to be indicative of ionic interactions as opposed to covalent interactions. A study of the nature of the metal-halide bond in cluster **V**, however, has suggested a weak covalency to the $Pd_3(\mu_3\text{-}X)$ interaction.[8] It was therefore of interest to study the interaction of $[Pt_3(\mu_3\text{-}CO)(\mu\text{-}dppm)_3]^{2+}$, **1**, with the halide ions to give the adducts with chloride, **2a**, bromide, **2b**, and iodide, **2c**. Insight into the coordinative nature of these ligands at the vacant site opposite the carbonyl bridge position on the dicationic cluster have been developed with regard to preference for site occupancy. Attempts have also been made to qualitatively investigate the bonding in these systems, particularly with respect to the degree of ionic or covalent character in the $Pt_3(\mu_3\text{-}X)$ bonds. The results for clusters **2a-2c** are compared and contrasted with those for the analogous tripalladium clusters. These studies were conducted via ^1H, $^{31}P\{^1H\}$, $^{13}C\{^1H\}$ and ^{195}Pt NMR, UV-Visible and IR spectroscopies.

2.2 RESULTS

2.2.1 Synthesis of the Complexes $[Pt_3(\mu_3\text{-}CO)(\mu\text{-}dppm)_3X]^{1+}$

The major chemical results are shown in Equation 2.1.

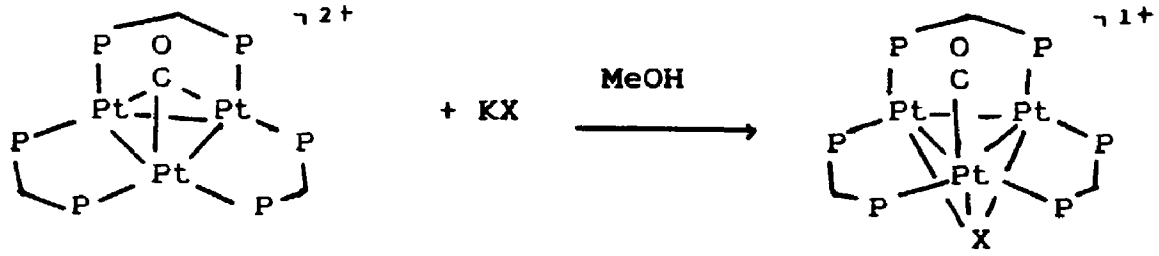

1

2a: $X=Cl^-$
2b: $X=Br^-$
2c: $X=I^-$

Equation 2.1

Reaction of 1 with excess KCl, KBr and KI in methanol yielded 2a-2c. These clusters were isolated by removing the methanol under reduced pressure and washing the solid with distilled water to remove excess KPF_6 or KO_2CCF_3. The orange solid was then dried under high vacuum.

2.2.2 Structural Features and Spectroscopic Characterization of 2a-2c

The clusters $[Pt_3(\mu_3\text{-}CO)(\mu_3\text{-}X)(\mu\text{-}dppm)_3]^{1+}$ are composed of a triangular metal core in which the platinum atoms are directly bound to each other. The platinum triangle is spanned by three edge-bridging dppm ligands and is capped by a triply bridging carbonyl. The halide ion completes a distorted trigonal bipyramidal arrangement.

The infrared spectra of **2a-2c** displayed carbonyl stretching frequencies in the narrow range of 1753 to 1767 cm^{-1} (Table 2.1). These are similar to the values of 1750 and 1765 cm^{-1} observed for $[Pt_3(\mu_3\text{-}CO)(CF_3CO_2)(\mu\text{-}dppm)_3][CF_3CO_2]$,[10] **3**, and $[Pt_3(\mu_3\text{-}CO)(\mu\text{-}dppm)_3][PF_6]_2$,[11] **1**, respectively and can be compared with the infrared band at 1810 cm^{-1} for CO bound at a threefold site on a Pt(111) surface.[12]

The ^1H NMR spectra of each of **2a-2c** consisted of an AB quartet for the $CH^aH^bP_2$ protons (Table 2.2). This results from the absence of a plane of symmetry containing the $Pt_3P_6C_3$ atoms of the $Pt_3(\mu\text{-}dppm)_3$ unit due to the presence of the μ_3-CO on one face of the platinum triangle and the halide ion on the opposite face. The $^2J(H^aH^b)$ value was found to be 14 Hz and the δ (H^a) and δ (H^b) values lay in the range of 5.57 to 6.08 ppm. These results compare favourably with those for the analogous tripalladium clusters where $^2J(H^aH^b)$ was also 14 Hz and the δ (H^a) and δ (H^b) values ranged from 4.72 to 4.93 ppm.

The $^{31}P\{^1H\}$ NMR spectra of **2a-2c** contained singlet resonances with complex and incompletely resolved satellites due to the coupling to ^{195}Pt (Table 2.3). The complexity arises in part from the superposition of resonances due to the Pt_3P_6 systems containing 0 (29% natural abundance), 1 (44% natural abundance), 2 (23% natural abundance) and 3 (4% natural abundance) ^{195}Pt atoms. Isotopomer 1 gives spectra analogous to those of

the palladium complexes. The more complex spectra of the other isotopomers are superimposed. The δ ^{31}P values fall in the narrow range -17.1 to -17.9 ppm with ^{1}J(PtP) from 3700 to 3890 Hz. These can be compared with the δ ^{31}P values for the analogous palladium clusters which fall in the range -14.2 to -14.5 ppm. Large ^{3}J(PP) couplings of 165 Hz were observed in the satellite spectra of 2a-2c. The observation of such long range couplings is characteristic of approximately linear P-Pt-Pt-P units, and is a very useful criterion for the presence of such units.[11,13-16] The ^{2}J(PtP) coupling was too small to be measured in the spectra of complexes **2a** and **2b** but was found to be 25 Hz for complex **2c** (Figure 2.1).

The ^{195}Pt NMR spectra consist of triplets arising from the isotopomer containing a single ^{195}Pt atom due to coupling to two directly bound phosphorous atoms (Table 2.3). Satellite spectra arising from the isotopomer with two ^{195}Pt atoms were also observed and allowed the coupling constant of ^{1}J(PtPt) = 500 Hz to be determined. This value is comparable to values found in other triangular Pt_3 clusters[17,18] (Figure 2.2).

The ^{13}C{^{1}H} NMR spectra of clusters **2a**, **2b** and **2c** consisted of a septet (^{1}J(PtC) = 890 HZ, **2a**; ^{1}J(PtC) = 896 Hz, **2b**; ^{1}J(PtC) = 850 Hz, **2c**) of septets (^{2}J(PC) = 17.5 Hz, **2a**; ^{2}J(PC) = 20.1 Hz, **2b**; ^{2}J(PC) = 18.4 Hz, **2c**) (Table 2.4). The relative intensities of the ^{195}Pt satellites were 1:12:49:84:49:12:1 which is the expected

TABLE 2.1: IR Data for Complexes 2a-2c[a]

Complex	ν_{CO} (cm^{-1})
2a	1767
2b	1753
2c	1765

[a] Samples run as Nujol mulls.

TABLE 2.2: ^1H NMR Data for Complexes 2a-2c

Complex	2a	2b	2c
δ (H^a) (ppm)[a]	5.97	5.84	6.08
δ (H^b) (ppm)	5.72	5.71	5.57
$^2J(H^aH^b)$ (Hz)	14	14	14

[a] Solvent was acetone-d_6.

TABLE 2.3: ^{31}P and ^{195}Pt NMR Data for the Complexes $[Pt_3(\mu_3\text{-}CO)(\mu_3\text{-}X)(\mu\text{-}dppm)_3]^{1+}$ where X = Cl, 2a; X = Br, 2b; X = I, 2c.

Complex	2a	2b	2c
δ ^{31}P (ppm)[a,b]	-17.6	-17.1	-17.8
$^{1}J(PtP)$ (Hz)	3700	3800	3890
$^{2}J(PtP)$ (Hz)	0	0	25
$^{3}J(PP)$ (Hz)	165	160	165
δ ^{195}Pt (ppm)[c]	-2991	-3044	-3059
$^{1}J(PtP)$ (Hz)	3720	3830	3890
$^{1}J(PtPt)$ (Hz)	500	----	500

[a] δ ^{31}P in ppm referenced to H_3PO_4.

[b] Solvent was acetone-d_6.

[c] δ ^{195}Pt in ppm referenced to aqueous K_2PtCl_4.

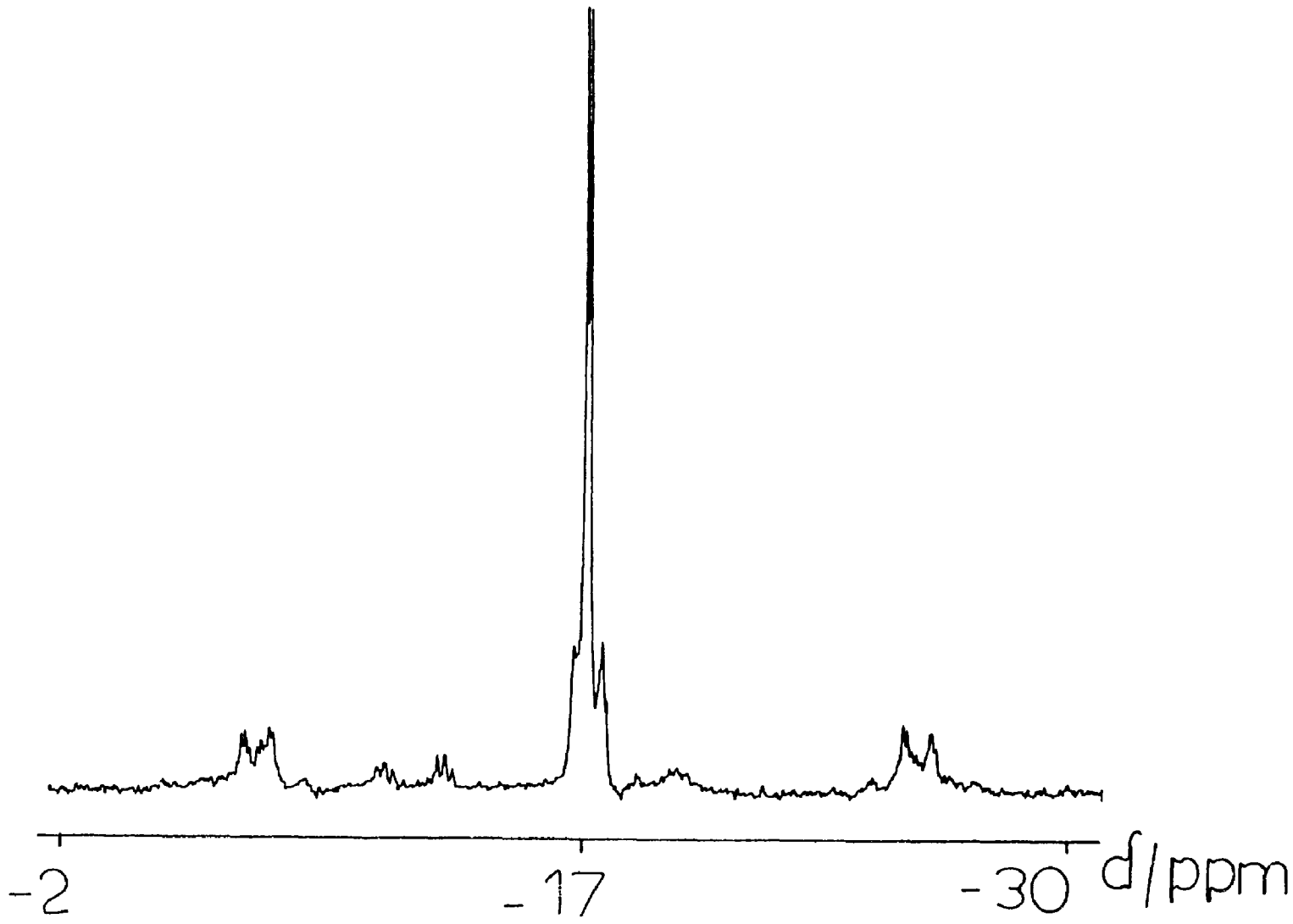

FIGURE 2.1: $^{31}P\{^{1}H\}$ NMR Spectrum of **2c**

FIGURE 2.2: $^{195}Pt\{^{1}H\}$ NMR Spectrum of 2c

TABLE 2.4: ^{13}C NMR Data for complexes **2a**, **2b**, and **2c**.

Complex	2a	2b	2c
δ ^{13}C (ppm)[a,b]	197.00	195.80	192.69
$^{1}J(PtC)$ (Hz)	890	896	850
$^{2}J(PC)$ (Hz)	17.5	20.1	18.4

[a] δ ^{13}C in ppm referenced to Me_4Si.

[b] Solvent was acetone-d_6.

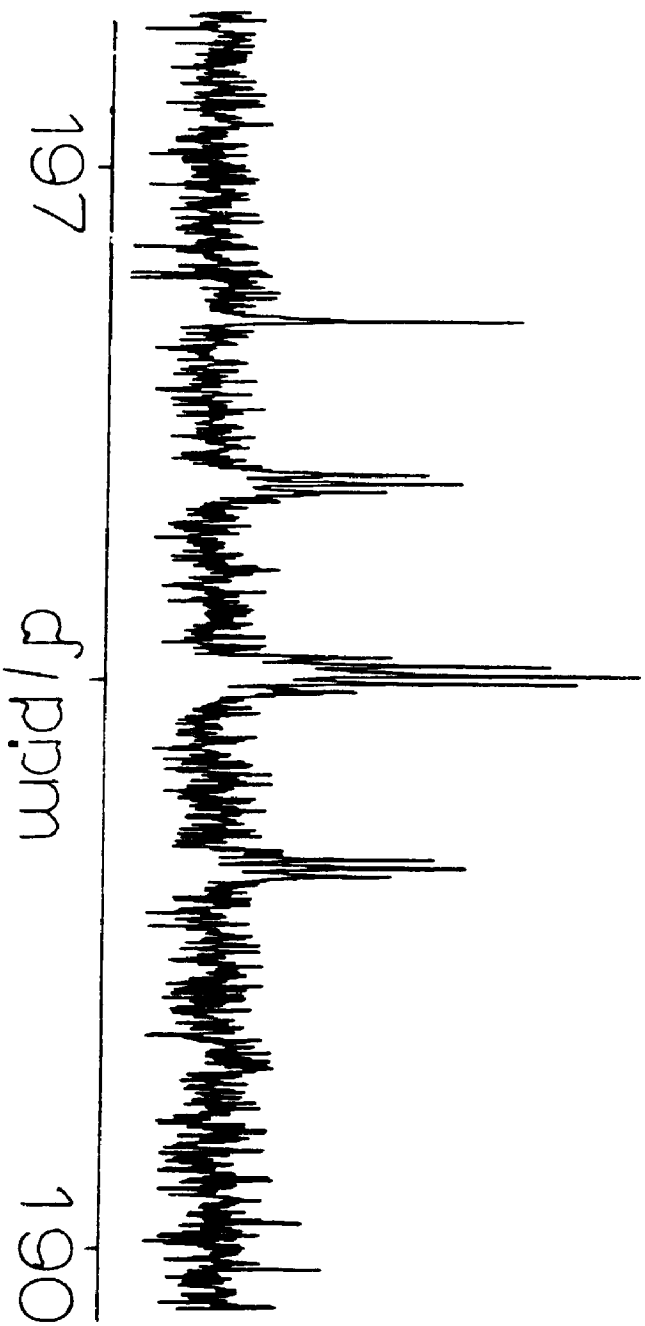

FIGURE 2.3: $^{13}C\{^{1}H\}$ NMR Spectrum of 2c

ratio for a carbonyl carbon atom bridging 3 platinum centres. This arises due to superposition of spectra due to four potential isotopomers containing 0-3 ^{195}Pt atoms. The outermost satellites were not observed due to their weak intensity (Figure 2.3).

2.2.3 Ligand Exchange Studies via UV-Visible Spectroscopy

The reaction of 1 with KCl, KBr or KI in varying molar ratios less than unity yielded an immediate conversion to the respective halogenated species 2a, 2b, or 2c (Figure 2.4). These conversions were monitored by visible spectroscopy. The relative changes in absorbance varied linearly with respect to the amount of halide ion added below a molar ratio of cluster to halide of unity. No further changes were observed beyond this ratio.

Anion exchanges in the halogenated clusters resulted in an immediate conversion to product. The reaction of 2a with KBr or KI led to immediate conversion to 2b or 2c, respectively. Similarly, addition of KI to 2b resulted in immediate conversion to 2c. Neither 2b nor 2c, however, revealed any change in the presence of excess KCl. The ease of the exchange reactions is most likely due to the weak nature of the $Pt_3(\mu_3\text{-}X)$ bond.

2.2.4 Reactions of 2a, 2b and 2c with CO

The addition of extra CO ligands to the Pt_3 halide adduct clusters was studied. It is known that one or two

FIGURE 2.4: **Ligand Exchange Study: The Titration of 2b with KI**

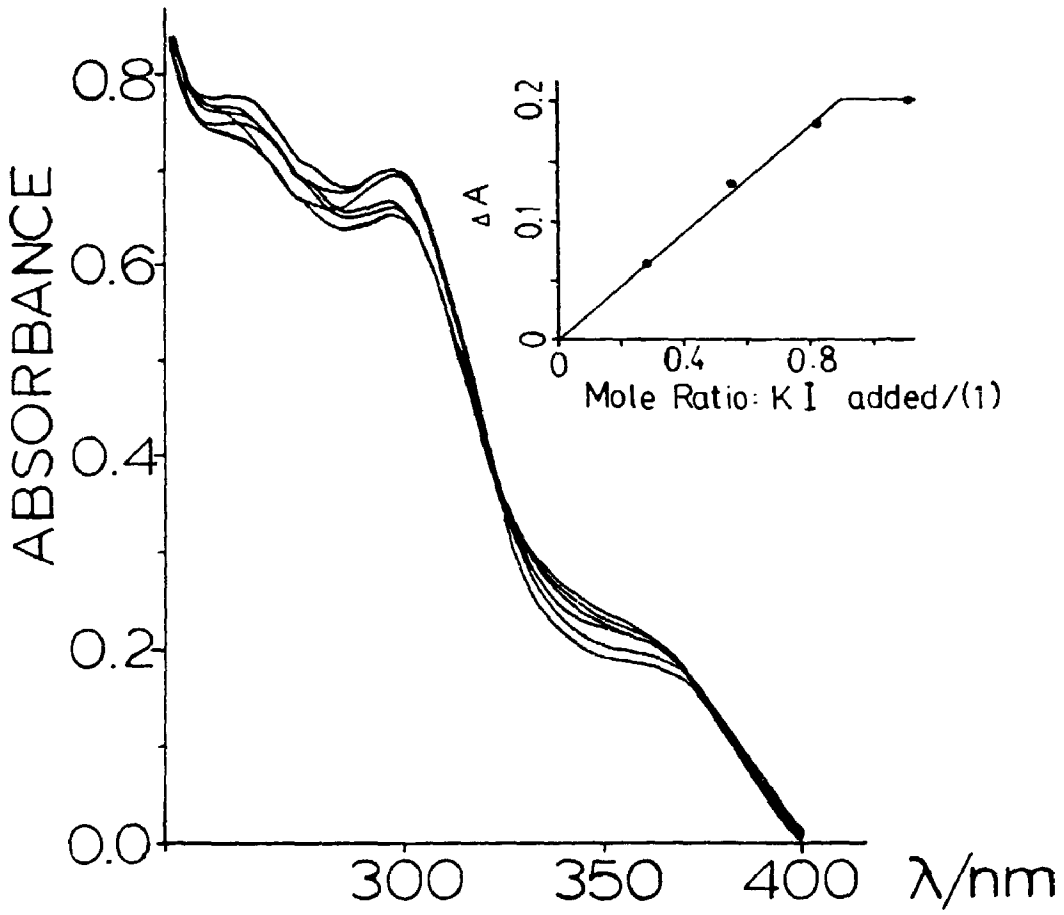

carbonyl ligands are able to undergo rapid, reversible coordination to the 42 electron complex cations $[M_3(\mu_3\text{-}CO)(\mu\text{-}dppm)_3]^{2+}$, M = Pt and Pd, and it was of interest to see whether an additional CO ligand could be added to the Pt_3 halide adduct clusters.[14]

Placing the chloride, bromide and iodide clusters under positive pressure of CO resulted in no coordination of extra CO ligands. The halide ions appear to prevent access of CO to the metal centres. This result is informative in that it demonstrates the relative strength of the $Pt_3(\mu_3\text{-}X)$ interaction. This is somewhat surprising in light of the ease with which exchange reactions occur with the various halide ions.

2.3 DISCUSSION

The crystallographic results for $[Pd_3(\mu_3\text{-}CO)(\mu_3\text{-}Cl)\text{-}(\mu\text{-}dppm)_3]^{1+}$ revealed Pd-Cl separations of 2.741(4) - 3.161(4) Å. These bond distances are too long to be considered indicative of normal covalent bonding. A consideration of the results of spectral titrations of these clusters with halide ions and their absorption spectra resulted in the conclusion that a weak covalency does exist in the $Pd_3(\mu_3\text{-}X)$ unit.

The spectral titrations of **1** with halide ions revealed a sharp endpoint at a 1:1 molar ratio which indicated a quantitative formation of **2a-2c**. The equilibrium constants for the formation of **2a-2c** followed

the sequence I » Br » Cl » CF_3CO_2 which is that expected for a covalent type of interaction at a soft platinum acceptor.

It was observed for the Pd_3 systems that those halide ions which were expected to bind most strongly yielded the higher energy absorption bands in their UV-Visible spectra (λ_{max} = 463 nm, X = Cl; λ_{max} = 459 nm, X = Br; λ_{max} = 456 nm, X = I). The absorption spectra for the Pt_3-halide clusters however yielded no distinctive peaks that could be monitored as in the palladium case. The positions of a shoulder were therefore monitored (λ= 368 nm, X = Cl; λ = 368 nm, X = Br). The position of the shoulder for the cluster in which X = I could not be accurately assigned. While no conclusions about the nature of the $Pt_3(\mu_3-X)$ interaction were able to be made from the UV-Visible spectra of these Pt_3 adduct clusters, it is clear that absorption spectra for these species lie much further into the UV region than those for the analogous Pd_3 clusters. It is possible, on the basis of the results of the spectral titrations, to suggest that some degree of covalency also exists for the $Pt_3(\mu_3-X)$ interaction.

The halide exchange reactions must be considered to be occurring by a dissociative mechanism since the cavity defined by the phenyl groups of the bridging dppm ligands could not accommodate two halide ions. The ease of the observed reactions is due to the relatively weak nature of the $Pt_3(\mu_3-X)$ interaction.

2.4 CONCLUSIONS

These trinuclear cluster systems have revealed some novel coordination chemistry at the μ_3-face position for which there are few precedents.[3] The presence of a weak covalent bonding interaction between the dicationic Pt cluster and the monoanionic ligands Cl, Br and I can be considered to have potentially profound effects on the chemistry of these trinuclear systems.

The high stability constants for halide addition, together with the lability of the coordinated halide, is very unusual, and suggests that many other ligands might be capable of coordination at the μ_3-site.

2.5 REFERENCES

1. S.J. Cartwright, K.R. Dixon and A.D. Rattray, *Inorg. Chem.*, (1980), **19**, 1120.
2. G.W. Bushnell, K.R. Dixon, R. Ono and A. Pidcock, *Can. J. Chem.*, (1984), **62**, 696.
3. J.W.A. van der Velden, J.J. Bour, R. Pet, W.P. Bosman and J.H. Noordik, *Inorg. Chem.*, (1983), **22**, 3112.
4. J. Estienne, *Acta Cryst.*, (1986), **C42**, 1512.
5. N. Bresciani, N. Marsich, G. Nardin and L. Randaccio, *Inorg. Chem.*, (1974), **10**, L5.
6. G. Nardin, L. Randaccio and E. Zangrando, *J. Chem. Soc., Dalton Trans.*, (1975), 2566.
7 H. Hoberg, K. Radine, C. Kruger and M. Romao, *Z. Naturforsch*, (1985), **40b**, 607.
8. Lj. Manojlovic-Muir, K.W. Muir, B.R. Lloyd and R.J. Puddephatt, *J. Chem. Soc., Chem. Commun.*, (1985), 536.
9. T. Matsubara and C. Creutz, *J. Am. Chem. Soc.*, (1978), **100**, 6257.
10. B.R. Lloyd, Ph.D. Thesis, University of Western Ontario, 1985.
11. G. Ferguson. B.R. Lloyd and R.J. Puddephatt, *Organometallics*, (1986), **5**, 344.
12. B.E. Haydem and A.M. Bradshaw, *Surf. Sci.*, (1983), **125**, 787.

13. M. Rashidi and R.J. Puddephatt, *J. Am. Chem. Soc.*, (1986), **108**, 7111.

14. B.R. Lloyd, A.M. Bradford and R.J. Puddephatt, *Organometallics*, (1987), **6**, 424.

15. S.S.M. Ling, N. Hadj-Bagheri, Lj. Manojlovic-Muir, K.W. Muir and R.J. Puddephatt, *Inorg. Chem.*, (1987), **26**, 231.

16. M.P. Brown, S.J. Franklin, R.J. Puddephatt, M.A. Thomson and K.R. Seddon, *J. Organomet. Chem.*, (1979), **178**, 281.

17. A. Moor, P.S. Pregosin and L.M. Veranzi, *Inorg. Chim. Acta.*, (1981), **48**, 153.

18. A. Moor, P.S. Pregosin and L.M. Veranzi, *Inorg. Chim. Acta.*, (1982), **61**, 135.

CHAPTER 3

THE ADDITION OF PR_3 AND $P(OR)_3$ TO $[Pt_3(\mu_3\text{-}CO)(\mu\text{-}dppm)_3]^{2+}$: A NOVEL CLASS OF CLUSTERS CONTAINING THE ASYMMETRIC (μ_3-CO) UNIT

3.1 INTRODUCTION

Transition metals exhibit a pronounced tendency to form complexes with trivalent compounds of phosphorus. Tertiary phosphines, and to a lesser extent tertiary phosphite ligands, play a major role in the chemistry of low valent platinum cluster complexes.[1-8] These ligands exhibit a wide range of steric and electronic effects which are able to markedly influence the chemistry of the complexes into which they are incorporated. For example, the nuclearity of the clusters obtained by the reduction of cis-$[PtCl_2(CO)(PR_3)]$ is sensitive to the steric and/or electronic requirements of the tertiary phosphine used.[9] The use of phosphines with large cone angles such as P^tBu_3 (182°) and $P(C_6H_{11})_3$ (170°) stabilize clusters of the type $[Pt_3(\mu\text{-}CO)_3(PR_3)_3]$, whereas the use of phosphines such as PPh_3 (145°) and PMe_2Ph (122°), with intermediate cone angles and electronic parameters, destabilize these same clusters.

Farrar and co-workers have investigated the exchange of phosphine ligands in the compounds $[Pt_3(\mu_3\text{-}CO)_3L_3]$ where

L is a bulky phosphine such as $P(C_6H_{11})_3$, P^iPr_3 or P^tBu_3.[10] They found that the phosphines, L, exchange readily and quickly with less bulky phosphines, L', and, depending on how much of the free phosphine, L', is used, various amounts of mixed phosphine clusters are formed.

It has also been shown that some phosphine ligands, L, add reversibly to the 42 electron clusters $[Pt_3(\mu\text{-}CO)_3L_3]$ to give $[Pt_3(\mu\text{-}CO)_3L_4]$ and this can lead to ligand substitution reactions or, especially with less bulky ligands, L', to cluster fragmentation.[11-13]

The simplest surface reaction which can be mimicked by a coordinatively unsaturated cluster is non-dissociative chemisorption.[14] In the terminology of coordination chemistry this is just ligand addition or complex formation. This chapter reports the results of the addition of tertiary phosphine and phsophite ligands to the cluster cation $[Pt_3(\mu_3\text{-}CO)(\mu\text{-}dppm)_3]^{2+}$, 1. The interest is in whether the ligands add at terminal or bridging sites,[15-20,22,24] in how ligand addition affects the $Pt_3(\mu_3\text{-}CO)$ linkage,[19,20] and in whether the added ligand or carbonyl ligand is fluxional.[15-17,20] With respect to the surface analogy, it is believed that PH_3 and PF_3 add as terminal ligands on the Pt(111) and Ni(111) surfaces.[23]

3.2 RESULTS

3.2.1 Synthesis of the Complexes $[Pt_3(\mu_3\text{-}CO)(\mu\text{-}dppm)_3L][PF_6]_2$

The chemistry is shown in Scheme 3.1.

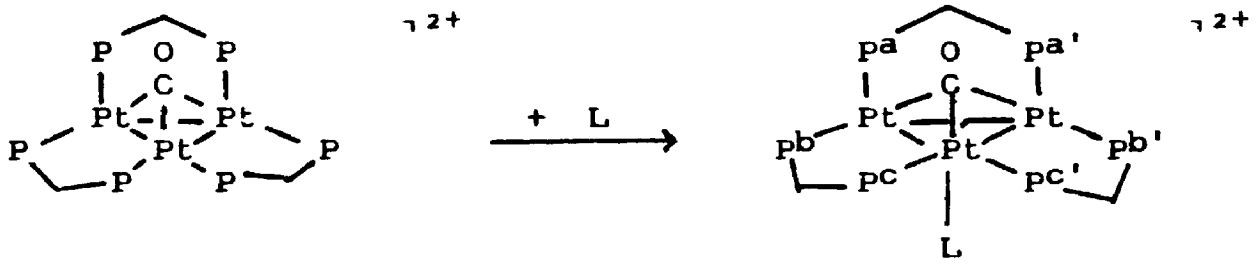

1

2a: L = $P^d(OMe)_3$
2b: L = $P^d(OEt)_3$
2c: L = $P^d(OPh)_3$
2d: L = P^dMe_2Ph
2e: L = P^dMePh_2
2f: L = P^dPh_3
2g: L = P^dF_3

Scheme 3.1

The reaction of complex 1 with the less bulky phosphine and phosphite ligands $P(OMe)_3$, $P(OEt)_3$, $P(OPh)_3$ and PMe_2Ph gave the corresponding complexes 2a-2d, respectively, in quantitative yield. These complexes were thermally stable and could be isolated in analytically pure form as the hexafluorophosphate salts which were red solids. With the bulkier ligands, $PMePh_2$ and PPh_3, adduct formation was reversible and the adducts 2e and 2f could not be isolated in pure form. Similarly, the volatile ligand PF_3 formed a complex 2g, as determined by NMR

spectroscopy, but partial loss of PF_3 occurred on attempted isolation.

3.2.2 The Characterization of $[Pt_3(\mu_3\text{-}CO)(\mu\text{-}dppm)_3\{P(OPh)_3\}][PF_6]_2\cdot Me_2CO$ by X-ray Crystallography

The structure of 2c was solved by Drs. Muir and Manojlovic-Muir at the University of Glasgow. Crystals of complex 2c $[PF_6]_2$ were grown by fractional recrystallization from an acetone/pentane mixture and consisted of well separated cations, anions and solvent molecules. The structure of the cation (Figures 3.1 and 3.2) is characterized by bond lengths and angles, as shown in Table 3.1. It contains an approximately equilateral triangular Pt_3 cluster with each edge of the triangle bridged by a dppm ligand to form a Pt_2P_2C dimetallacycle. Rotational orientation of the dppm ligands about the Pt-Pt bonds and conformations of the Pt_2P_2C rings are such as to afford a Pt_3P_6 skeleton substantially distorted from an idealized latitudinal M_3L_6 geometry. The largest distortions involve the phosphorus atoms coordinated to the platinum centre to which the $P(OPh)_3$ ligand is also bound [Pt(1)]. Thus the P(1) and P(6) atoms lie 0.321(8) and 0.669(7) Å away from the Pt_3 plane on the side opposite to that of the $P(OPh)_3$ ligand. In the Pt_2P_2C rings the methylene groups are pointing towards the $P(OPh)_3$ ligand while the atoms C(1), C(2) and C(3) are displaced from the

FIGURE 3.1: ORTEP Diagram of 2c (1)

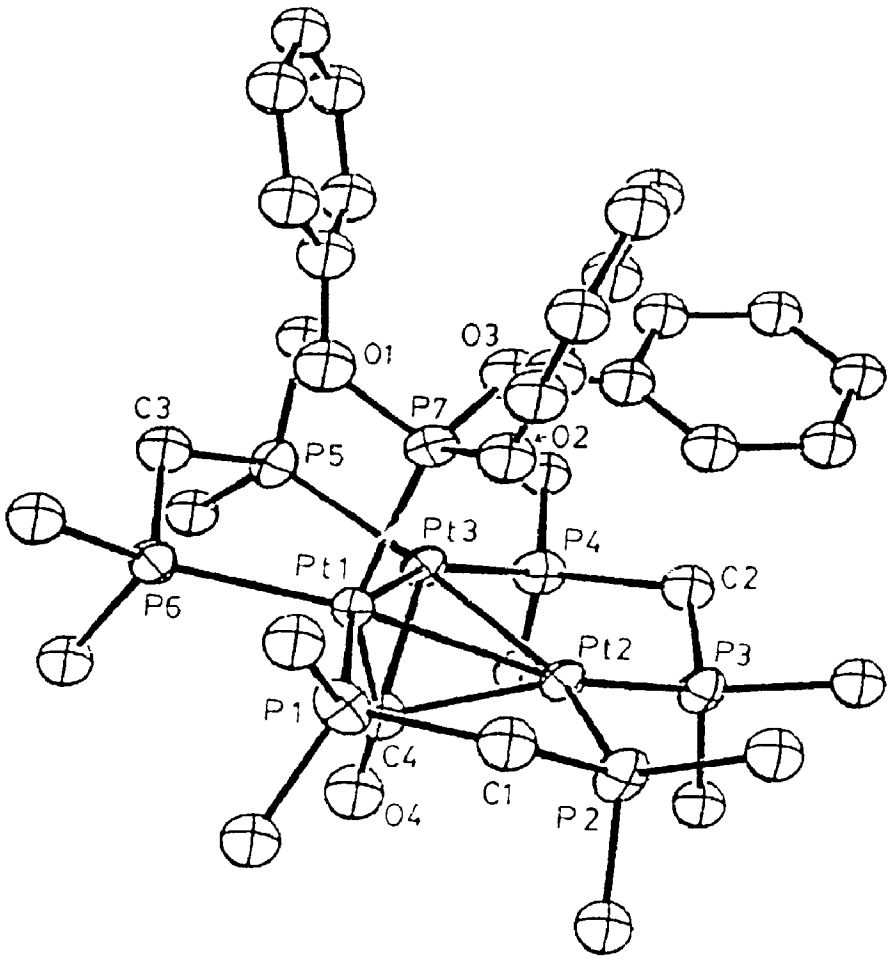

FIGURE 3.2: ORTEP Diagram of 2c (2)

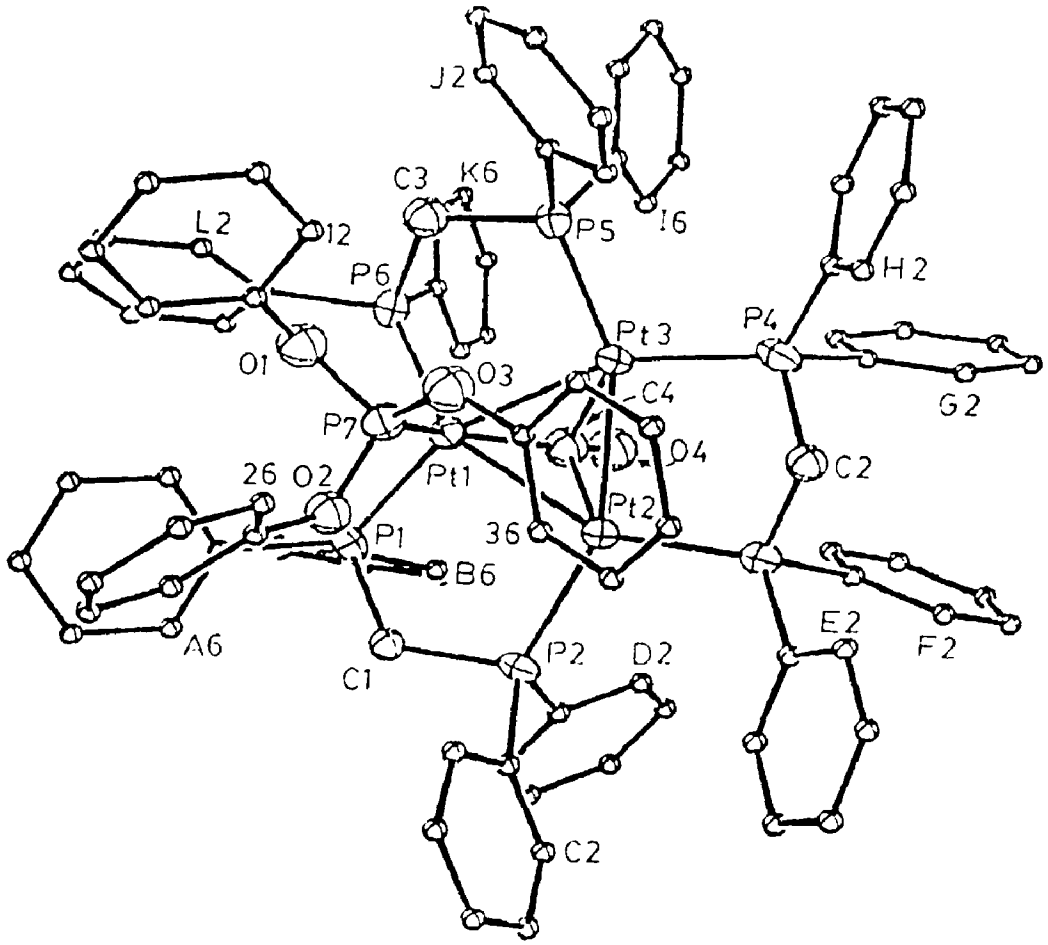

TABLE 3.1: Selected Bond Lengths and Angles in $[Pt_3(\mu_3\text{-}CO)(\mu\text{-}dppm)_3\{P(OPh)_3\}]^{2+}$, 2c

Bond Angles (°)		Bond Angles (°)	
Pt(2) - Pt(1) - Pt(3)	59.9(1)	Pt(2) - Pt(1) - P(1)	98.2(2)
Pt(2) - Pt(1) - P(6)	148.8(2)	Pt(2) - Pt(1) - P(7)	94.2(2)
Pt(2) - Pt(1) - C(4)	53.4(8)	Pt(3) - Pt(1) - P(1)	156.9(2)
Pt(3) - Pt(1) - P(6)	93.2(2)	Pt(3) - Pt(1) - P(7)	90.5(2)
Pt(3) - Pt(1) - C(4)	57.4(8)	P(1) - Pt(1) - P(6)	105.1(3)
P(1) - Pt(1) - P(7)	99.1(3)	P(1) - Pt(1) - C(4)	104.7(9)
P(6) - Pt(1) - P(7)	102.1(3)	P(6) - Pt(1) - C(4)	100.1(8)
P(7) - Pt(1) - C(4)	141.8(8)	Pt(1) - Pt(2) - Pt(3)	59.5(1)
Pt(1) - Pt(2) - P(2)	95.1(2)	Pt(1) - Pt(2) - P(3)	153.3(2)
Pt(1) - Pt(2) - C(4)	45.9(8)	Pt(3) - Pt(2) - P(2)	154.6(2)
Pt(3) - Pt(2) - P(3)	93.9(2)	Pt(3) - Pt(2) - C(4)	55.5(8)
P(2) - Pt(2) - P(3)	111.5(3)	P(2) - Pt(2) - C(4)	107.9(8)
P(3) - Pt(2) - C(4)	122.9(8)	Pt(1) - Pt(3) - Pt(2)	60.6(1)
Pt(1) - Pt(3) - P(4)	156.3(2)	Pt(1) - Pt(3) - P(5)	95.0(2)
Pt(1) - Pt(3) - C(4)	45.7(8)	Pt(2) - Pt(3) - P(4)	95.7(2)
Pt(2) - Pt(3) - P(5)	155.2(2)	Pt(2) - Pt(3) - C(4)	51.6(7)
P(4) - Pt(3) - P(5)	108.7(3)	P(4) - Pt(3) - C(4)	120.3(7)
P(5) - Pt(3) - C(4)	115.5(7)	Pt(1) - P(1) - C(1)	106.2(9)
Pt(1) - P(7) - O(2)	110.7(8)	Pt(2) - P(2) - C(1)	110.0(8)
O(1) - P(7) - O(2)	106.9(11)	Pt(2) - P(3) - C(2)	110.4(9)
O(2) - P(7) - O(3)	10.68(10)	Pt(1) - P(7) - O(1)	109.8(8)
P(7) - O(2) - C(21)	130.1(20)	Pt(1) - P(7) - O(3)	124.0(8)
P(1) - C(1) - P(2)	121.5(14)	O(1) - P(7) - O(3)	96.9(11)
P(5) - C(3) - P(6)	114.6(15)	P(7) - O(1) - C(11)	131.1(15)
Pt(1) - C(4) - Pt(3)	76.8(10)	P(7) - O(3) - C(31)	141.3(18)
Pt(2) - C(4) - Pt(3)	72.9(8)	P(3) - C(2) - P(4)	111.6(13)
Pt(3) - C(4) - O(4)	119.9(20)	Pt(1) - C(4) - Pt(2)	80.7(11)
Pt(2) - C(4) - O(4)	121.1(19)	Pt(1) - C(4) - O(4)	154.6(21)

Bond Lengths (Å)		Bond Lengths (Å)	
Pt(1) - Pt(2)	2.656(2)[a]	Pt(1) - Pt(3)	2.626(2)
Pt(1) - P(1)	2.341(8)	Pt(1) - P(6)	2.335(8)
Pt(1) - P(7)	2.293(8)	Pt(1) - C(4)	1.93(3)
Pt(2) - Pt(3)	2.636(2)	Pt(2) - P(2)	2.323(8)
Pt(2) - P(3)	2.290(8)	Pt(2) - C(4)	2.16(3)
Pt(3) - P(4)	2.288(8)	Pt(3) - P(5)	2.300(8)
Pt(3) - C(4)	2.27(3)	P(1) - C(1)	1.81(3)
P(2) - C(1)	1.88(3)	P(3) - C(2)	1.76(3)
P(4) - C(2)	1.89(3)	P(5) - C(3)	1.83(3)
P(6) - C(3)	1.82(3)	P(7) - O(1)	1.56(2)
P(7) - O(2)	1.57(2)	P(7) - O(3)	1.59(2)
O(1) - C(11)	1.40(4)	O(2) - C(21)	1.44(4)
O(3) - C(31)	1.37(3)	O(4) - C(4)	1.21(4)

[a] Estimated standard deviations in the least significant digit are shown in parentheses, here and throughout the paper.

Pt_3 plane by 0.23(2), 0.81(3) and 0.21(3) A, respectively. In such a conformation of the $Pt_3P_6C_3$ skeleton the phenyl rings are directed away from the bulky $P(OPh)_3$ ligand and the steric hindrance, which is severe, is thus minimized.

The Pt-Pt distances of 2.656(2), 2.636(2) and 2.626(2) A differ only slightly from each other and their mean value of 2.639(2) A is similar to the mean Pt-Pt distance in complex 1 which is 2.634 A.[21] Thus the addition of the phosphite ligand to 1 increases the cluster electron count from 42 to 44 electrons, but it does not significantly affect the Pt-Pt bond lengths. This is in accord with our recent findings on related complexes.[16,18,25] The Pt-P bond lengths involving the Pt(1) atom [2.341(8) and 2.335(8) A], however, are longer than those involving Pt(2) and Pt(3) [2.288(8) - 2.323(8) A]. This difference could reflect a rehybridization of platinum orbitals due to the higher coordination number of Pt(1). The Pt(1)-P(7) distance of 2.293(8) A is within the range of Pt-P bond lengths in phosphite complexes.[26]

The carbonyl ligand adopts a distorted triply bridging geometry, binding more strongly to Pt(1) than to Pt(2) or Pt(3). This is apparent from the respective Pt-C distances of 1.92(3), 2.16(3) and 2.27(3) A. This is also apparent from the Pt(1)-C-O bond angle of 155(2)° which is significantly larger than the Pt(2)-C-O and Pt(3)-C-O angles of 121(2) and 120(2)°. It is interesting to compare the geometry of the $Pt_3(\mu_3\text{-}CO)$ unit in 2c with those

previously observed in the complexes $[Pt_3(\mu_3\text{-}CO)(\mu\text{-}dppm)_3]^{2+}$, 1, $[Pt_3(\mu_3\text{-}CO)(\mu_3\text{-}SnF_3)(\mu\text{-}dppm)_3]^{2+}$, 3, and $[Pt_3(\mu_3\text{-}CO)(SCN)(\mu\text{-}dppm)_3]^{1+}$, 4. A brief summary provided in Table 3.2, where the μ-dppm ligands are omitted for clarity, shows that the Pt-Pt distances are very similar for the 42 electron cluster, 1, the 44 electron cluster with an additional triply bridging ligand, 3, and the 44 electron clusters with an additional terminal ligand, 4 and 2c. The distortion of the triply bridging carbonyl ligand from the symmetrical μ_3-bonding mode is significant in the weakly bound thiocyanante adduct, 4, and it is even greater in the more strongly bound triphenylphosphite adduct, 2c. This distortion will be considered further in the discussion section of this chapter.

3.2.3 Characterization of Complexes 2a-2g by Spectroscopic Methods

The values for the ν(CO) stretching frequencies were in the narrow range of 1774 to 1780 cm^{-1} for the stable clusters 2a-2d. This is in the range of stretching frequencies for μ_3-CO groups but is higher than ν(CO) = 1765 cm^{-1} for the parent cluster, 1. It should be noted that complex 3, with a symmetrical $Pt_3(\mu_3\text{-}CO)$ group, has a still higher value of ν(CO) = 1827 cm^{-1}, and it is therefore possible that the higher ν(CO) values are characteristic of 44 electron clusters and are not

TABLE 3.2: A Comparison of Selected Structural and Spectroscopic Data for Some $Pt_3(\mu_3\text{-}CO)$ Complexes.

Complex	1[2]	3[9,a]	4[7]	2c
$Pt^1\text{-}Pt^2$/Å	2.638(1)	2.639(3)	2.620(1)	2.656(2)
$Pt^1\text{-}Pt^3$/Å	2.650(1)		2.625(1)	2.626(2)
$Pt^2\text{-}Pt^3$/Å	2.613(1)		2.623(1)	2.636(2)
Pt^1-C /Å	2.095(9)	2.16(5)	2.042(13)	1.93(3)
Pt^2-C /Å	2.089(8)		2.165(13)	2.16(3)
Pt^3-C /Å	2.080(9)		2.175(13)	2.27(3)
Pt^1 C O/°	131.8(6)	135(2)	143.8(11)	154.6(21)
Pt^2 C O/°	133.1(7)		129.8(10)	121.1(14)
Pt^3 C O/°	134.9(7)		128.9(10)	119.9(20)
ν(CO)/cm^{-1}	1765	1827	1810	1779
$^1J(PtC)$[b]/Hz	770	650	868	630
$^1J(Pt^1C)$ /Hz	---	---	---	960
$^1J(Pt^2C)$[c]/Hz	---	---	---	493
$\delta(^{13}CO)$/ppm	205	198	198	194

[a] This complex has crystallographically imposed threefold symmetry.

[b] For 4 and 2c, this is the average value in the fast fluxionality region.

[c] $^1J(Pt^2C) = {}^1J(Pt^3C)$ in all cases.

primarily dependent on whether the $Pt_3(\mu_3\text{-}CO)$ group is symmetrical or not (Table 3.2).

The complexes 2 were fluxional at room temperature and so NMR spectra were obtained at low temperature, typically at -90°C in acetone-d_6 solution. The ^1H NMR spectrum in the CH_2P_2 region (Table 3.3) contained two "AB" quartets with relative areas 2:1 as expected for the static structure 2, which has no plane of symmetry containing the $Pt_3(PCP)_3$ unit.

The ^{31}P NMR spectra of the complexes are informative and the spectrum of 2a will be described as a typical example (Figure 3.3). Data for all complexes are given in Table 3.4. In these $Pt_3(\mu\text{-dppm})_3$ complexes, the largest J(PP) couplings are the trans-like couplings through the PtPt bonds which in 2 are $^3J(P^aP^c)$ and $^3J(P^bP^{b'})$. The spectra contain two doublet resonances and a singlet resonance and the singlet is then readily assigned to P^b. The magnitude of $^3J(P^bP^{b'})$ = 150 Hz, is obtained from the ^{195}Pt satellite spectra, while $^3J(P^aP^c)$ = 170 Hz. These are typical values for complexes 2 (Table 3.4). The resonances due to P^a [δ = -10.8, $^1J(PtP)$ = 3930 Hz] and P^c [δ = -35.6, $^1J(PtP)$ = 2500 Hz] are assigned by correlation of $^1J(PtP)$ values with the Pt-P bond distances (PtP^c longer than PtP^a, Table 3.1) and from a general trend that the ^{31}P chemical shifts are more negative when bound to platinum atoms with higher steric hindrance.[26]

TABLE 3.3: ^1H NMR Data (-80°C) for Complexes **2a-2d** in Acetone-d_6

Complex[a]	$P_2CH^aH^b$ δ_a	δ_b	$^2J(H^aH^b)$	$P_2CH^cH^d$ δ_c	δ_d	$^2J(H^cH^d)$	δ He	J(PH)
2a	4.91	4.86	14	5.93	5.88	14	3.51	10.8
2b	4.46		--	5.69	5.55	14	4.30	7
2c	4.92	4.80	14	5.75	5.62	14	--	--
2d	--	--	--	--	--	--	1.64	13

[a] **2a**, $P(OCH_3^e)_3$; **2b**, $P(OCH_2^eCH_3^f)_3$, $\delta(H^f)$ = 1.3, t, $^3J(H^eH^f)$ = 7; **2c**, $P(OC_6H_5)_3$; **2d**, $P(CH_3^e)_2C_6H_5$, spectrum very poorly resolved in the CH_2 region and assignments are not given.

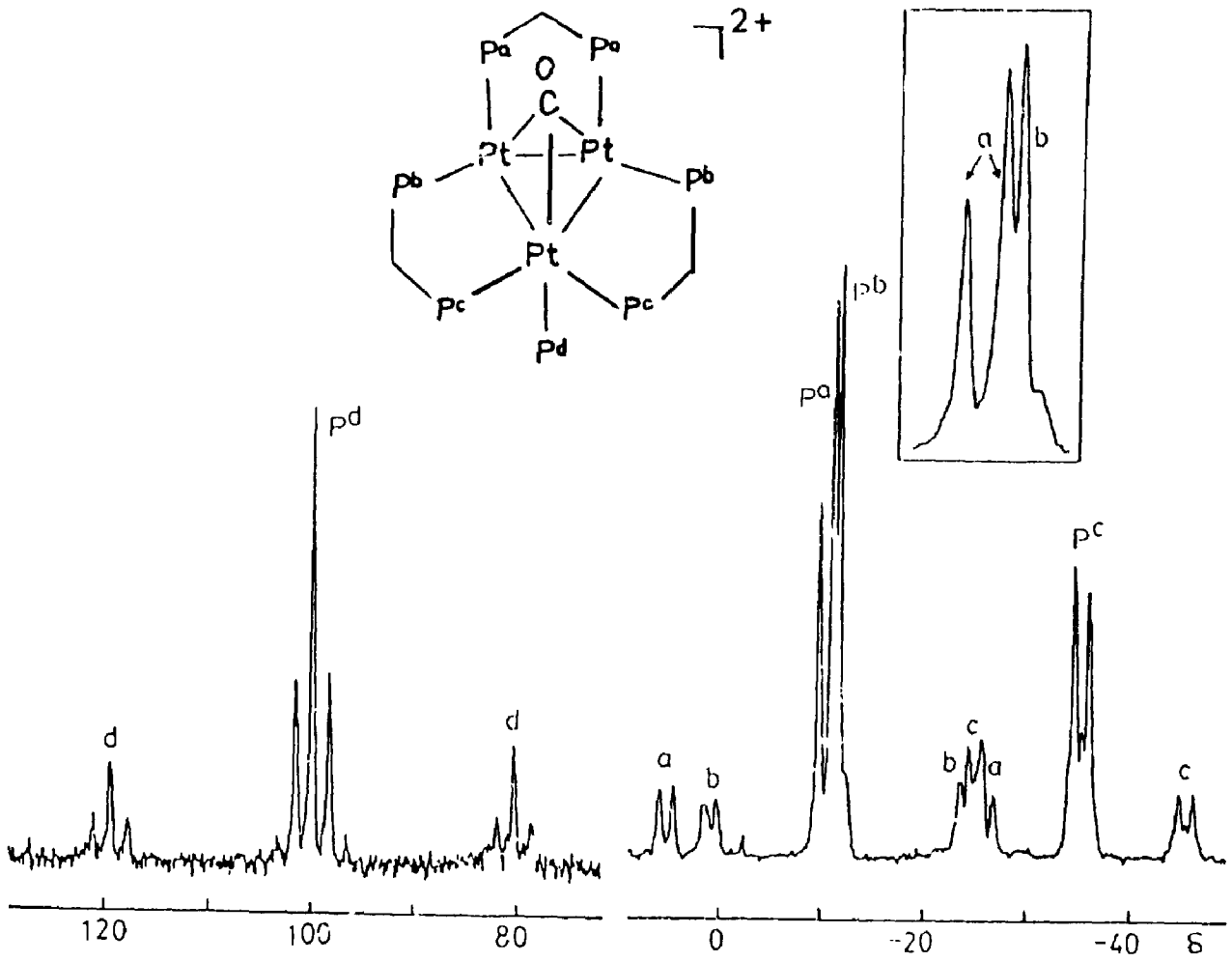

FIGURE 3.3: $^{31}P\{^{1}H\}$ NMR Spectrum of **2a**

TABLE 3.4: ^{31}P NMR Data (-92°C) for the Clusters 2a-2f

Complex	2a	2b	2c	2d	2e	2f	
$\delta(P^a)$	-10.8	-10.0	-12.4	-13.9	-16.1	-15.4	-5.1[a]
$^1J(PtP^a)$	3930	3820	3930	3820	3800	3860	3860
$^3J(P^aP^c)$	170	180	170	170	170	170	170
$\delta(P^b)$	-12.1	-14.6	-13.6	-13.6	-15.3	-7.9	
$^1J(PtP^b)$	3080	3060	3000	3080	3100	2780	
$^3J(P^bP^{b'})$	150	150	150	150	160	---	
$\delta(P^c)$	-35.6	-37.9	-35.7	-42.4	-42.5	-43.1	-38.7[a]
$^1J(PtP^c)$	2500	2400	2665	2640	2600	2660	2660
$^3J(P^aP^c)$	170	180	170	170	170	170	170
$\delta(P^d)$	100.	97.8	91.9	-35.6	-18.8	-7.0	
$^1J(Pt^1P^d)$	4910	4990	5080	2800	2750	2670	
$^2J(Pt^2P^d)$	420	410	430	186	240	220	

[a] Complex 2f gives 2 P^a and P^c resonances, see text.

The resonance due to the $P(OMe)_3$ ligand was at δ = 100.3, and appeared as a 1:4:1 triplet [due to coupling to Pt^1, $^1J(PtP)$ = 4910 Hz] of 1:8:18:8:1 quintets [due to coupling to Pt^2 and Pt^3, $^2J(PtP)$ = 420 Hz]. These parameters are typical for the phosphite adducts, but lower J(PtP) values were found for the phosphine complexes as seen in Table 3.4.

The ^{13}C NMR spectrum of **2a***, enriched with ^{13}CO, gave $\delta(^{13}CO)$ = 194.5 ppm, and appeared as a 1:1 doublet [coupling to $P(OMe)_3$, $^2J(PC)$ = 142 Hz] of 1:4:1 triplets [due to coupling to Pt^1, $^1J(PtC)$ = 996 Hz] of 1:8:18:8:1 quintets [due to Pt^2 and Pt^3, $^1J(PtC)$ = 468 Hz] (Table 3.5.).

TABLE 3.5: ^{13}C NMR Data for Complexes 2 in CD_2Cl_2

Complex	2a	2c	2g
δ (CO)/ppm	194.5	194.0	194.0
$^1J(Pt^1C)$/Hz	996	960	---
$^1J(Pt^2C)$/Hz	468	463	---
$J_{av}(PtC)$/Hz[a]	630[b]	630[c]	640
$^2J(P^dC)$ /Hz	142	146	144

[a] Experimental value in region of rapid fluxionality.

[b] Calculated value $J_{av}(PtC)$ = 1/3 x 996 + 2/3 x 468 = 644 Hz.

[c] Calculated value $J_{av}(PtC)$ = 1/3 x 960 + 2/3 x 463 = 629 Hz.

The above spectroscopic data clearly show that the structures in solution are of the type found in the solid state for 2c. In particular, the phosphine or phosphite adducts adopt a terminal bonding position and the carbonyl group is asymmetrically bridging with a much stronger interaction with Pt^1 than with Pt^2 or Pt^3.

For the bulky PPh_3 derivative, 2f, the ^{31}P NMR spectrum at -90°C showed a doubling of some of the resonances and data are given in Table 3.4. It is not clear if the extreme steric hindrance expected for this species causes non-equivalence of pairs of atoms, $P^aP^{a'}$ and $P^cP^{c'}$, within a given molecule or if two atropisomers are for· ·d.[27] The former is perhaps more probable since only one signal due to coordinated PPh_3 was resolved.

3.2.4 Fluxionality of Complexes 2a-2f

The clusters 2a-2e were found to be fluxional in the sense that the ligand L could migrate around the triangular face of the cluster 2 as shown in Equation 3.1.

For 2a, which was studied in most detail, the ^{31}P NMR spectrum at 59° C showed a single broad resonance due to the dppm phosphorus atoms thus indicating apparent threefold symmetry for the complex (Figure 3.4). The resonance due to the $P(OMe)_3$ ligand occurred as a sharp septet due to coupling to six "equivalent" dppm phosphorus atoms and had broad satellites due to $^1J(PtP)$ = 1900 Hz. The calculated value for rapid intramolecular fluxionality

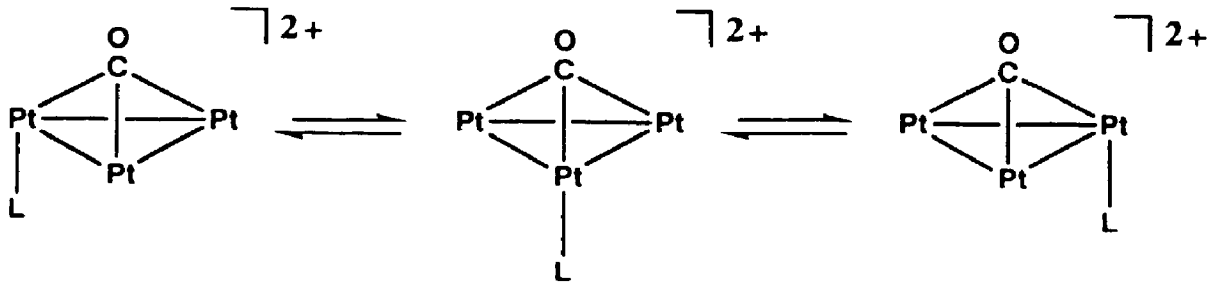

Fluxionality of Phosphine and Phosphite Adduct Clusters

Equation 3.1

would be $^{1}J(PtP) \approx 1/3 \times 4910 + 2/3 \times 420 = 1917$ Hz, in reasonable agreement. The ^{195}Pt satellites were sharper at 100°C in DMF solution with $^{1}J(PtP) = 1910$ Hz, but the complex began to decompose under these conditions. Finally, in the presence of free $P(OMe)_3$, no exchange between free and coordinated $P(OMe)_3$ could be detected by NMR at 59°C in acetone.

Further evidence on the nature of the fluxionality was obtained by ^{13}C NMR spectroscopy of **2a** and **2c** (Figure 3.5). At +59°C the ^{13}CO resonance in each case still occurred as a doublet with $^{2}J(PC) = 144$ Hz, due to coupling to the phosphite phosphorus, but an average ^{195}Pt coupling of $^{1}J(PtC) = 630$ Hz was observed (Figure 3.5).

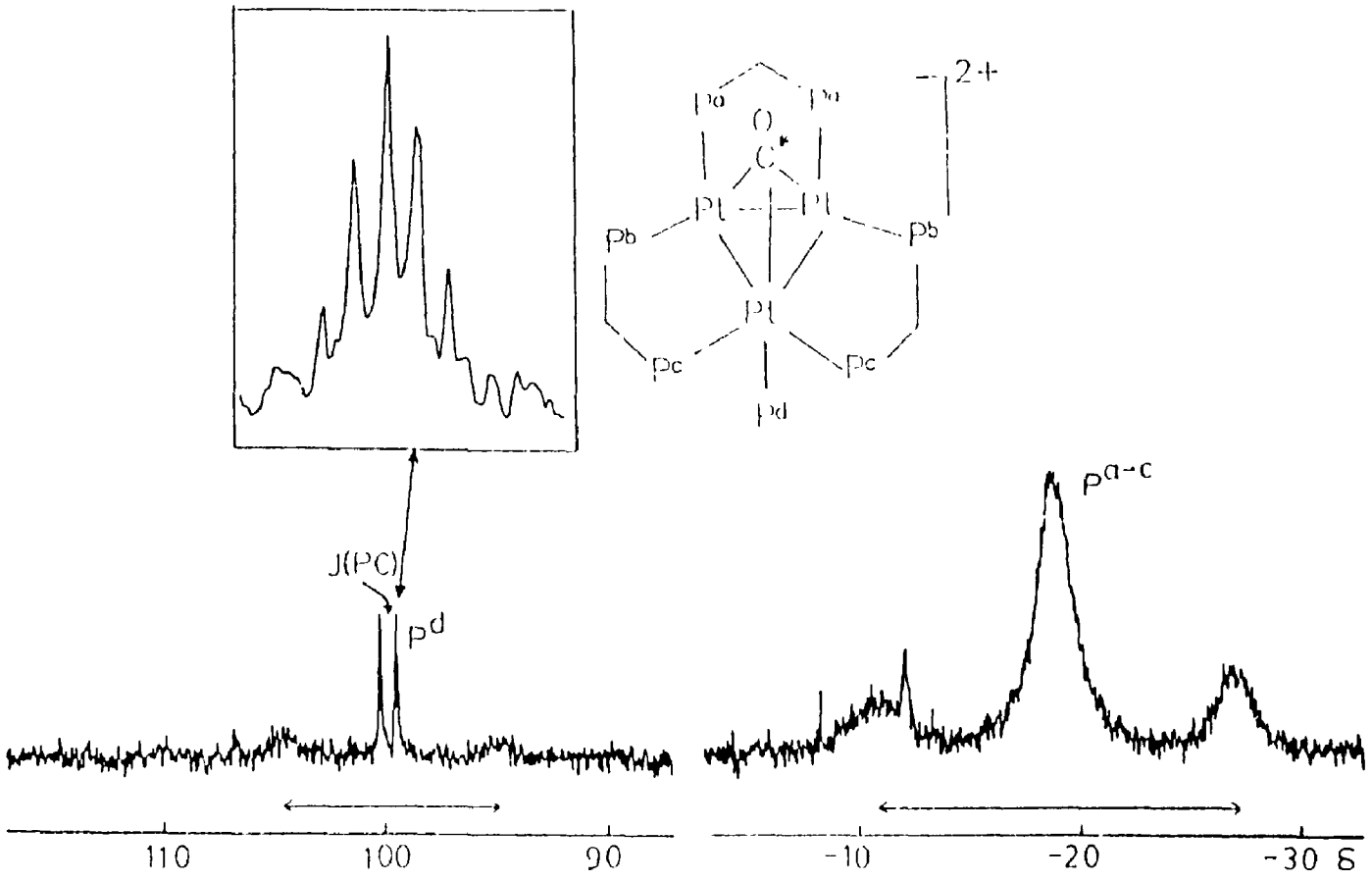

FIGURE 3.4: $^{31}P\{^{1}H\}$ NMR Spectrum of 2a at 59°C

FIGURE 3.5: $^{13}C\{^{1}H\}$ NMR Spectrum for 2a at 50°C

The calculated average value of $^{1}J(PtC)$ = 1/3 x 996 + 2/3 x 468 = 644 Hz. Thus the carbonyl appears to be symmetrically triply bridging in the fast fluxionality region but the coupling $^{2}J(PC)$ to the phosphite ligand is maintained. This shows that the fluxionality does not involve reversible dissociation of either the phosphite or carbonyl ligand and so supports the mechanism of Equation 3.1. A transition state with a $Pt_3(\mu_3\text{-}PX_3)$ group and symmetrical $Pt_3(\mu_3\text{-}CO)$ group is probable but not proved.[28] The results described above are in sharp contrast to those obtained for the triphenylphosphine adduct **2f**. For this complex at -43°C, sharp singlet resonances due to dppm and PPh_3 phosphorus atoms were observed, the latter having no ^{195}Pt satellites. The chemical shifts were close to those for free **1** and PPh_3. At this temperature the equilibrium strongly favors **1** and PPh_3 over **2f**, but it is probable that there is fast exchange also. As discussed earlier, the steric bulk of PPh_3 appears to be at the limit for access to the Pt_3 plane of **1**. It is not clear if the intramolecular migration of Equation 3.1 can occur in this case since the complex is almost completely dissociated at temperatures where it might occur.

The fluxionality observed for **2a-2e** appears to be unique in cluster complexes and is probably due to a small energy difference between the structures with terminal and $\mu_3\text{-}PR_3$ ligands. Phosphine or phosphite fluxionality in transition metal clusters has previously been considered

not to occur.[29-31] A related fluxionality of a diphosphine ligand has recently been reported.[32-34]

3.2.5 Spectroscopic Characterization of $[Pt_3(\mu_3\text{-}CO)(\mu\text{-}dppm)_3(PF_3)]^{2+}$, 2g

Based on the above studies of fluxionality, it seemed that the most probable ligand to form a complex with a $Pt_3(\mu_3\text{-}PX_3)$ group was PF_3, which has π-acceptor properties similar to those of CO. An isolobal analogy also exists between PF_3 and $[SnF_3]^-$, which forms the symmetrical $Pt_3(\mu_3\text{-}SnF_3)$ group in 3. This suggested that the PF_3 adduct might have structure 5 rather than 2g.

The PF_3 adduct must be characterized in solution in the presence of some free PF_3, since partial dissociation occurs on attempted isolation. Even at -92°C, in CD_2Cl_2 solution, the ^{31}P NMR spectrum contained only one resonance due to the μ-dppm ligands (Table 3.3) at δ = -17.7 [^1J(PtP) = 3370 Hz], while the PF_3 signal occurred as a broad, poorly resolved quartet at δ = -15.9 [^1J(PF) = -1440 Hz]. In the ^{13}C NMR spectrum at -92°C the carbonyl resonance was at δ = 194.0 as a 1:1 doublet [$^2J(F_3PCO)$ = 144 Hz] of 1:12:49:84:49:12:1 septets [due to coupling to three "equivalent" platinum atoms, ^1J(PtC) =640 Hz].

There are strong similarities between the above spectra and those due to the complexes 2a and 2b in the high temperature limiting spectra where phosphite fluxionality is rapid, but there is also a strong

resemblance to the spectrum of 3 which contains a symmetrical μ_3-SnF_3^- ligand. [$^{31}P\{^1H\}$ NMR: 2a: δ (P^{a-c}) = -20.1 ppm, $^1J(PtP^{a-c})$ = 3270 Hz, δ P^d = 98.6 ppm, $^1J(PtP^d)$ = 1885 Hz; 3: δ (P^{a-c}) = -1.1 ppm, $^1J(PtP^{a-c})$ = 3684 Hz]. $^{13}C\{^1H\}$ NMR: 2a: $^1J(PtC)$ = 630 Hz, $^2J(PC)$ = 144 Hz; 3: $^1J(PtC)$ = 650 Hz.] Thus the PF_3 adduct either has structure 2g, but it is still undergoing rapid intramolecular fluxionality of the PF_3 ligand even at -92°C, or it has structure 5. In either case, the prediction that PF_3 would have a stronger tendency than the phosphite or phosphine ligands to form the $Pt_3(\mu_3\text{-}PX_3)$ group is clearly confirmed. Attempts to grow crystals of 2g or 5 suitable for X-ray structure determination have so far been unsuccessful.

3.3 DISCUSSION

For the ligand PPh_3 it was possible to measure the equilibrium constant, K, for the formation of 2f by integration of ^{31}P NMR resonances due to free reagents and complex 2f over the narrow temperature region -83 to -92°C. At higher temperatures, exchange broadening was severe and the equilibrium was unfavorable, and -92°C was the lower limit of temperature which could be studied in acetone-d_6. The approximate thermodynamic parameters were ΔH° = -42 ± 10 kJ mol^{-1} and ΔS° = -200 ± 40 JK^{-1} mol^{-1}. Thus, as expected, the enthalpy term favors complex formation but the entropy term does not.

The ^{31}P NMR experiment showed that exchange between free and coordinated PPh_3 occurred rapidly at room temperature, but similar exchange between free and coordinated $P(OMe)_3$ in **2a** did not occur rapidly on the NMR time scale at temperatures up to 100°C. The ligand exchange with PPh_3, therefore, almost certainly occurs by the dissociative mechanism of Scheme 3.1. Exchange could occur with the smaller ligands but at a much slower rate.

This work has shown (i) that phosphine and phosphite ligands add to complex **1** in a terminal bonding mode and (ii) that this ligand addition leads to a slippage of the μ_3-carbonyl ligand towards the platinum atom with the highest coordination number in complexes **2**. This observation can be rationalized if the μ_3-CO ligand acts to a large extent as a π-acceptor ligand[16,25] and this interpretation has been expressed elegantly by Evans.[20] According to extended Huckel MO calculations (EHMO), the platinum acceptor orbital is a $5d_{z^2}6p_z$ hybrid orbital and the enhanced backbonding can then be understood in terms of the bonding interactions shown in **6**.

While this interaction might be expected to lead to a lower value of ν(CO) in **2** compared to **1**, the opposite effect was observed (Table 3.2). One possible reason for this is that the geometry of the $Pt_3(\mu_3$-CO) unit changes from an almost regular triple bridging mode in **1** to that which may be regarded as a semi-bridging mode in **2c** (Table 3.2). This is not just a solid state effect since

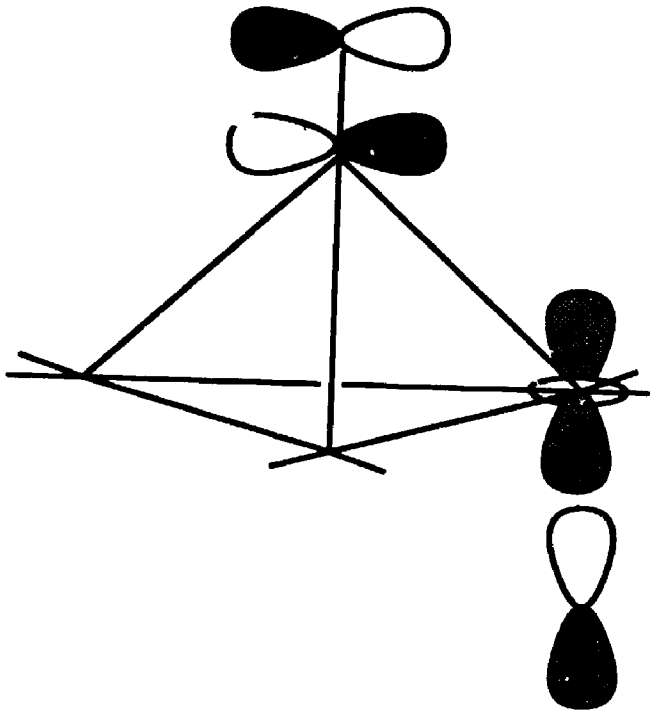

6

the low temperature ^{13}C NMR spectrum in the carbonyl region of 2a shows a much larger coupling to Pt^1 [$^1J(Pt^1C)$ = 996 Hz] than to Pt^2 or Pt^3 [$^1J(Pt^2C) = {}^1J(Pt^3C)$ = 468 Hz]. The geometry of the $Pt_3(\mu_3\text{-}CO)$ unit is intermediate between that expected for a symmetrical (μ_3-CO) group and that expected for a terminal carbonyl bound to Pt^1, and the slight increase in ν(CO) for 2 compared to 1 is not unreasonable on that basis.

Evans has suggested,[20] based on EHMO calculations, that the symmetrical structure $[Pt_3(\mu_3\text{-}CO)_2(\mu\text{-}dppm)_3]^{2+}$, 6, is slightly more stable than the structure of

$[Pt_3(\mu_3\text{-}CO)(CO)(\mu\text{-}dppm)_3]^{2+}$, 7, analogous to 2. The symmetrical structure was also consistent with the NMR data, but the observation of a terminal carbonyl stretching band in the IR indicated that 7 was the correct structure, but that it was fluxional even at -90°C. There are now good examples, 3 and 2c, for which the added ligand is clearly in a μ_3-bridging site or a terminal site, respectively; hence the spectroscopic properties of each type of complex are now established (Table 3.2). Unfortunately, the IR and NMR parameters are very similar for 3 and 2a in the rapid fluxionality region. Thus for the PF_3 complex it is not possible to distinguish between structure 5 or a rapidly fluxional 2g. The similarities of the bonding properties of CO and PF_3 are well-known, and so it is not unreasonable that 2g and 5 are very similar in energy as are 6 and 7. However, there are no examples of bridging PX_3 ligands and so the possibility that 5 is the correct structure is particularly intriguing. For rapid fluxionality of 2g at -90°C, $\Delta G^{\ddagger}$ is probably $\leq$ 42 kJ mol^{-1}, and this may be considered an upper limit of the thermodynamic preference for 2g over 5. Whilst the structure 2g is perhaps more probable than 5, this work does show the feasibility of synthesis of a $Pt_3(\mu_3\text{-}PF_3)$ group and hence other $M_3(\mu_3\text{-}PF_3)$ groups.

3.4 CONCLUSIONS

The chemistry of these trinuclear carbonyl clusters of platinum with tertiary phosphine and phosphite ligands has revealed some unique insights into the formation and nature of the asymmetric μ_3-CO ligand, and has confirmed the suggestion made by Evans that the μ_3-carbonyl behaves primarily as a π-acceptor ligand. The phosphine and phosphite ligands display a unique fluxionality not previously observed in cluster chemistry involving rapid migration about the Pt_3 triangle. The ease of this fluxionality is probably due to both the coordinative unsaturation of **1** and the lowered activation energy for fluxionality created by the presence of the asymmetric μ_3-CO. Finally, this work demonstrates the feasibility of the synthesis of not only the $Pt_3(\mu_3\text{-}PF_3)$ group but also other $M_3(\mu_3\text{-}PF_3)$ groups which have not been seen before.

3.5 REFERENCES

1. J. Chatt and P. Chini, *J. Chem. Soc. A*, (1970), 1538.
2. A. Albinati, *Inorg. Chim. Acta*, (1977), **22**, L3.
3. A. Albinati, G. Cartman and A. Musco, *Inorg. Chim. Acta*, (1976), **16**, L3.
4. R.G.Vranka, L.F. Dahl, P. Chini and J. Chatt, *J. Am. Chem. Soc.*, (1969), **91**, 1574.
5. A.A. Frew, R.H. Hill, Lj. Manojlovic-Muir, K.W. Muir and R.J. Puddephatt, *J. Chem. Soc., Chem. Commun.*, (1982), 198.
6. A. Moor, P.S. Pregosin, L.M. Veranzi and A.J. Welch, *Inorg. Chim. Acta*, (1984), **85**, 103.
7. J.P. Barbier, R. Bender, P. Braunstein, J. Fischer and L. Ricard, *J. Chem. Res.*, (1978), (S) 230; (M) 2913.
8. R. Bender, P. Braunstein, J. Fischer, L. Ricard and A. Mitschler, *Nouv. J. Chim.*, (1981), **5**, 81.
9. D.G. Evans, M.F. Hallam, D.M.P. Mingos and W.M. Wardle, *J. Chem. Soc., Dalton Trans.*, (1987), 1889.
10. C.S. Browning, D.H. Farrar, R. Gukathasan and S.A. Morris, *Organometallics*, (1985), **4**, 1750.
11. D.M.P. Mingos and W.M. Wardle, *Transition Met. Chem.*, (1985), **10**, 441.
12. N.K. Eremenko, E.G. Mednikov and S.S. Kurasov, *Russ. Chem. Rev.*, (1985), **54**, 394.
13. D.M.P. Mingos, I.D Williams and M.J. Watson, *J. Chem. Soc., Dalton Trans.*, (1988), 1509.

14. E.L. Meutterties, T.N. Rhodin, E. Baird, C.F. Brucker and W.R. Pretzer, *Chem. Rev.*, (1979),**79**, 91.

15. B.R. Lloyd, A.M. Bradford and R.J. Puddephatt, *Organometallics*, (1987), **6**, 424.

16. G. Ferguson, B.R. Lloyd, Lj. Manojlovic-Muir, K.W. Muir and R.J. Puddephatt, *Inorg. Chem.*, (1986), **25**, 41900.

17. M.C. Jennings and R.J. Puddephatt, *Inorg. Chem.*, (1988), **27**, 4280.

18. M.C. Jennings, Lj. Manojlovic-Muir, K.W. Muir and R.J. Puddephatt, *J. Chem. Soc., Chem. Commun.*, (1989), in press.

19. C. Mealli, *J. Am. Chem. Soc.*, (1985), **107**, 2245.

20. D.G. Evans, *J. Organomet. Chem.*, (1988), **352**, 397.

21. G. Ferguson, B.R. Lloyd and R.J. Puddephatt, *Organometallics*, (1986), **5**, 344.

22. M.C. Jennings, Lj. Manojlovic-Muir and R.J. Puddephatt, *J. Am. Chem. Soc.*, (1989), **111**, 745.

23. G.E. Mitchell, M.A. Henderson and M. A. White, *Surf. Sci.*, (1987), **191**, 425. M.D. Alvey and J. Yates, *J. Am. Chem. Soc.*, (1988), **110**, 1782.

24. A.M. Bradford, M.C. Jennings and R.J.Puddephatt, *Organometallics*, (1988), **7**, 792.

25. S.S.M. Ling, N. Hadj-Bagheri, Lj. Manojlovic-Muir, K.W. Muir and R.J. Puddephatt, *Inorg. Chem.*, (1987), **26**, 231.

26. Q.-B. Bao, S.J. Geib, A.L. Rheingold and T.B. Brill, *Inorg. Chem.*, (1987), **26**, 3453.

27. R.J. Blau, J.H. Espensen, S. Kim and R.A. Jacobson, *Inorg. Chem.*, (1986), **25**, 757.

28. A transition state with a μ_2-PR_3 group is also possible, but is considered to be less likely because steric hindrance would be greater.

29. D.H. Farrar and J.A. Lunniss, *J. Chem. Soc., Dalton Trans.*, (1987), 1249.

30. R.F. Alex and R.K. Pomeroy, *Organometallics*, (1987), **6**, 2437.

31. M.R. Shaffer and J.B. Keister, *Organometallics*, (1986), **5**, 561.

32. K.A. Sutin, J.W. Kolis, M. Mlekuz, P. Bougeard, B.G. Sayer, M.A. Quilliam, R. Faggiani, C.J.L. Lock, M.J. McGlinchey and G. Jaouen, *Organometallics*, (1987), **6**, 439.

33. P.A.W. Dean, J.J. Vittal and R.S. Srivastava, *Canad. J. Chem.*, (1987), **65**, 2628.

34. A.M. Bradford and R.J. Puddephatt, *New J. Chem.*, (1988), **12**, 427.

CHAPTER 4

NEW 46 ELECTRON CLUSTERS: THE REACTION OF $[Pt_3(\mu_3\text{-}CO)(\mu\text{-}dppm)_3]^{2+}$ WITH BIDENTATE PHOSPHORUS AND SULPHUR-CONTAINING LIGANDS

4.1 INTRODUCTION

The idea that two metals kept in close proximity could react cooperatively with substrate molecules has led to a very wide development of ligand systems able to lock together 2 metals in such a position.[1-5] This is especially true of diphosphines with the general formula $R_2P(CH_2)_nPR_2$. Of such ligands those containing only one central atom (n= 1) such as dppm ($Ph_2PCH_2PPh_2$) and dmpm ($Me_2PCH_2PMe_2$) are very efficient bridging ligands as a result of their ability to form closed (in the case of metal-metal bonded species) or open five membered rings.[6,7] The metal-phosphorus bonds formed in such systems are very strong and bridging diphosphines are effectively able to lock together 2 metal centres to prevent dissociation from dimer to monomer, to promote bridging by other groups and to promote binuclear reactions involving the cleavage and formation of metal-metal bonds. Such reactions are invoked in heterogeneous catalysis using binuclear or cluster complexes.

The dithiocarbamates ($S_2CNR_2^-$), and the carbon disulphide adducts of the tertiary phosphines (PR_3CS_2), are also able to act as bridging ligands. Bridging dithiocarbamate ligands can have several forms (Figure 4.1).

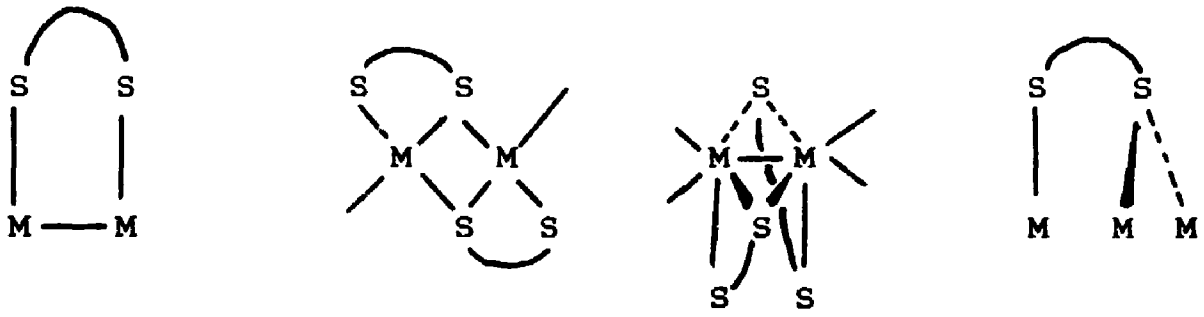

FIGURE 4.1:[8] Bridging Dithiocarbamate Ligands

It has been previously established that monodentate phosphorus and sulphur-containing ligands react readily with $[Pt_3(\mu_3\text{-}CO)(\mu\text{-}dppm)_3]^{2+}$, 1,[8-11] and the investigation of its reactions with bidentates was of interest to see whether the ligands add at terminal or bridging sites, how ligand addition affects the $Pt_3(\mu_3\text{-}CO)$ linkage and in whether steric or electronic factors influence the fluxionality of the product clusters. The complex $[Pt_3(\mu\text{-}CO)(\mu\text{-}dmpm)_4][BPh_4]_2$, 2, has been previously reported by our group and it is also of interest to compare the structures of the clusters reported in this chapter with that of 2.[12]

4.2 RESULTS

4.2.1 Formation of the Complexes

$[Pt_3(\mu\text{-}CO)(\mu\text{-}dppm)_3L_2]^{(2+n)+}$

The major chemical results are shown in Scheme 4.1.

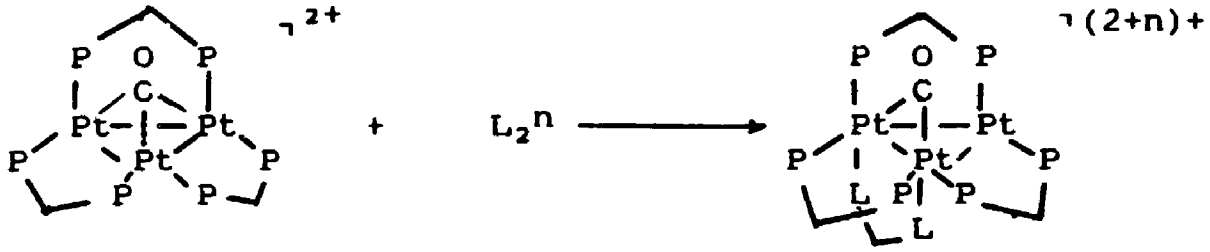

1

3a: $L_2=Me_2NCS_2$ n=-1
3b: $L_2=Et_2NCS_2$ n=-1
3c: $L_2=Et_3PCS_2$ n=0
3d: $L_2=(C_6H_{11})_3PCS_2$ n=0
3e: $L_2=Me_2PCH_2PMe_2$ n=0
3f: $L_2=Ph_2PCH_2PPh_2$ n=0

Scheme 4.1

As monitored by $^{31}P\{^1H\}$ NMR spectroscopy, the reaction of $[Pt_3(\mu_3\text{-}CO)(\mu\text{-}dppm)_3]^{2+}$, 1, with dimethyl and diethyldithiocarbamate, triethyl and tricyclohexylphosphine carbon disulphide, and bis(dimethylphosphino)methane gave the corresponding complexes 3a-3e, respectively in 93% yield. These complexes were thermally stable and could be isolated in analytically pure form as the hexafluorophosphate salts. Reaction of 1 with the bulkier dppm ligand yielded an equilibrium between 1, free dppm and 3f. Pure 3f could be isolated as a black solid by crystallization at low temperature in the presence of

excess dppm, and by separating the black crystals of 3f by hand from the red crystals of 1 which also formed.

4.2.2 The Structure of $[Pt_3(\mu_3\text{-}CO)(\mu\text{-}dppm)_3(\mu\text{-}S_2CNMe_2)][PF_6]\cdot Me_2CO$

The structure of complex 3a was solved by Drs. Muir and Manojlovic-Muir of the University of Glasgow. The complex cation contains an isosceles triangle of platinum atoms with a dppm ligand bridging each edge of the triangle (Figure 4.2). The Pt(1)-Pt(3) bond is further supported by bridging carbonyl and dimethyldithiocarbamate ligands on opposite sides of the triangle. The Pt_2P_2C atoms of each $Pt_2(\mu$-dppm) unit adopt an envelope conformation with the methylene groups C(2) and C(3) bent towards the bridging dimethyldithiocarbamate ligand. This conformation serves to direct the phenyl groups attached to these carbon atoms away from the dimethyldithiocarbamate, thus minimizing steric hindrance.

The Pt(2) centre differs both sterically and electronically from Pt(1) and Pt(3). This difference has little influence however on the Pt-Pt bond lengths in that the Pt(1)-Pt(3) distance of 2.622(1) Å is only marginally longer than the effectively equal Pt(1)-Pt(2) and Pt(2)-Pt(3) distances of 2.612(1) and 2.605(1) Å, respectively. It is particularly interesting to note that the mean Pt-Pt bond length of 2.613(1) Å in this 46 electron cluster is significantly shorter than the

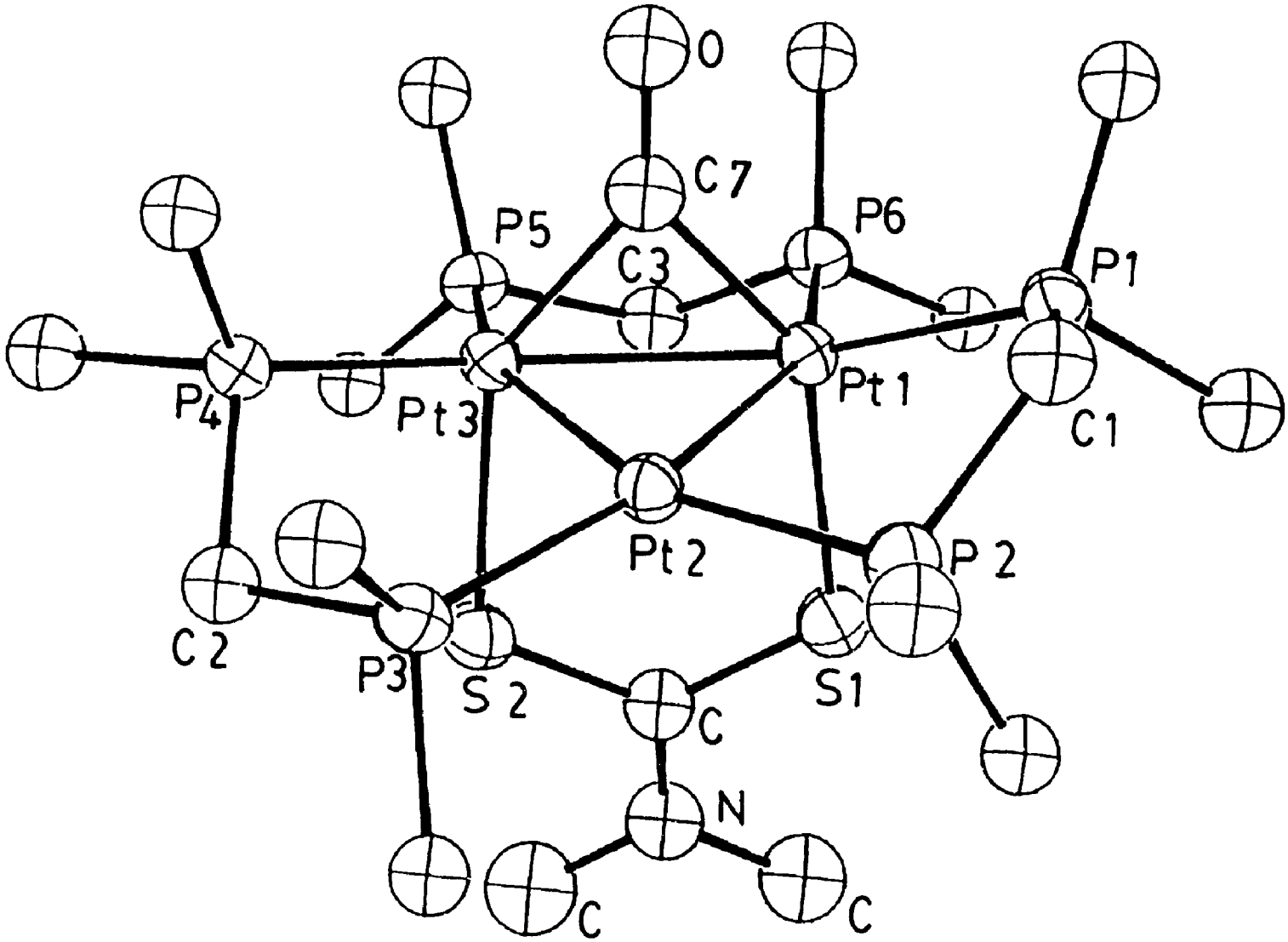

FIGURE 4.2: ORTEP Diagram of **3a**

corresponding average values of 2.634(2), 2.639(2) and 2.632(1) Å for the related 42, 44 and 46 electron clusters $[Pt_3(\mu_3\text{-}CO)(\mu\text{-}dppm)_3]^{2+}$,[13] $[Pt_3(\mu_3\text{-}CO)(\mu\text{-}dppm)_3\{P(OPh)_3\}]^{2+}$[14] and $[Pt_3(\mu\text{-}CO)(\mu\text{-}dmpm)_4]^{2+}$[12]. It seems that the extra electrons in **3a** go into π-type metal bonding orbitals as opposed to nonbonding or antibonding orbitals.

The Pt-P bond lengths display a sensitivity to their environment in that the shortest Pt-P bonds involve the four-coordinate Pt(2) atom. Next in length are Pt(1)-P(1) and Pt(3)-P(4) followed by Pt(1)-P(6) and Pt(3)-P(5). These differences could arise as a result of a rehybridization of Pt orbitals due to the higher coordination numbers of Pt(1) and Pt(3), or it could simply be the result of steric congestion at these same sites. These distances are all in the expected range for Pt-P single bonds however.

The average Pt-S distance of 2.492(4) Å in **3a** is significantly longer than that of 2.331(7) Å[15] found for $Pt_2Cl_3(PEt_3)_2(S_2CNMe_2)$ where the dithiocarbamate ligand bridges two platinum centres which are not bound to each other, and of 2.339(4) Å for $Pt(S_2CNEt_2)_2PPh_3$[16] and 2.31 Å[17] for $Pt(S_2CNEt_2)_2$ where the dithiocarbamate ligands chelate to the platinum atom. Steric factors could play a role in these lengthened Pt-S bonds. It should be mentioned at this point however that only a small number of dithiocarbamate complexes of platinum are known and that this strucutre is the first in which the dithiocarbamate

ligand bridges two platinum centres with a metal-metal bond. The ligand Pt-S bond lengths could therefore also be characteristic of this type of structure.

The carbonyl ligand of **3a** bridges Pt(1) and Pt(3) with Pt–C distances of 2.01(1) Å. The corresponding distance for the unique platinum, Pt(2), is 2.67(1) Å and does not indicate any interaction between the bridging carbonyl and this platinum atom. It is interesting to compare this geometry to that of $[Pt_3(\mu\text{-CO})(\mu\text{-dmpm})_4]^{2+}$, **2**, and a summary is given in Table 4.1 where the μ-dppm and dmpm ligands in the plane of the platinum triangle are ommitted for clarity. The carbonyl ligand distortion from the symmetrical μ_3-bridging mode is significant for the dmpm adduct, **2**, and is even greater for the dithiocarbamate adduct, **3a**. The slippage of the μ_3-carbonyl ligand towards the platinum atoms with the highest coordination number can be rationalized if the μ_3-CO acts to a large extent as a π-acceptor ligand and this interpretation has been expressed by Evans.[18] Such slippage has also been observed in the SCN^- and $P(OPh)_3$ adduct clusters of $[Pt_3(\mu_3\text{-CO})(\mu\text{-dppm})_3]^{2+}$, **1**.[14] The difference in the degree of CO slippage between **2** and **3a** is consistent with the fact that the sulphur atoms of the anionic dithiocarbamate ligand are better donors than the dmpm phosphorus atoms.

TABLE 4.1: A Comparison of Selected Structural and Spectroscopic Data for Some $Pt_3(\mu\text{-}CO)$ Complexes[a]

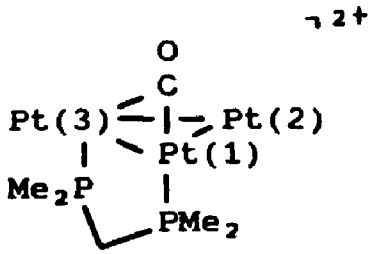

2

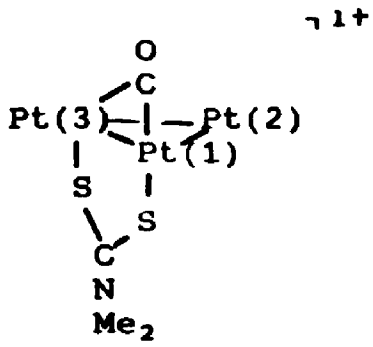

3a

Complex	2	3a
Pt(1)-Pt(2)/(Å)	2.628(1)	2.612(1)
Pt(1)-Pt(3)/(Å)	2.648(1)	2.622(1)
Pt(2)-Pt(3)/(Å)	2.620(1)	2.605(1)
Pt(1)-C(4)/(Å)	2.049(8)	2.01(1)
Pt(2)-C(4)/(Å)	2.43(1)	2.67(1)
Pt(3)-C(4)/(Å)	2.061(9)	2.02(1)
ν(CO)/cm^{-1}[b]	1730	1736
^1J(PtC)/Hz[c]	730	780
δ (^{13}CO)/ppm	---	207.48

[a] The dmpm and dppm ligands in the Pt_3 plane are omitted for clarity in 2 and 3a, respectively.

[b] Samples run as Nujol mulls.

[c] Solvent: Acetone-d_6.

4.2.3 Characterization of Complexes 3a-3f by Spectroscopic Methods

The values for the ν(CO) stretching frequencies ranged from 1729 to 1759 cm^{-1} (Table 4.2) . The ν(CO) value of 1729 cm^{-1} was observed for complex 3e which has a μ_2-CO ligand by analogy with complex 2. Although all frequencies are in the range expected for bridging carbonyl groups all are lower than the ν(CO) value of 1765 cm^{-1} observed for complex 1. It is possible that these lower ν(CO) values are characteristic of 46 electron clusters and are not primarily dependent of whether the $Pt_3(\mu_3$-CO) group is symmetrical or not. ν(CS) values of 1036 to 1102 cm^{-1} were observed for 3a-3d which are characteristic of C-S single bonds. This is consistent with the x-ray analysis of 3a which shows the dimethyldithiocarbamate bridging two platinum centres (Table 4.2).

All complexes with the exception of 3e were fluxional even at -90°C. Spectra were therefore obtained at room temperature in acetone-d_6 solution.

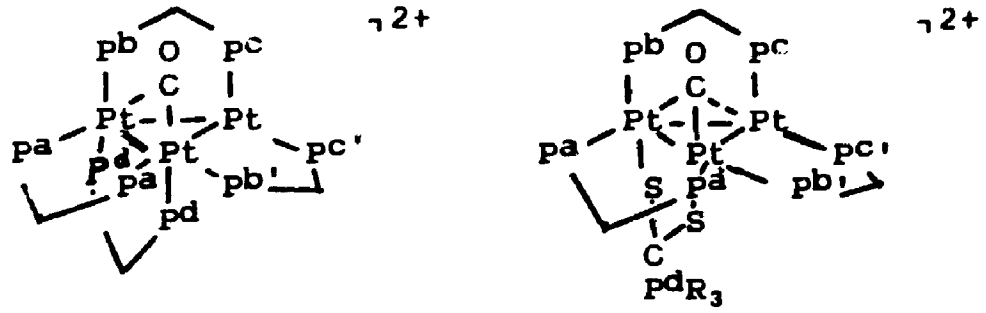

3e or 3f 3c or 3d

FIGURE 4.3: NMR Labelling Scheme

TABLE 4.2: IR Data for Complexes 3a-3f[a]

Complex	ν(CO)/cm^{-1}	ν(C3)/cm^{-1}	ν(CN)/cm^{-1}
3a	1736	1102	1588
3b	1741	1098	1564
3c	1754	1036	
3d	1752	1098	
3e	1729	--	
3f	1759	--	

[a] Samples run as Nujol mulls.

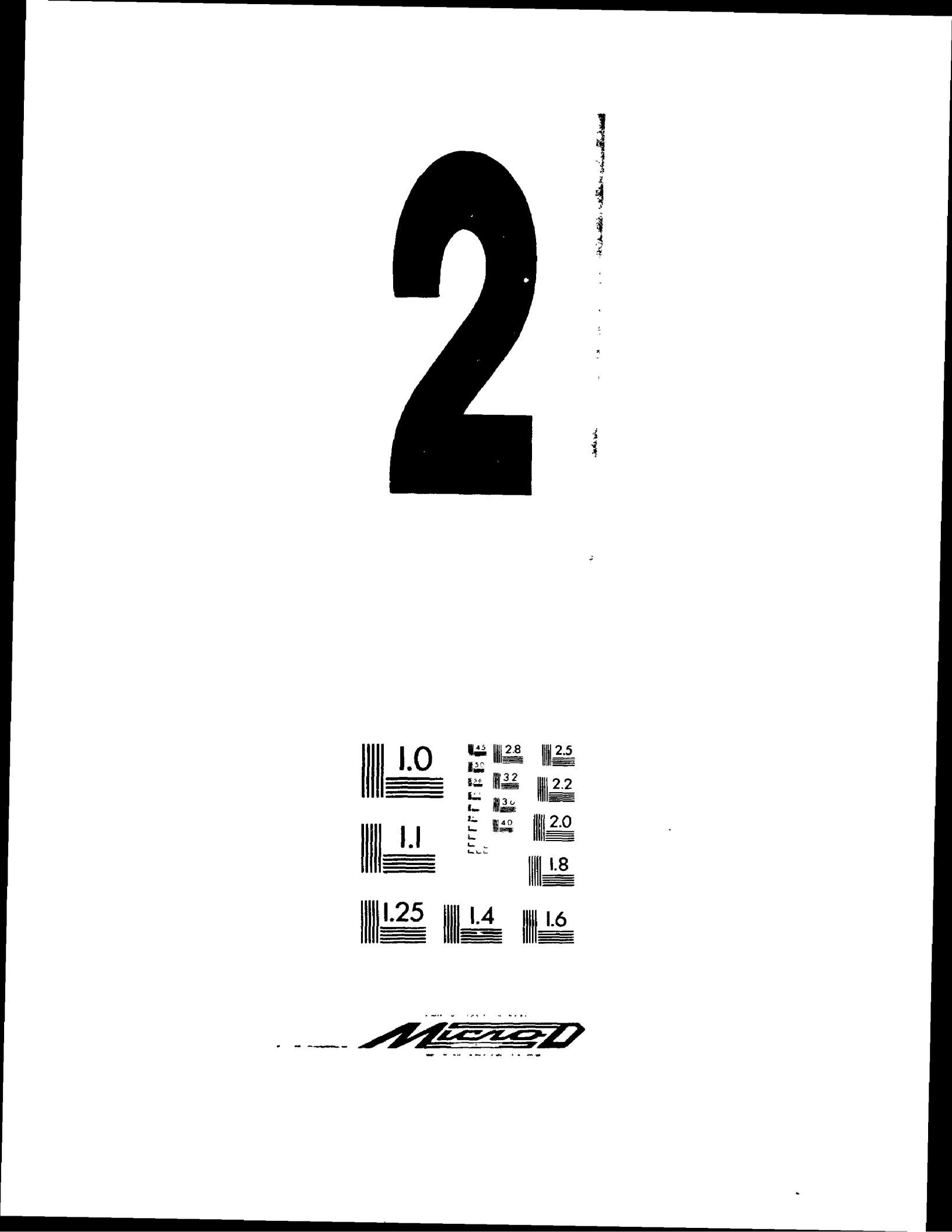
2
1.0
1.1
1.25
1.4
1.6
1.8
2.0
2.2
2.5
2.8
3.2
3.6
4.0
4.5
5.0
5.6
MicroD

A diagram outlining the assignments of the phosphorus atoms is shown in Figure 4.3.

$^{195}Pt\{^{1}H\}$ NMR spectra were obtained for complexes **3d** and **3f**. The spectrum of **3d** enriched with ^{13}CO consisted of a doublet of triplets with δ = -2435 ppm, $^{1}J(PtP^{a,b,c})$ = 3200 Hz, $^{3}J(PtP^{d})$ = 150 Hz and $^{1}J(PtC)$ = 700 Hz (Figure 4.4). The spectrum of **3f** on the other hand consisted of a broad triplet at δ = -2887 ppm with $^{1}J(PtP^{a,b,c})$ = 2800 Hz. Other couplings could not be determined due to the broadness of the resonance. The coordination of ligands with different donor atoms appears to have a large effect on the ^{195}Pt chemical shifts observed for these clusters.

The $^{31}P\{^{1}H\}$ NMR spectra of **3a-3d** contained singlet resonances with platinum satellites which appeared as doublets due to trans coupling between the dppm phosphorus atoms in the plane of the platinum triangle (Table 4.3). The J(PP) values were in the narrow range of 180 to 200 Hz. The spectra of complexes **3c** and **3d** contained another resonance at 54.4 and 48.9 ppm respectively due to the phosphorus atoms in the ligands Et_3PCS_2 and $(C_6H_{11})_3PCS_2$ (Figure 4.5). These resonances displayed the septet pattern characteristic of ligands which triply bridge three platinum centres with the intensities of the inner five lines of the septet being 1:4:7:4:1. This is a clear indication of the fluxionality of these ligands about

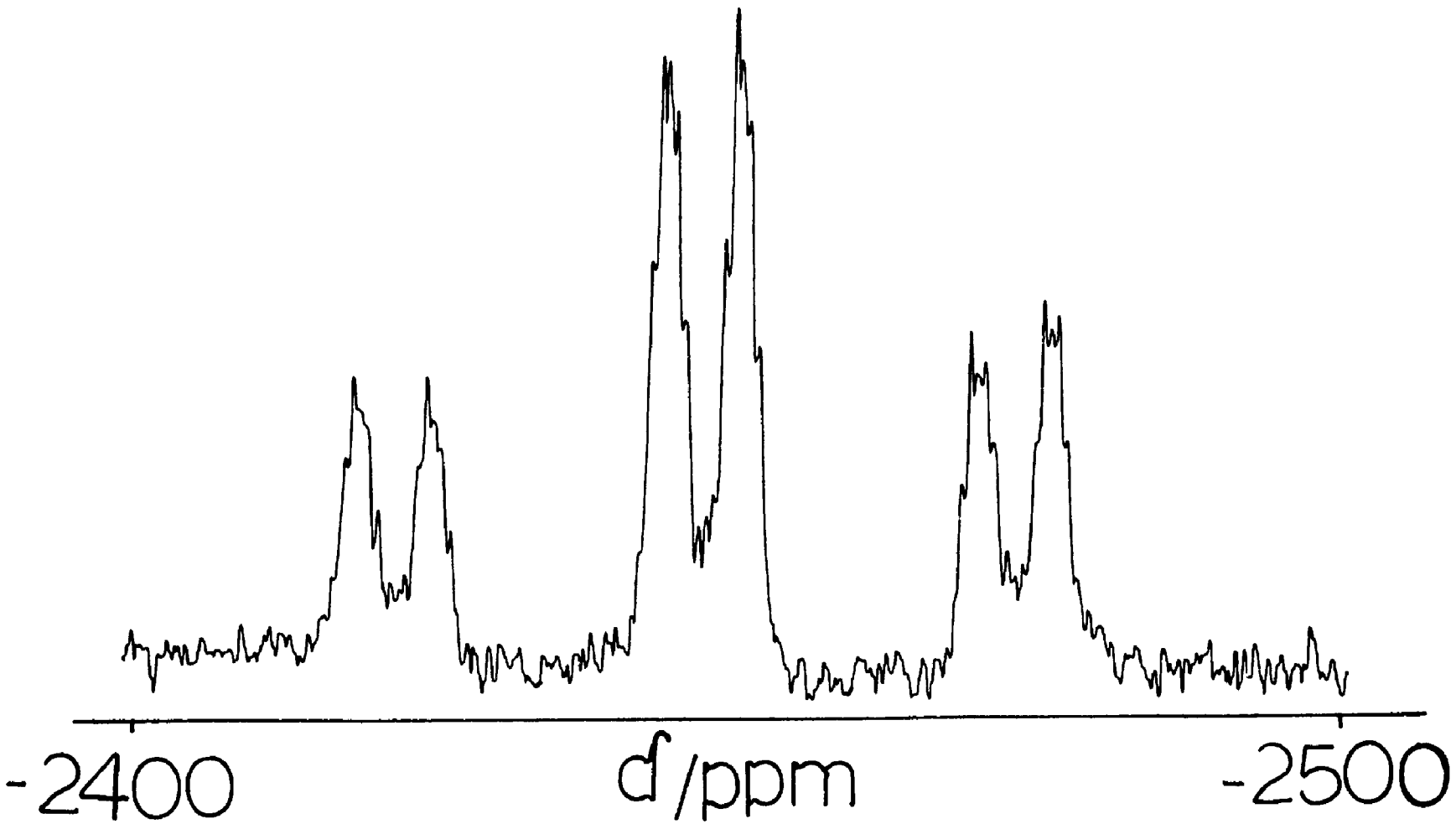

FIGURE 4.4: $^{195}Pt\{^{1}H\}$ NMR Spectrum of ^{13}C O Enriched 3d

TABLE 4.3: ^{31}P NMR Data for Complexes **3a-3d** and **3f**[a]

Complex	3a	3b	3c	3d	3f
δ P^a/ppm[b,d]	-32.1	-32.1	-26.4	-26.9	-43.2
$^1J(PtP^a)$/Hz	3280	3110	3100	3180	2900
$^2J(PtP^a)$/Hz	120	135	90	100	270
$^3J(P^aP^{a'})$/Hz	200	185	185	180	190
δ P^b/ppm[c]			54.4	48.9	-22.1
$^3J(PtP^b)$/Hz			170	156	720
$J(P^aP^b)$/Hz			0	0	0

[a] Spectra run at 20°C.

[b] Singlet resonances.

[c] Septet resonances.

[d] Ref. is H_3PO_4.

FIGURE 4.5: $^{31}P\{^{1}H\}$ NMR Spectrum of **3d**

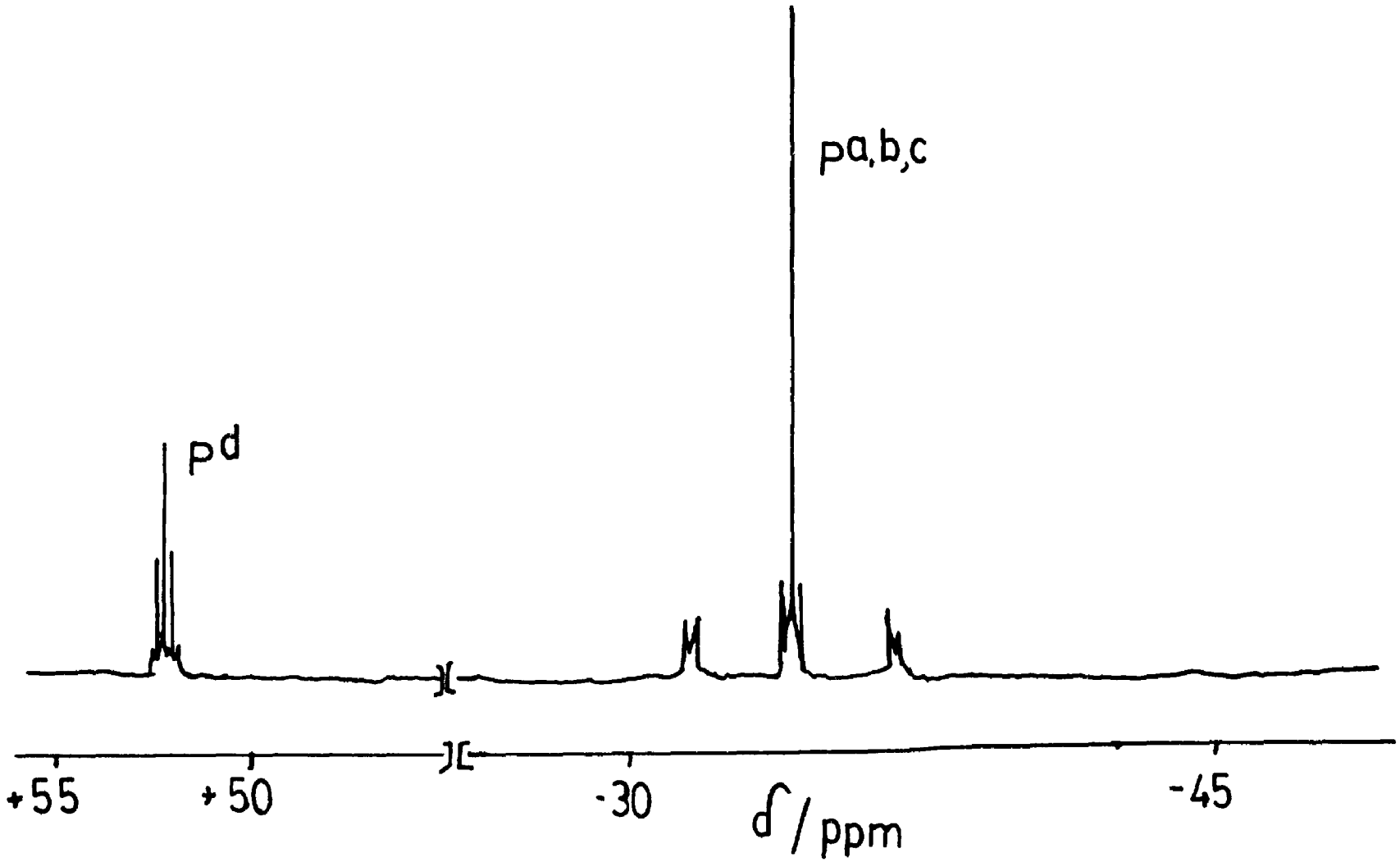

the triplatinum centres of 3c and 3d. $^{3}J(PtP^{d})$ in these clusters was found to be 170 and 166 Hz respectively.

Complex 3f was also fluxional, with the $^{31}P\{^{1}H\}$ NMR spectrum consisting of two resonances in a 3:1 intensity ratio: one due to $P^{a}P^{b}$ and P^{c} and the other due to P^{d} of the additional dppm ligand. The resonance due to P^{d} is particularly interesting in that it appears as a septet with the two outer resonances being too small to be observed. The observed $^{1}J(PtP)$ value for this resonance is 720 Hz. The true value for $^{1}J(PtP)$ however is 3 X 720 = 2160 Hz which is close to the $^{1}J(PtP^{d})$ value of 2592 Hz found for 2. Aspects of this unusual fluxionality of a dppm ligand of a triplatinum cluster have been reported in the chemical literature[19] and will be discussed in more detail later in this chapter.

Complex 3e was the only nonfluxional complex of those studied. The $^{31}P\{^{1}H\}$ NMR spectrum of 3e consisted of four resonances of approximately equal intensity (Table 4.4). Of these resonances two were doublets with platinum satellites and large $^{3}J(PP)$ couplings of 215 Hz. The platinum satellites of the singlet resonances were doublets with $^{3}J(PP)$ = 205 Hz (Figure 4.6). The structure of complex 3e is analogous to 2 and on the basis of this and the fact that the largest J(PP) coupling is the trans coupling through the Pt-Pt bonds the singlet resonances were assigned to P^{b} and P^{d} while the doublet resonances were assigned to P^{a} and P^{c}. The first doublet at -25.5 ppm

FIGURE 4.6: $^{31}P\{^{1}H\}$ NMR Spectrum of 3c

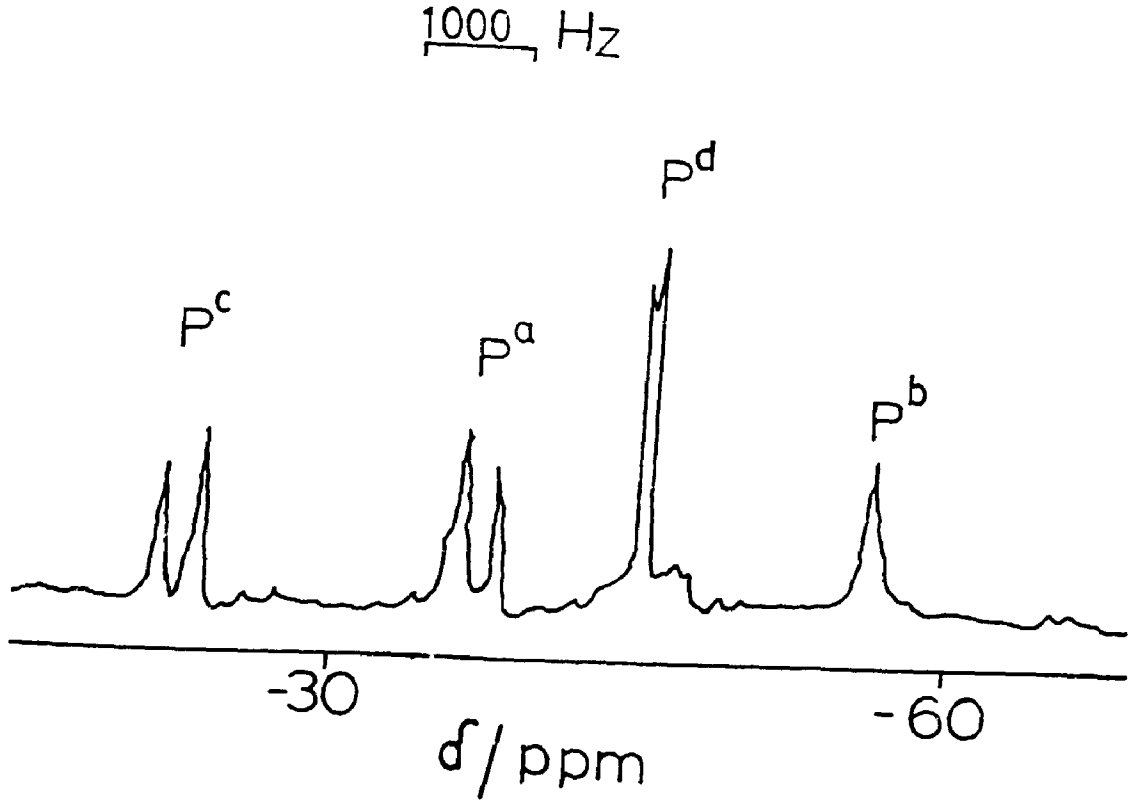

TABLE 4.4: ^{31}P NMR Data for Complex 3e[a]

Complex	3e
δ P^a/ppm[b,c]	-25.5
$^1J(PtP^a)$/Hz	3265
$^3J(P^aP^c)$/Hz	215
δ P^b/ppm[d]	-61.5
$^1J(PtP^b)$/Hz	3060
$^3J(P^bP^{b'})$/Hz	205
δ P^c/ppm[c]	-39.0
$^1J(PtP^c)$/Hz	2140
$^3J(P^aP^c)$/Hz	215
δ P^d/ppm[d]	-46.0
$^1J(PtP^d)$Hz	2070
$^3J(PP)$/Hz	205

[a] Spectrum run at 20°C.

[b] Ref. is H_3PO_4.

[c] Doublet resonance.

[d] Singlet resonance.

was assigned to P^a while the second at -39.0 ppm was assigned to P^c. The singlet resonance at -61.5 ppm was assigned to P^b and the one at -46.0 ppm was assigned to P^d. These assignments were made on the basis of the structure of complex **2**.

The $^{13}C\{^1H\}$ NMR spectra for the fluxional clusters **3a-3d** and **3f** enriched with ^{13}CO consisted of septet resonances with chemical shifts ranging from 207.48 to 215.78 ppm and $^1J(PtC)$ values ranging from 680 to 780 Hz (Table 4.5 and Figure 4.7). These parameters can be compared with those observed for the static cluster **3e** where $\delta(^{13}CO)$ = 219.12 ppm and $^1J(PtC)$ = 793 Hz. This cluster has a μ_2-CO by analogy with complex **2** as does **3f**. It is interesting to note that while the chemical shifts for these carbonyl resonances are all in the range expected for bridging carbonyls, the $^1J(PtC)$ values for clusters **3a-3d** and **3f** are significantly lower than that of **3e** with the doubly bridging carbonyl, possibly indicating the presence of a certain degree of asymmetry in the μ_3-CO ligand. The differences in chemical shift values and coupling constants between μ_2-CO groups and asymmetric μ_3-CO groups does not appear to be large and no definitve range of values can be given for either parameter.

The ^1H NMR spectra of each of **3a-3d** and **3f** contained AB quartets due to the methylene protons of the μ-dppm ligands in the plane of the platinum triangle. This inequivalence is generated by the presence of a bridging

FIGURE 4.7: $^{13}C\{^{1}H\}$ NMR Spectrum of 3a

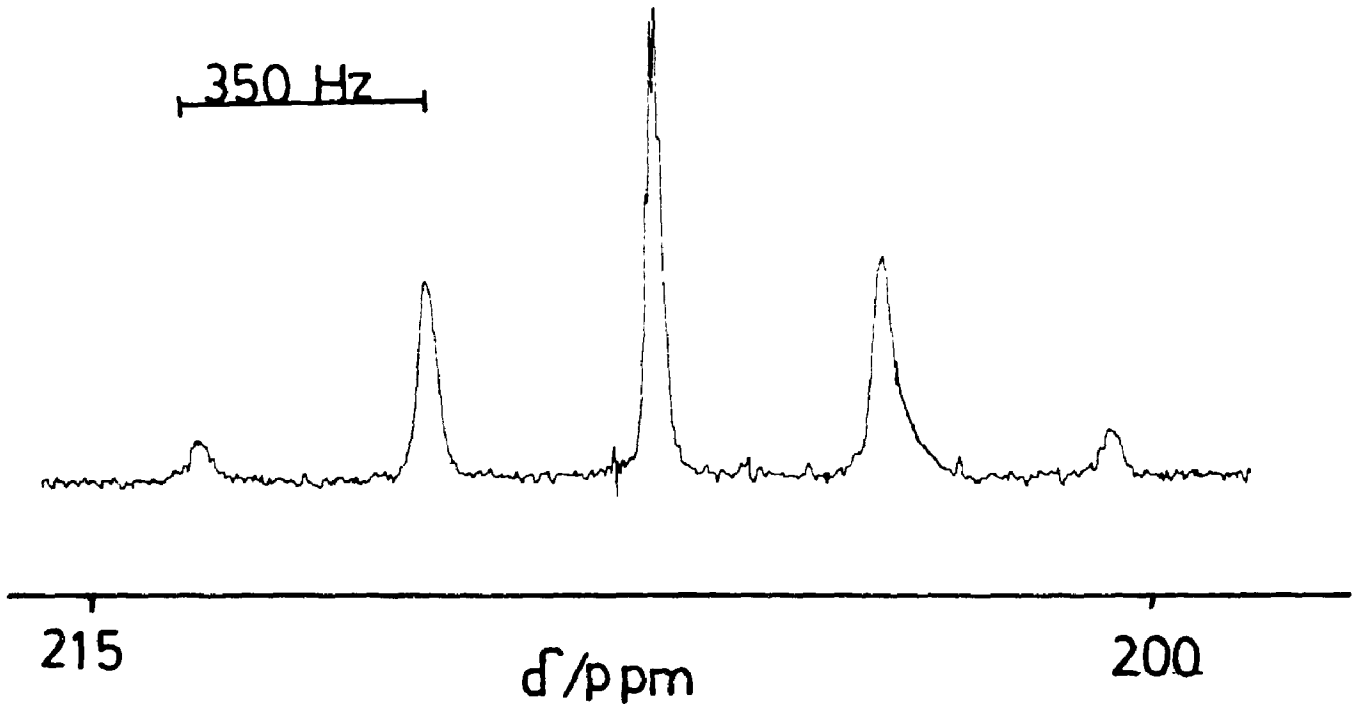

TABLE 4.5: ^{13}C NMR Data for Complexes **3a-3f**

Complex	δ ^{13}CO (ppm)	$^{1}J_{(PtC)}$ (Hz)	$^{2}J_{(P^aC)}$ (Hz)[a]	$^{2}J_{(P^bC)}$ (Hz)[b]
3a	207.48	780	9	--
3b	--	--	-	--
3c	211.92	760	-	--
3d	213.10	745	-	--
3e[c]	219.12	793	-	--
3f	215.75	680	-	--

[a] P^a refers to the dppm phosphorus atoms in the plane of the platinum triangle.

[b] P^b refers to the phosphorus atoms perpendicular to the platinum triangle.

[c] The only nonfluxional cluster.

carbonyl on one side of the platinum triangle and another ligand on the other side. For complex 3f the resonance due to the methylene protons on the dppm ligand below the plane of the triangle is obscured by those on the dppm ligands in the plane.

Other resonances due to the protons on the various alkyl groups of the dithiocarbamate and trialkylphosphine carbon disulphide ligands are observed in the expected regions with the appropriate splitting patterns due to coupling (Experimental Section).

The ^{1}H NMR spectrum of 3e is very complex and did not provide any useful structural information.

4.2.4 Fluxionality of Complexes 3a-3d and 3f

The clusters 3a-3d and 3f were fluxional in the sense that the added ligands could migrate around the triangular face of the platinum cluster.[19] This is a new form of fluxionality, especially for the bidentate dppm ligand below the plane of the platinum triangle in 3f, although related fluxionality of a diphosphine ligand has been reported.[20,21] As has been mentioned earlier, the thermodynamic parameters for the formation of 3f were obtained by measuring the equilibrium constant using $^{31}P\{^{1}H\}$ NMR at temperatures from 20 to -28°C were $\Delta H^{\circ} = -55 \pm 10$ kJ mol^{-1} and $\Delta S^{\circ} = -145 \pm 50$ JK^{-1} mol^{-1}. The ΔG° values were -12.5 kJ mol^{-1} (20°C), -15.9 kJ mol^{-1} (3°C), -17.3 kJ mol^{-1} (-13°C) and -19.5 kJ mol^{-1} (-28°C).

The mechanism of fluxionality is likely to occur as shown in 4.1 involving an intermediate with a monodentate dppm, although a concerted phosphorus shift is also possible.

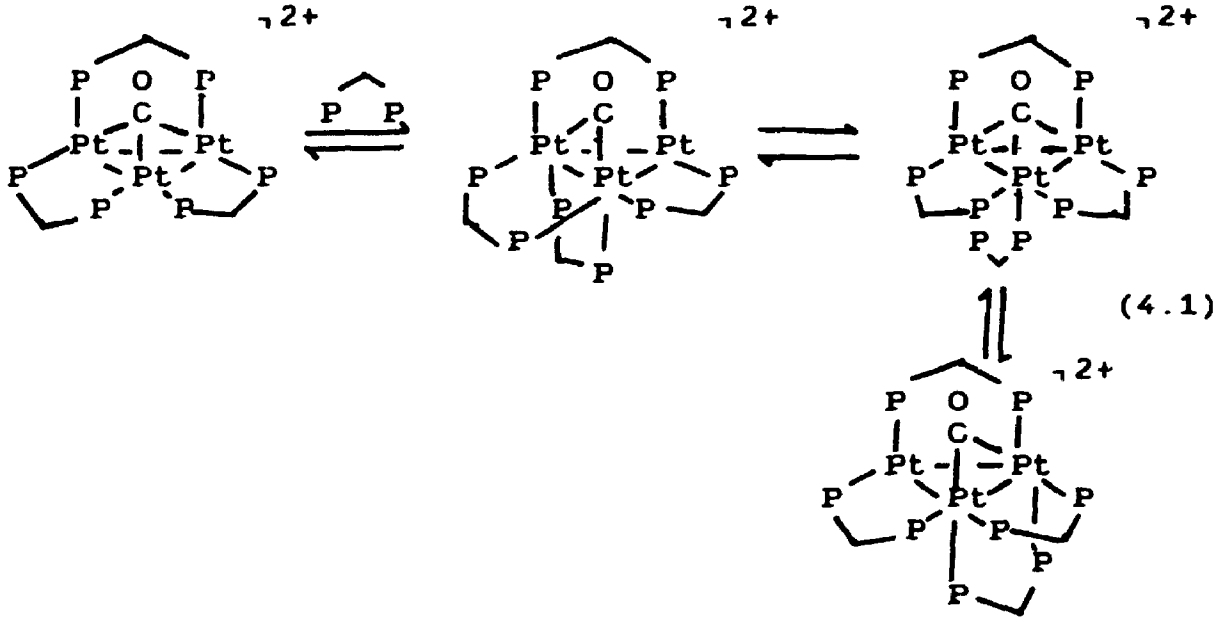

(4.1)

Complete fluxionality must include the six contributing species shown in 4.2 in simplified form.

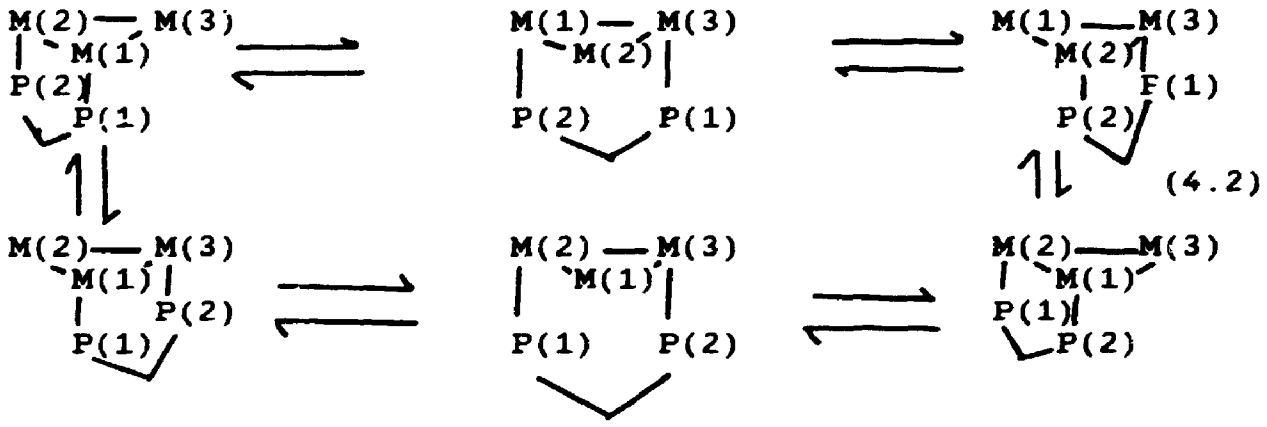

(4.2)

TABLE 4.6: ^{31}P NMR Data for Complex 3f at -124°C

δ ^{31}P (ppm)[a,c]	$^{1}J_{(PtP)}$ (Hz)	$^{3}J_{(PP)}$ (Hz)[c]
-8.81	2440	220
-34.23[b]	3160	--
-36.22	2180	208
-38.04	3008	240
-40.03	--	--
-51.12	3560	220
-54.10	1520	220
-78.66	2920	200
-32.28[d]	--	--

[a] Ref. is H_3PO_4.

[b] Singlet resonance. All other resonances are doublets.

[c] Solvent is Acetone-d_6/$CHCl_2F$.

[d] Due to free dppm.

A mechanism of fluxionality involving complete dissociation of dppm is precluded by the NMR data. Such a mechanism which clearly can occur, although slowly on the NMR time scale, would lead to a coalescence of resonances due to P^d and free dppm in addition to a loss of $J(PtP^d)$ coupling. It is clear that the type of fluxionality shown in Equations 4.1 and 4.2 is possible only for coordinatively unsaturated clusters and we know of no precedents.

The fluxionality of the added dppm ligand in **3f** could be frozen out at -124°C using a mixture of acetone-d_6 and $CHCl_2F$ as solvent (Table 4.6). Eight sets of resonances were observed in addition to a singlet due to free dppm in solution. Unambiguous assignments of the eight sets of resonances could not be made but it seems that steric interactions in $[Pt_3(\mu_3\text{-}CO)(\mu\text{-dppm})_4]^{2+}$, **3f**, are great enough to render each of the dppm phosphorus atoms inequivalent giving eight sets of resonances instead of four.

4.3 DISCUSSION

Thermodynamic parameters for the formation of **3f**, obtained by measuring the equilibrium constant using $^{31}P\{^1H\}$ NMR at temperatures from 20 to -28°C, were $\Delta H° = -55 \pm 10$ kJ mol^{-1} and $\Delta S° = -145 \pm 50$ JK^{-1} mol^{-1}. Hence the enthalpy term favours complex formation while the entropy term does not.

The $^{31}P\{^{1}H\}$ NMR experiment showed that exchange between free and coordinated dppm occurred rapidly at room temperature. Similar exchange between free and coordinated dmpm in **3e** did not occur rapidly on the NMR time scale. The ligand exchange with dppm almost certainly occurs by a dissociative mechanism.

This work has shown that diphosphine and disulphide ligands add to **1** as ligands which bridge adjacent metal sites and that this ligand addition leads to a slippage of the μ_3-carbonyl ligand towards the platinum atoms with the highest coordination numbers in complexes **3**. According to extended Huckel molecular orbital (EHMO) calculations the platinum acceptor orbital is a $5d_z^2 6_{pz}$ hybrid orbital and enhanced backbonding can then be understood in terms of the bonding interactions shown in Figure 4.8. This interaction might be expected to lead to a lower value of ν(CO) in **3** compared to **1** which is exactly what is observed (Table 4.2). The slip distortion towards a μ_2-coordination mode observed for complexes **3** should also occur for the 46 electron cluster $[Pt_3(\mu_3\text{-}CO)(\mu\text{-}dppm)_3(CO)_2]^{2+}$, to give $[Pt_3(\mu_2\text{-}CO)(\mu\text{-}dppm)_3(CO)_2]^{2+}$,[18] since this form is 0.2 eV more stable than the triply bridged isomer according to EHMO calculations.

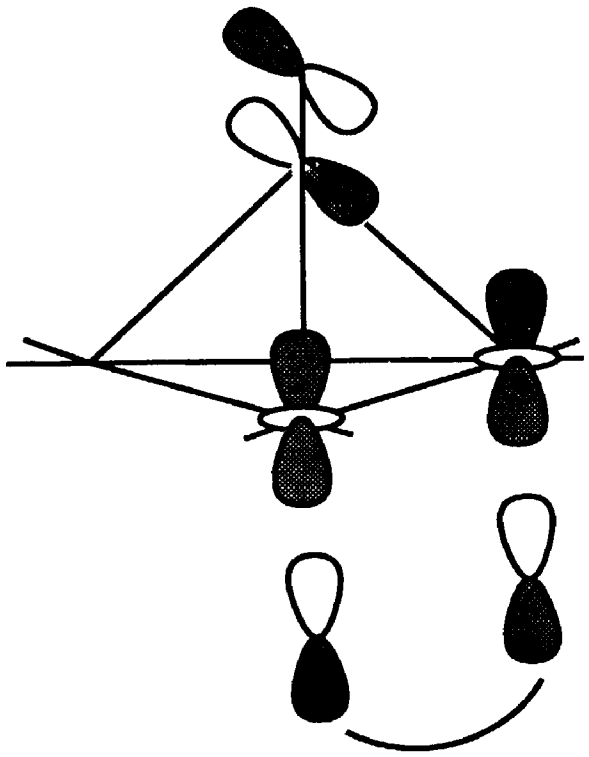

FIGURE 4.8: Bonding Interactions for Complexes **3a-3f**

4.4 CONCLUSIONS

All ligands examined in this chapter are 4 electron donors which add to complex **1** to give isolable 46 electron clusters. Ligand addition occurs to adjacent metal centres due to the formation of highly stable 5-membered rings as the ligands bridge 2 metal centres bound to each other. The observed fluxionality of complexes **3a-3d** and complex **3f**

is due to the coordinative unsaturation of the triplatinum cluster in addition to the steric and electronic properties of the added ligand. These properties can be altered by varying the substituents on the phosphorus atoms of the diphosphine ligands . It is interesting to note that while complex **2** is static the dppm analogue, **3f**, is highly fluxional. Complex **3e**, with a dmpm ligand below the plane of the platinum triangle, is also static. The fluxionality observed in **3f** may be due to the steric strain caused by the addition of a fourth dppm ligand to this cluster. $^{13}C\{^{1}H\}$ NMR data however does not rule out the possibility that there may also be some degree of asymmetry associated with the carbonyl group of complex **3f** in that the $^{1}J(PtC)$ value is significantly lower than that for both **2** and **3e** which do not exhibit fluxionality and have μ_2-CO groups. This would be consistent with the fact that we know that the dppm phosphorus atoms are poorer donors than the dmpm phosphorus atoms and could possibly result in the formation of an asymmetric μ_3-CO group. Such groups would serve to lower the activation energy for fluxionality. Just how much an asymmetric μ_3-CO group would contribute to the fluxionality observed for **3f** as opposed to steric factors is difficult to determine. It is obvious however that the fluxionality observed for complexes **3a-3d** can be accounted for by the presence of such groups.

4.5 REFERENCES

1. E.L. Meutterties, *Bull. Soc. Chim. Belg.*, (1975), **84**, 959.
2. R. Poilblanc, *J. Organomet. Chem.*, (1975), **94**, 241.
3. R. Poilblanc, *Nouv. J. Chim.*, (1978), **2**, 145.
4. E.L. Meutterties and J. Stein, *J. Chem. Rev.*, (1979), **79**,479.
5. J.P. Collman, R.K. Rothrock, R.G. Finke and E.J. Rose Munch, *Inorg. Chem.*, (1982), **21**, 146.
6. B. Chaudret, B. Delavaux and R. Poilblanc, *Coordination Chemistry Reviews*, (1988), **86**, 191.
7. R.J. Puddephatt, *Chem. Soc. Rev.*, (1983), **99**, 1 and references therein.
8. F.A. Cotton and G. Wilkinson, *Advanced Inorganic Chemistry*, Wiley-Interscience: New York, 1980. 4th Ed.
9. A.M. Bradford, M.C. Jennings and R.J. Puddephatt, *Organometallics*, (1988), **7**, 792.
10. G. Ferguson, B.R. Lloyd, Lj. Manojlovic-Muir, K.W. Muir and R.J. Puddephatt, *Inorg. Chem.*, (1986), **25**, 4190.
11. M.C. Jennings, N.C. Payne and R.J. Puddephatt, *Inorg. Chem.*, (1987), **26**, 3776.
12. S.S. Ling, N. Hadj-Bagheri, Lj. Manojlovic-Muir, K.W. Muir and R.J. Puddephatt, *Inorg. Chem.*, (1987), **26**, 231.

13. G. Ferguson, B.R. Lloyd and R.J. Puddephatt, *Organometallics*, (1986), **5**, 344.

14. A.M. Bradford, G. Douglas, Lj. Manojlovic-Muir, K.W. Muir and R.J. Puddephatt, Submitted for publication.

15. A.B. Goel, S.Goel, D. Van Derveer and C.G. Brinkley, *Inorg. Chim Acta.*, (1982), **64**, L173.

16. J.P. Fackler Jr., L.D. Thompson, I.J.B. Lin, T.A. Stephenson, R.O. Gould, J.M.C. Alison and A.J.F. Fraser, *Inorg. Chem.*, (1982), **21**, 2397.

17. D. Coucouvanis, *Progress in Inorganic Chemistry*, (1970), **11**, 233.

18. D.G.Evans, *J. Organomet. Chem.*, (1988), **352**, 397.

19. A.M. Bradford and R.J. Puddephatt, *New J. Chem.*, (1988), **12**, 427.

20. K.A. Sutin, J.W. Kolis, M. Mlekuz, P. Bougeard, B.G. Sayer, M.A. Quilliam, R. Faggiani, C.J.L. Lock, M.J. McGlinchey and G. Jaouen, *Organometallics*, (1987), **6**, 439.

21. B.R. Lloyd, A.M. Bradford and R.J. Puddephatt, *Organometallics*, (1987), **6**, 424.

CHAPTER 5

PLATINUM-MONOISOCYANIDE CLUSTERS: THE REACTION OF $[Pt_3(\mu_3\text{-}CO)(\mu\text{-}dppm)_3]^{2+}$ WITH ONE MOLAR EQUIVALENT OF ISOCYANIDE

5.1 INTRODUCTION

While much work has been done on the reactivity of carbon monoxide with metal clusters and surfaces,[1-3] relatively little attention has been paid to the isocyanides, CNR, which are isoelectronic with CO. Isocyanide bonds to metal centres have two essential components: a σ component involving donation of the lone pair of electrons on carbon to the metal, and a π component in which the electron density of the metal is transferred to the π^* orbitals of the ligand.[4,5]

Valence-bond pictures for isocyanides and carbon monoxide, as well as for metal complexes of these ligands, emphasize the similarities of both the ligands and their complexes

There are, however, important differences between

isocyanides and CO. Metal-isocyanide complexes with the metal in a low oxidation state (0, -1) are uncommon while a large variety of analogous metal carbonyl complexes are known. In contrast, isocyanide complexes of metals with higher oxidation states (+1, +2) are reasonably common compared to the analogous CO species. Isocyanides are better σ-donor ligands than CO and are, therefore, better able to stabilize high oxidation state complexes.[3]

Several bonding modes have been observed for isocyanides bound to metal atoms. Some of these are illustrated in Figure 5.1 and a few representative examples will be discussed.

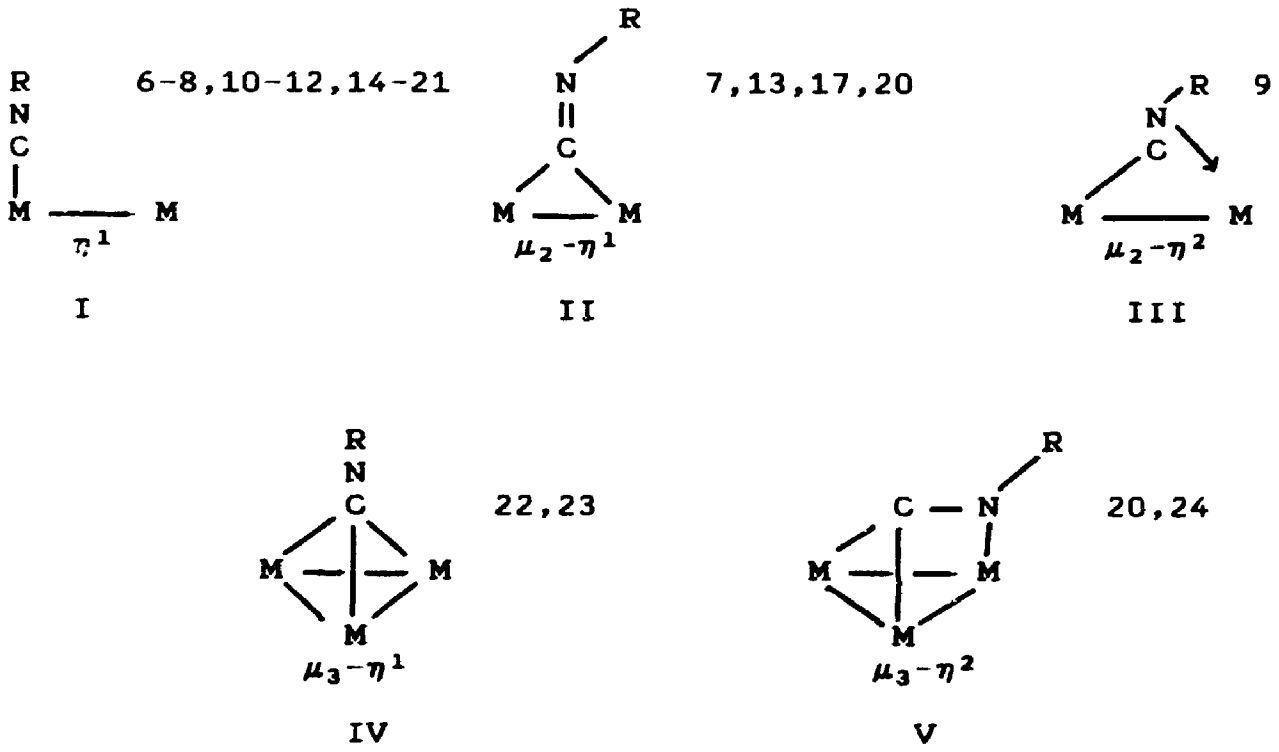

FIGURE 5.1: Bonding Modes of Isocyanides

Molecular examples of the type V interaction have only been observed in a few instances. The complex $[Ni_4\{CNC(CH_3)_3\}_7]$[24] has three μ_2-η^2 bridging isocyanides, each of which acts as a four electron donor, while the complexes $[Pt_7(2,6\text{-}Me_2C_6H_3NC)_{12}]$,[20] $[Os_6(CO)_{18}$-$(4\text{-}MeC_6H_4NC)_2]$[25] and $[Fe_3(CO)_9\{CNC(CH_3)_3\}]$[26] all possess μ_3-η^2 isocyanides. Novel examples of isocyanide coordination to metal centres are found in $[Ru_5(CO)_{14}\{CNC(CH_3)_3\}_2]$[27] which contains an isocyanide bound to all five ruthenium atoms in a μ_5-η^2 fashion and acts as a six electron donor, as well as $[Co_3(CO)_9\{CNC(Cr(CO)_5)\}]$[22] and $[Ni_3(\mu_3\text{-}CNMe)(\mu_3\text{-}I)(CNMe)_2(dppm)_2]^{1+}$ which both have isocyanides bound in symmetric μ_3-η^1 modes. Several examples of symmetric μ_3-η^1 CO clusters are known. These include the complexes $[Cp_3Ni_3(\mu_3\text{-}CO)_2]$,[28] which have two carbonyls capping each face of the nickel triangle, as well as $[Pd_3(\mu_3\text{-}CO)(\mu\text{-}dppm)_3]^{2+}$[29] and $[Pt_3(\mu_3\text{-}CO)(\mu\text{-}dppm)_3]^{2+}$, 1.

Studies on the adsorption of MeNC on Pt(111) surfaces show that the isocyanide is adsorbed in two different forms.[23] Infrared spectroscopy reveals the presence of terminal (ν(NC) = 2180 cm^{-1}) and bridging (ν(NC) = 1685 cm^{-1}) isocyanide groups bound to the metal through the isocyanide carbon atoms.

On the other hand, when carbon monoxide is adsorbed onto a Pt(111) surface, the on-top (terminal) sites are occupied first. At higher coverages the twofold (μ_2) sites

are preferred. Recently it has been shown that threefold (μ_3) sites are also occupied at high coverage and that the energy difference between the μ_3-CO and the μ_2-CO groups is only 4 ± 1 kJ mol^{-1}.[30] In all cases the CO interacts with the metal centres through the carbon atom.

Due to the similarities that often exist between carbon monoxide and the isocyanides and due to the fact that relatively little attention has been paid to the reactivities of isocyanides with metal clusters, it was of interest to investigate the reactions that occur between $[Pt_3(\mu_3\text{-}CO)(\mu\text{-}dppm)_3]^{2+}$, **1**, and various isocyanides. This chapter reports the results of the addition of one molar equivalent of isocyanide to complex **1**. Our interest here is in whether the ligands add at terminal or bridging sites, in how ligand addition affects the $Pt_3(\mu_3\text{-}CO)$ linkage and in whether the isocyanide is able to displace the μ_3-carbonyl from the cluster. The results of the addition of excess isocyanide to complex **1** will be reported in the following chapter.

5.2 RESULTS

5.2.1 Synthesis

The major chemical results are shown in Equation 5.1.

As monitored by ^{31}P NMR spectroscopy, reaction of complex **1** with an equimolar amount of cyclohexyl and tertiary-butyl isocyanide in acetone proceeded via the formation of an intermediate with the isocyanide on the

formation of an intermediate with the isocyanide on the same face of the cluster as the carbonyl ligand. This is followed by dissociation of the isocyanide and finally coordination to the opposite face of the triplatinum cluster. Intermediate formation was not observed with $2,6\text{-}Me_2C_6H_3NC$. It was also nonreversible in that cooling solutions of the final products did not result in subsequent reformation of the intermediate. Complexes 3a-3c were isolated as their hexafluorophosphate salts in greater than 90% yield by removing the acetone under reduced pressure and by crystallization from an acetone/pentane mixture.

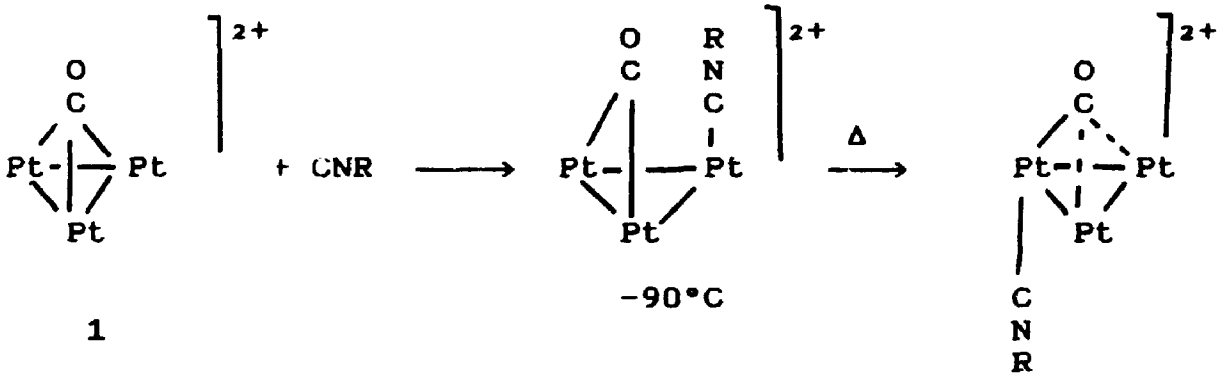

2a:	R = Cy	3a:	R = Cy
2b:	R = ^{t}Bu	3b:	R = ^{t}Bu
2c :	R = $2,6\text{-}Me_2C_6H_3$	3c:	R = $2,6\text{-}Me_2C_6H_3$
		3d:	R = Me

*dppm ligands omitted for clarity.

Equation 5.1

Reaction of complex 1 with methyl isocyanide resulted in the formation of complex 3d. This complex was

characterized exclusively by $^{31}P\{^{1}H\}$ NMR.

5.2.2 The Structure of $[Pt_3(\mu_3\text{-}CO)(CNC_6H_{11})(\mu\text{-}dppm)_3][PF_6]_2\cdot(CH_3)_2CO$: Characterization by X-ray Crystallography

The structure of complex 3a was determined by Drs. Muir and Manojlovic-Muir at the University of Glasgow. Crystals of complex $3a[PF_6]_2$ were grown by fractional recrystallization from an acetone/pentane mixture and consisted of well separated cations, anions and solvent molecules. The structure of the cation (Figure 5.2) is characterized by the bond lengths shown in Table 5.1. The structure was disordered and, as a result, it could not be completely solved. It could only be refined to an R value of 10%. Important information however can still be extracted from the structure.

The platinum cluster contains an isosceles triangle of platinum atoms with each edge of the triangle bridged by a dppm ligand to form a Pt_2P_2C dimetallacycle. The rotational orientation of the dppm ligands about the Pt-Pt bonds and conformations of the Pt_2P_2C rings are such as to afford a Pt_3P_6 skeleton substantially distorted from an idealized latitudinal M_3L_6 geometry. In the Pt_2P_2C rings the two methylene groups closest to Pt(1) are situated below the plane of the Pt_3 triangle while the third is situated above the plane. In such a conformation of the $Pt_3P_6C_3$ skeleton the phenyl rings are directed away from

FIGURE 5.2: ORTEP Diagram of 3a

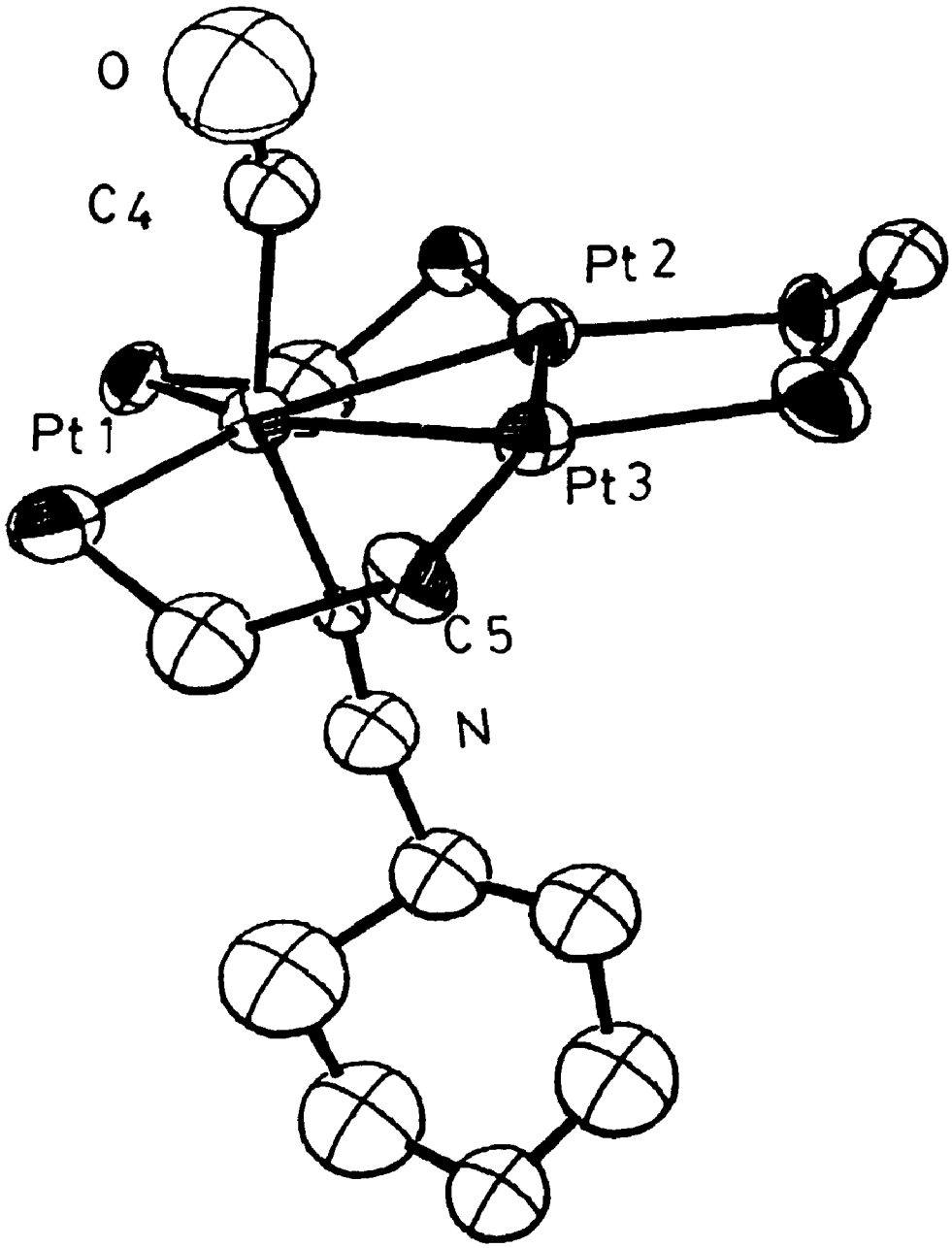

the CNC_6H_{11} ligand and the steric hindrance, which is severe, is thus minimized.

The platinum core is an isosceles triangle with two longer (2.626(3) A and 2.646(3) A) and one shorter (2.585(3) A) Pt-Pt distance.

TABLE 5.1: Bond Lengths for Complex 3a

Bond	Length (A)
Pt(1)-Pt(2)	2.646(3)
Pt(1)-Pt(3)	2.626(3)
Pt(2)-Pt(3)	2.585(3)
Pt(1)-C(4)	2.08(5)
Pt(1)-C(5)	1.90(4)
Pt(2) ···· C(4)	3.04(4)
Pt(3) ···· C(4)	2.97(5)
Pt(2) ···· C(5)	2.93(4)
Pt(3) ···· C(5)	3.01(4)

The average Pt-Pt bond length is 2.619(3) Å, which is significantly shorter than those found for the 42 electron clusters $[Pt_3(\mu_3\text{-}CO)(\mu\text{-}dppm)_3]^{2+}$,[30] 1, 2.634 Å; $[Pt_3(\mu\text{-}CO)(\mu\text{-}CNC_8H_9)_2(CNC_8H_9)\{P(C_6H_{11})_3\}_2]$,[17] 2.633(1) Å; $[Pt_3(\mu\text{-}CNC_8H_9)_3(CNC_8H_9)_2\{P(C_6H_{11})_3\}]$,[17] 2.632(1) Å; and $[Pt_3(\mu\text{-}CN^tBu)_3(CN^tBu)_3]$,[7] 2.633(1) Å. Hence the addition of isocyanide ligand to 1 increases the cluster electron count from 42 to 44 electrons, but does not have the effect of lengthening the Pt-Pt bonds. This is in agreement with our recent findings on related complexes.

In considering the Pt-Pt bond lengths in this cluster it is interesting to note that the addition of the terminal isocyanide has a greater effect on the geometry of the cluster core than does the addition of $P(OPh)_3$ where the cluster core is an equilateral triangle with an average Pt-Pt distance of 2.639 Å. This is within experimental error of that found for complex 1.[31]

The Pt-P bond lengths involving Pt(1) are longer than those involving Pt(2) and Pt(3). This difference could reflect a rehybridization of platinum orbitals due to the higher coordination number of Pt(1). The Pt(1)-C(5) distance of 1.90(4) Å is within the expected range of Pt-C bond lengths in complexes with terminal isocyanide ligands. The isocyanide ligand is not normal to the Pt_3 plane. Rather it is tilted in towards Pt(2) and Pt(3), probably to minimize steric repulsions between the C_6H_{11} ring of the isocyanide and the dppm phenyl rings. The

Pt(3)-C(5) and Pt(2)-C(5) distances of 3.01(4) and 2.93(4) Å, respectively, are too long for there to be any bonding interaction present between the isocyanide and the platinums.

The carbonyl ligand bonds to Pt(1) and not to Pt(2) or Pt(3). This is apparent from the respective Pt-C distances of 2.08(5), 3.04(5) and 2.97(5) Å. It is interesting to compare the geometry of the $Pt_3(CO)$ unit in 3a with those previously observed in the complexes $[Pt_3(\mu_3\text{-}CO)(\mu\text{-}dppm)_3]^{2+}$,[30] 1, $[Pt_3(\mu_3\text{-}CO)(\mu_3\text{-}SnF_3)(\mu\text{-}dppm)_3]^{1+}$,[32] 4, $[Pt_3(\mu_3\text{-}CO)(P\{OPh\}_3)(\mu\text{-}dppm)_3]^{2+}$,[31] 5, and $[Pt_3(\mu_3\text{-}CO)(SCN)(\mu\text{-}dppm)_3]^{1+}$,[33] 6. The distortion of the carbonyl is significant in the weakly bound thiocyanate adduct, is greater in the more strongly bound triphenylphosphite adduct, 5, and is greater still in the cyclohexyl isocyanide adduct, 3a. This distortion has already been considered in depth in Chapter 3 and it suffices to say that the extreme distortion observed for complex 3a is not surprising due to the fact that isocyanide is a good σ-donor ligand.

TABLE 5.2: IR Data for Complexes 3a-3c

Complex	ν(CO) cm^{-1}	ν(CNR) cm^{-1}
3a	1800	2165
3b	1779	2170
3c	1793	2131

5.2.3 Characterization of Complexes 3a-3c by Spectral Methods

The values for the ν(CO) stretching frequencies were in the narrow range of 1779 to 1800 cm^{-1} while those for the ν(CN) frequencies ranged from 2131 to 2170 cm^{-1} for complexes 3a-3c (Table 5.2). The ν(CO) frequencies fall in the range expected for μ_3-CO groups but are higher than ν(CO) = 1765 cm^{-1} for the parent cluster 1. The IR data, therefore, clearly indicate some degree of interaction between the carbonyl ligand and Pt(2) and Pt(3), as opposed to the X-ray structural data which imply that there is none. Due to the fact that the existence of disorder in the positioning of the isocyanide ligand would also be expected to create some uncertainty about the positioning of the carbonyl ligand, it may be that the Pt(3)-carbonyl and Pt(2)-carbonyl distances should be shorter than 2.97(5) and 3.04(5) Å, respectively, but still significantly longer

than Pt(1)-C(4) of 2.08(5) Å. Once again, as was found for the clusters reported in Chapter 3, the higher ν(CO) values are not necessarily indicative of an asymmetric $Pt_3(\mu_3\text{-CO})$ group, but may simply be characteristic of 44 electron cluster species. The ν(CN) values are in the expected range for terminal isocyanides.

The complexes 3a-3c were fluxional at room temperature and so NMR spectra were obtained at low temperature, typically at -90°C in acetone-d_6 solution. The ^{1}H NMR spectrum in the CH_2P_2 region contained two "AB" quartets with relative areas 2:1 as expected for the static structure shown below which has no plane of symmetry containing the $Pt_3(PCP)_3$ unit.

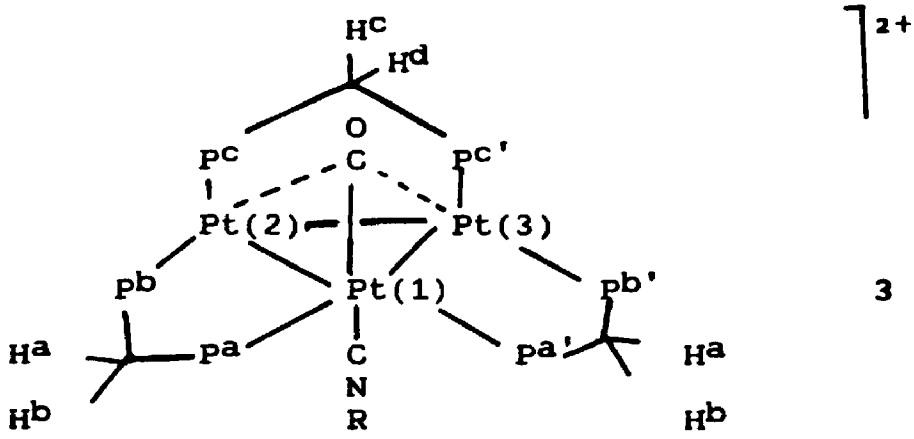

3

The ^{31}P{^{1}H} NMR spectra of the complexes are informative and the spectrum of 3a will be described as a typical example (Figure 5.3). Data for all complexes are given in Table 5.3. In these $Pt_3(\mu\text{-dppm})_3$ complexes, the largest J(PP) couplings are the trans-like couplings through the Pt-Pt bonds which, in complexes 3, are $^3J(P^aP^c)$

and $^{3}J(P^{b}P^{b'})$. The spectra contain two doublet resonances and a singlet resonance. The singlet is readily assigned to P^{b}. The magnitude of $^{3}J(P^{b}P^{b'})$, 200 Hz, is obtained from the ^{195}Pt satellite spectra while $^{3}J(P^{a}P^{c})$ = 170 Hz. These are typical values for complexes 3. The resonances due to P^{a} [δ = -49.6 ppm, $^{1}J(PtP)$ = 1840 Hz] and P^{c} [δ = 13.2 ppm, $^{1}J(PtP)$ = 4024 Hz] are assigned by correlation of $^{1}J(PtP)$ values with the Pt-P bond distances (PtP^{a} longer than PtP^{c}, Table 5.1). It should be mentioned at this point that while there is a general trend that the ^{31}P chemical shifts are more negative when bound to platinum atoms with higher steric hindrance in the phosphine and phosphite adducts of complex 1 (Chapter 3), no such trend is observed for the isocyanide adducts.

TABLE 5.3: $^{31}P\{^{1}H\}$ NMR Data for Complexes 3a-3d

	δ P^a (ppm)	$^1J(PtP^a)$ (Hz)	$^3J(P^aP^c)$ (Hz)	δ P^b (ppm)	$^1J(PtP^b)$ (Hz)	$^3J(P^bP')$ (Hz)	δ P^c (ppm)	$^1J(PtP^c)$ (Hz)	$^3J(P^aP^c)$ (Hz)
3a	-49.6	1840	170	-9.6	2510	200	-13.2	4024	170
3b	-52.2	1830	170	-10.6	2600	180	-13.2	4040	170
3c	-35.3	2680	160	-9.5	3200	160	-9.3	4020	160
3d	-48.5	1800	---	-9.0	2540	---	-13.9	3860	---

Ref.: H_3PO_4

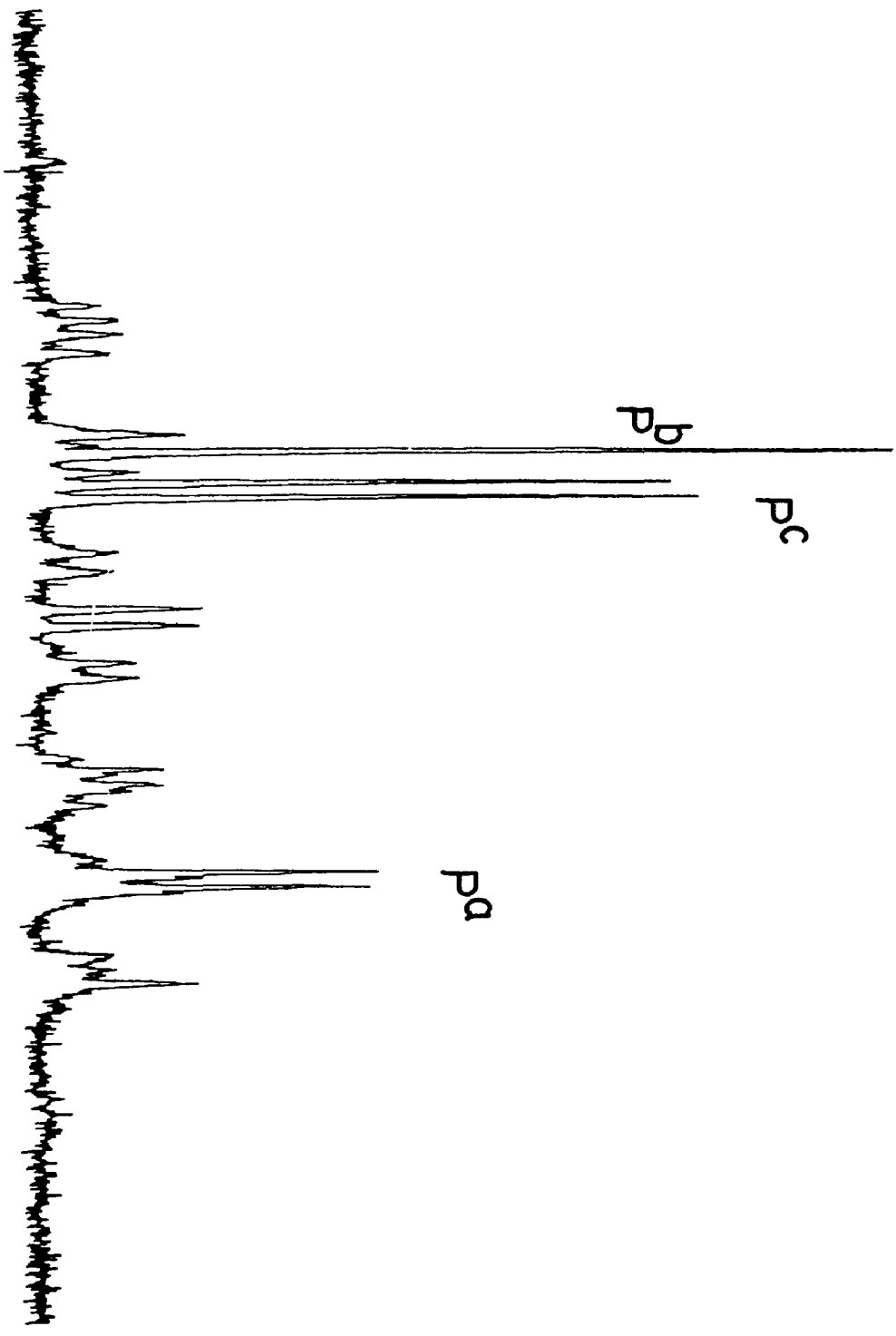

FIGURE 5.3: $^{31}P\{^{1}H\}$ NMR Spectrum of 3a

The $^{13}C\{^1H\}$ NMR spectrum **3a***, enriched with ^{13}CO, gave δ (^{13}CO) = 196.6 ppm, and appeared as a 1:4:1 triplet [due to coupling to Pt(1), $^1J(PtC)$ = 1175 Hz] of 1:8:18:8:1 quintets [due to coupling to Pt(2) and Pt(3), $^1J(PtC)$ = 458 Hz]. The spectrum is shown in Figure 5.4, and the data are in Table 5.4.

It is interesting to compare these parameters with those obtained for the platinum phosphite clusters discussed in Chapter 3. For the clusters $[Pt_3(\mu_3\text{-}CO)(P\{OMe\}_3)(\mu\text{-}dppm)_3]^{2+}$ and $[Pt_3(\mu_3\text{-}CO)(P\{OPh\}_3)(\mu\text{-}dppm)_3]^{2+}$ the $^1J(Pt(1)C)$ values were 996 and 960 Hz, respectively, while the $^1J(Pt(2)C)$ values were 468 and 463 Hz. These values support the conclusion that the (μ_3-CO) ligand is more distorted in the cluster isocyanide systems than in the cluster-tertiary phosphite and phosphine systems.

TABLE 5.4: ^{13}C NMR Data for Complexes **3a-3c**

	δ ^{13}C (ppm)[a]	$^1J(Pt(1)C)$ (Hz)[a]	$^1J(Pt(2)C)$ (Hz)[a]	δ ^{13}C (ppm)[b]	$^1J(PtC)$ (Hz)[b]	$^2J(PC)$ (Hz)[b]
3a	196.6	1175	458	195.6	685	11.4
3b	195.2	1190	455	194.0	688	--
3c	195.5	1200	400	195.3	685	11

[a] T = -82°C [b] T = 20°C.

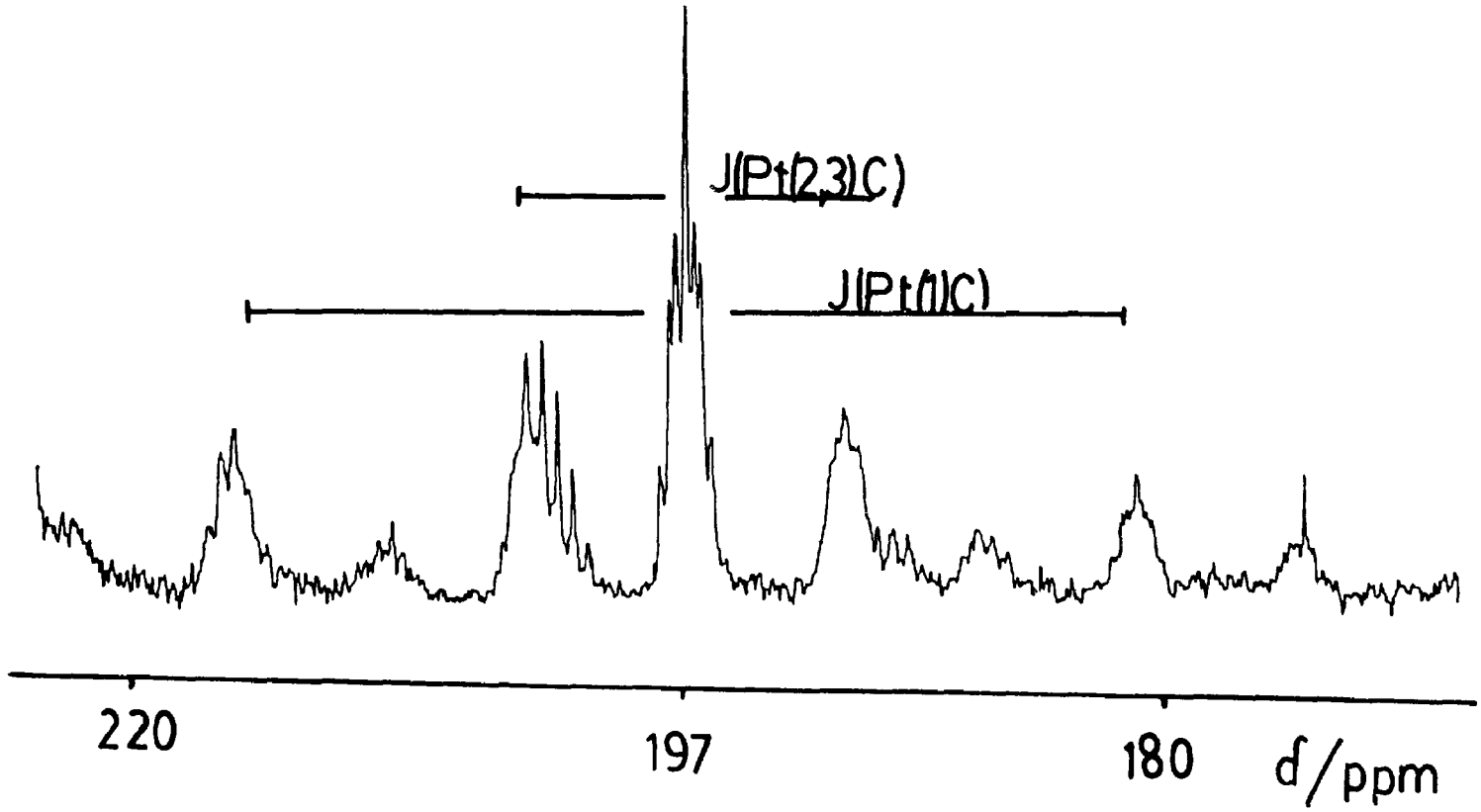

FIGURE 5.4 $^{13}C\{^{1}H\}$ NMR Spectrum of **3a**

The above spectroscopic data clearly show that the structures in solution are of the type found in the solid state for **3a**. In particular, the isocyanide ligand adopts a terminal bonding position and the carbonyl group is asymmetrically bridging with a much stronger interaction with Pt(1) than with Pt(2) or Pt(3).

The $^{195}Pt\{^{1}H\}$ NMR spectrum of **3a** consisted of two sets of resonances, one due to Pt(1) and the other due to Pt(2) and Pt(3) (Table 5.5). The resonance due to Pt(1) appeared as a triplet due to coupling to P^a [δ = -3247 ppm, $^{1}J(PtP^a)$ = 1860 Hz], while the resonance due to Pt(2) and Pt(3) appeared as a doublet of doublets due to coupling to both P^b and P^c [δ = -2132 ppm, $^{1}J(PtP^b)$ = 2500 Hz, $^{1}J(PtP^c)$ = 4100 Hz] (Figure 5.5). The ^{195}Pt NMR spectrum of ^{13}CO enriched **3c** helped to verify the presence of the asymmetric $Pt_3(\mu_3\text{-}CO)$ unit by clearly exhibiting the different Pt-^{13}C couplings [δ Pt(1) = -3269 ppm, $^{1}J(PtP^a)$ = 2540 Hz, $^{1}J(Pt(1)C)$ = 1200 Hz; δ Pt(2) = -2493 ppm, $^{1}J(Pt(2)P^b)$ = 3000 Hz, $^{1}J(Pt(2)C)$ = 4000 Hz, $^{1}J(Pt(2)C)$= 400 Hz].

5.2.4 Comparison of the Structures of Complexes 3 and $[Pt_3(\mu_3\text{-}CO)(CO)(\mu\text{-}dppm)_3]^{2+}$, 7

Due to the similarities that exist between carbonyl and isocyanide ligands, it is instructive to compare the clusters obtained by the addition of isocyanide and CO to complex 1. Studies have shown that CO adds rapidly and reversibly to complex 1 to give

FIGURE 5.5: $^{195}Pt(^{1}H)$ NMR Spectrum of 3a

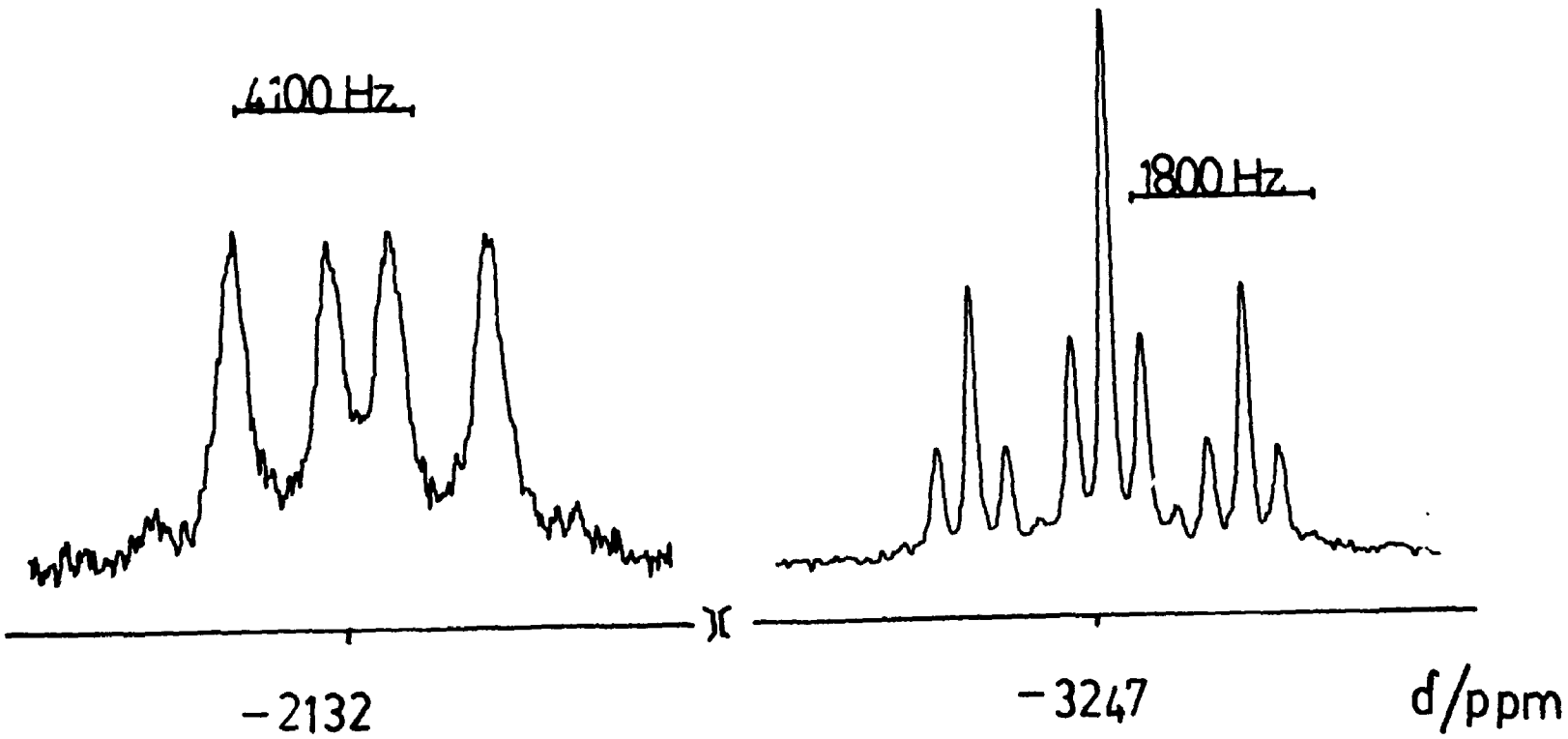

$[Pt_3(\mu_3\text{-}CO)(CO)(\mu\text{-}dppm)_3]^{2+}$,[35] **7**, under 1 atmosphere of CO. Both the low temperature $^{31}P\{^1H\}$ NMR and $^{13}C\{^1H\}$ NMR spectra indicate the presence of threefold symmetry in complex **7**. The $^{31}P\{^1H\}$ NMR spectrum yielded a singlet resonance with platinum satellites [δ = -16.6 ppm, $^1J(PtP)$ = 3400 Hz], while the $^{13}C\{^1H\}$ NMR spectrum yielded a single carbonyl resonance with platinum satellites [δ = 186.0 ppm, $^1J(PtC)$ = 590 Hz].

The ν(CO) stretching frequencies for complex **7** under a partial atmosphere of CO, however, showed bands at 1760 cm^{-1} and 2075 cm^{-1} indicating the presence of both a triply-bridging and terminal isocyanide, respectively. The ground state structure is therefore thought to be **8** which is directly analogous to that for complexes **3a-3c**.

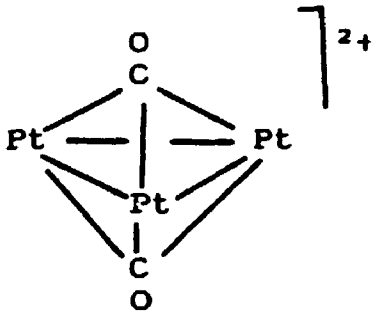

7

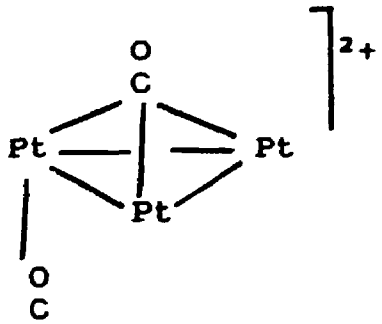

8

TABLE 5.5: $^{195}Pt\{^{1}H\}$ NMR Data for Complexes 3a-3c

	δ Pt(1) (ppm)	$^{1}J(Pt(1)P^{a})$ (Hz)	$^{1}J(Pt(1)Pt(2))$ (Hz)	δ Pt(2) (ppm)	$^{1}J(Pt(2)P^{b})$ (Hz)	$^{1}J(Pt(2)P^{c})$ (Hz)
3a	-3247	1860	740	-2132	2500	4100
3b	-3234	1940	920	-2141	2500	4100
3c	-3269	2540	900	-2493	3000	4000

Ref.: K_2PtCl_4

Species 7 and 8 are most likely in rapid equilibrium, even at -90°C, so that the structure appears to be 7 on the NMR time scale.

Evans has done extended Huckel molecular orbital (EHMO) calculations on the symmetrical cluster $[Pt_3(\mu_3\text{-}CO)_2(\mu\text{-}dppm)_3]^{2+}$, 7, and has found that the symmetrical structure is slightly more stable than the structure $[Pt_3(\mu_3\text{-}CO)(CO)(\mu\text{-}dppm)_3]^{2+}$,[34] 8.

5.2.5 Fluxionality in Complexes 3a-3c

The complexes 3a-3c were found to be fluxional in the sense that the terminal isocyanide can migrate around the triangular face of the cluster, by analogy with the fluxionality observed for the phosphine and phosphite adducts of complex 1, as shown in Equation 5.1.

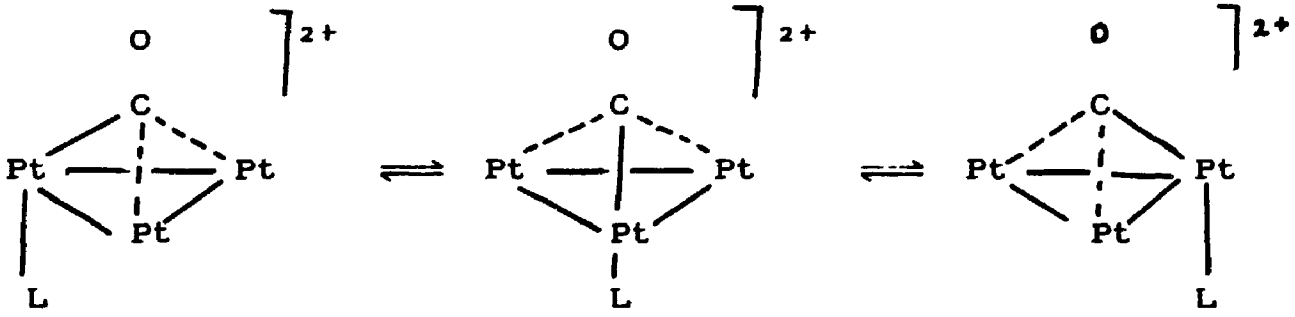

Equations 5.1

At high temperature, 60°C, the $^{31}P\{^1H\}$ NMR spectrum displayed a single broad resonance due to the dppm phosphorus atoms, and the $^{13}C\{^1H\}$ NMR resonance appeared as a 1:12:49:84:49:12:1 septet thus indicating apparent

FIGURE 5.6: $^{13}C\{^{1}H\}$ NMR Spectrum of 3c at 60°C

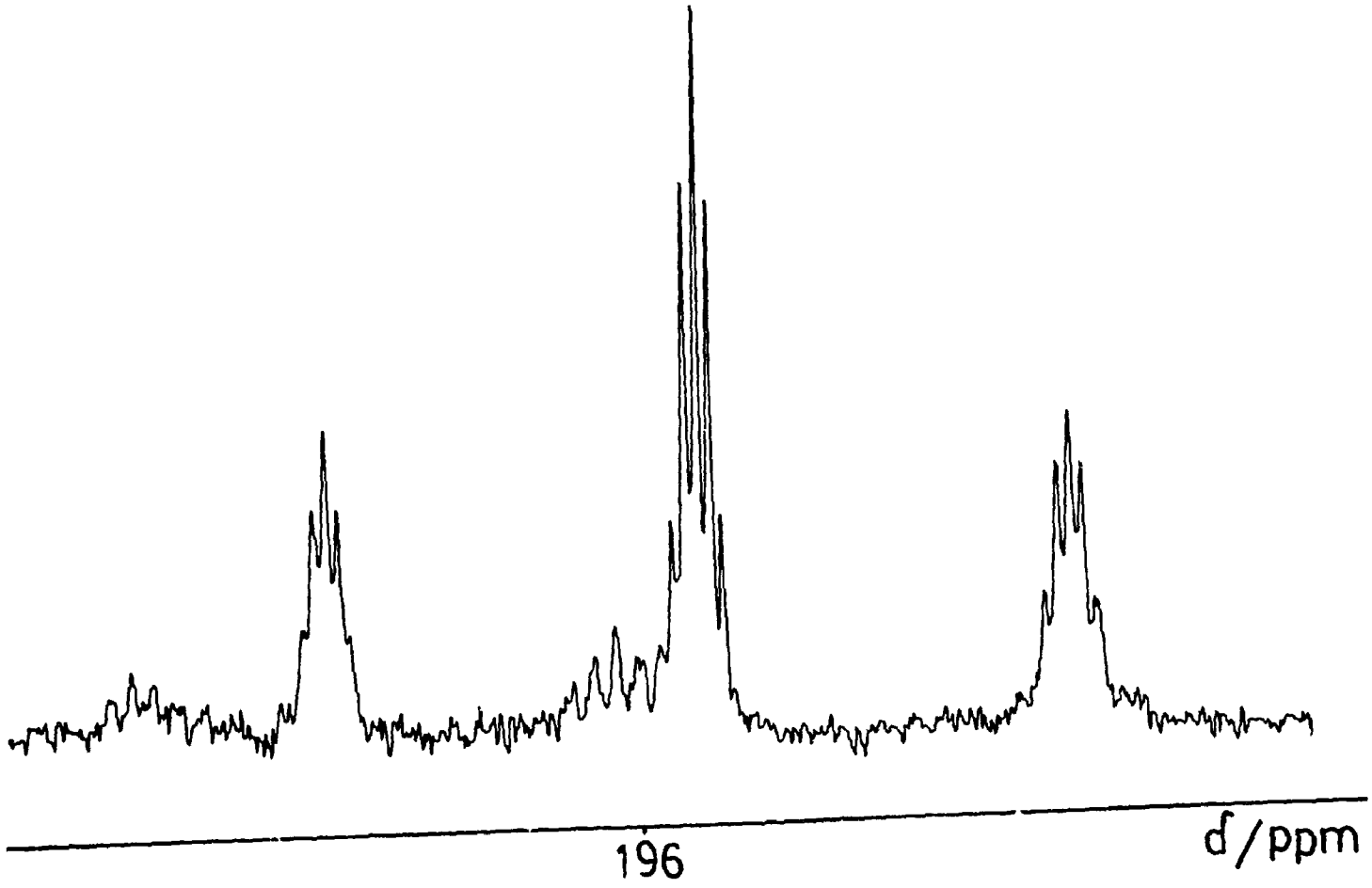

threefold symmetry for complexes **3** (Figure 5.6). The $^{1}J(PtC)$ value for rapid intramolecular fluxionality is 1/3 [$^{1}J(Pt(1)C)$] + 2/3 [$^{1}J(Pt(2)C)$]. [**3a**: $^{1}J(PtC)$ calc = 697 Hz, $^{1}J(PtC)$ obs = 685 Hz; **3b**: $^{1}J(PtC)$ calc = 700 Hz, $^{1}J(PtC)$ obs = 688 Hz; **3c**: $^{1}J(PtC)$ calc = 667 Hz, $^{1}J(PtC)$ obs = 685 Hz.]

5.2.6 Spectral Characterization of the Intermediate, 2

The intermediates observed in this reaction appeared immediately upon the addition of isocyanide to complex **1** at -92°C and persisted to 0°C. The $^{31}P\{^{1}H\}$ NMR spectrum consisted of three sets of resonances, all with platinum satellites [two sets of doublets and a singlet] (Table 5.6). The observed multiplicities are due to $^{3}J(PP)$ coupling across the Pt-Pt bonds (Figure 5.7). The phosphorus assignments were made on the basis of the fact that the $^{1}J(PtP)$ values for these Pt_3 clusters are known to decrease as the steric crowding around the phosphorus atoms becomes greater.

The $^{13}C\{^{1}H\}$ NMR spectra of **2a** and **2b** revealed the presence of μ_2-carbonyls [**2a**: δ = 217.2 ppm, $^{1}J(PtC)$ = 912 Hz; **2b**: δ= 220.4 ppm, $^{1}J(PtC)$ = 903 Hz] Table 5.7.

The intermediates were not fluxional as were the final products **3a** and **3b**. This is particularly evident in the $^{31}P\{^{1}H\}$ NMR spectra of the system in which cyclohexyl isocyanide is added to complex **1**. At -22°C resonances due to both the final product, **3a**, and the intermediate, **2a**,

TABLE 5.6: $^{31}P\{^{1}H\}$ Data for Intermediates **2a-2b**

	δ P^a (ppm)	$^1J(PtP^a)$ (Hz)	$^3J(P^aP^c)$ (Hz)	δ P^b (ppm)	$^1J(PtP^b)$ (Hz)	$^2J(PtP)$ (Hz)	δ P^c (ppm)	$^1J(PtP^c)$ (Hz)
2a	-39.7	2220	180	-60.4	3180	---	-25.2	3240
2b	-39.0	2120	180	-62.3	3030	410	-29.9	3400

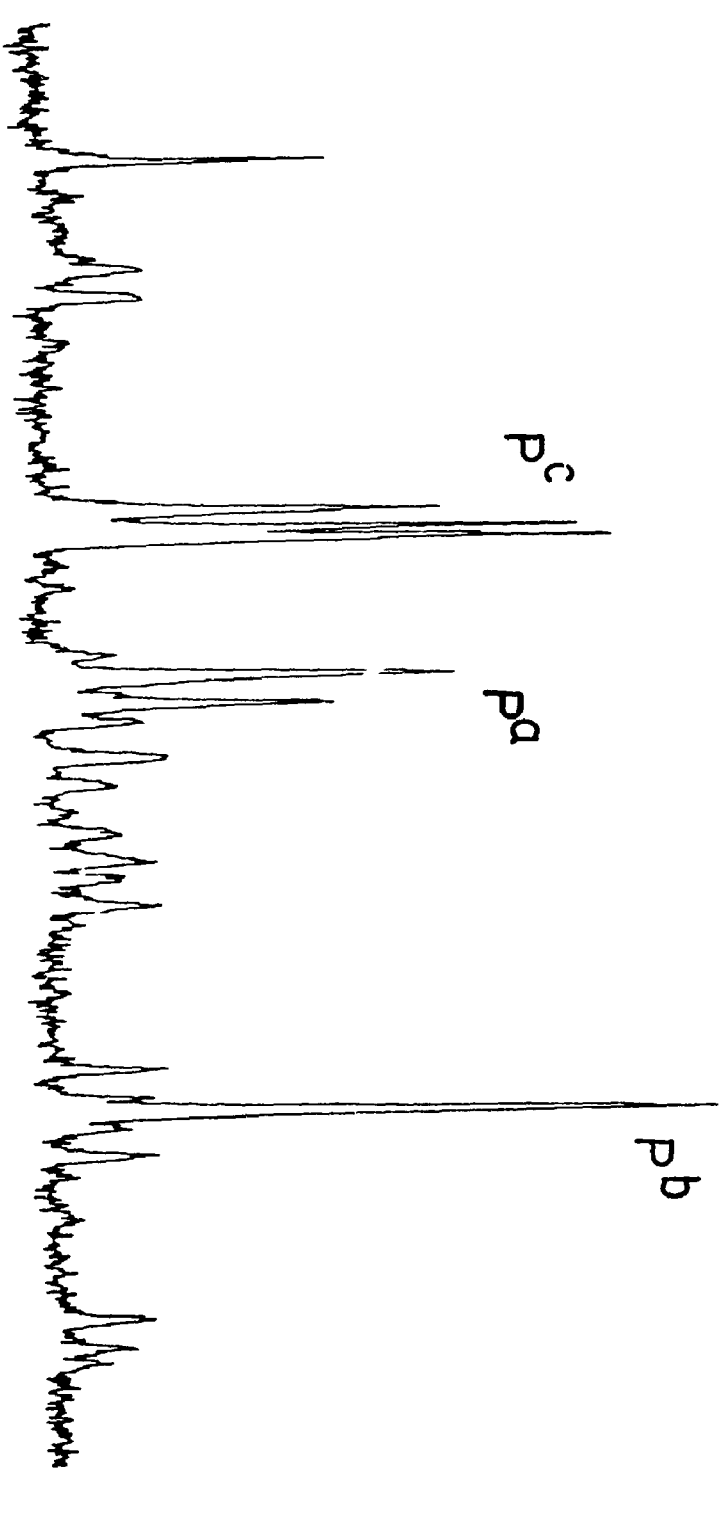

FIGURE 5.7: $^{31}P\{^{1}H\}$ NMR Spectrum of 2b

TABLE 5.7: $^{13}C\{^{1}H\}$ NMR Data for the Intermediate, 2

	^{13}C (ppm)	$^{1}J(PtC)$ (Hz)
2a	217.2	912
2b	220.4	903

are present. The resonances due to 3a, however, are significantly broadened due to the fluxionality of this species while those belonging to complex 2a were still sharp. The small energy differences between the μ_3, μ_2 and terminal modes of coordination for CO, in addition to the coordinative unsaturation of the metal centres, lead to an intramolecular fluxionality of terminally bound ligands on the face opposite to that occupied by the carbonyl, even for ligands where this has not been observed before. It is therefore reasonable to propose the type of structure shown below for the intermediate where both the μ_2-CO and the terminal isocyanide are present in the same face of the Pt_3 cluster.

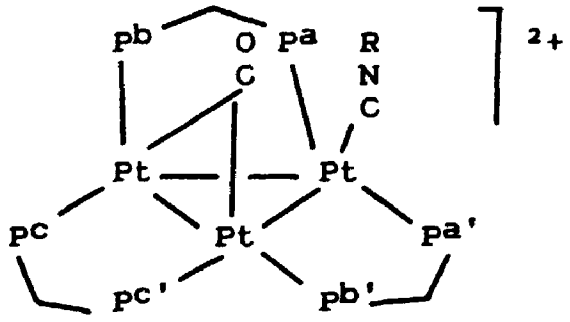

2

A space filling diagram of complex 1 was constructed in an effort to determine why the isocyanide would initially interact with complex 1 on the same face where the μ_3-carbonyl is situated (Figure 5.6). The diagram revealed that the dppm phenyl rings are pushed away from this face leaving it more open to attack than the vacant face of the cluster. This is most likely due to the presence of the carbonyl ligand.

Studies indicate that the intermediate, complex 2, is most likely the kinetic product in the interaction of isocyanide ligands with complex 1, while complex 3 is the thermodynamic product. This intermediate is a novel species and as far as we know, no such complexes have been observed in the reaction of trinuclear platinum complexes with isocyanides.

5.2.7 The Reaction of $[Pt_3(\mu_3\text{-}CO)(P\{OMe\}_3)(\mu\text{-}dppm)_3]^{2+}$ with $C_6H_{11}NC$

Studies were done on the reactivity of $[Pt_3(\mu_3\text{-}CO)(P\{OMe\}_3)(\mu\text{-}dppm)_3]^{2+}$, which was reported in Chapter 3, with cyclohexyl isocyanide. The impetus for this study was the finding reported by Mingos that isocyanide ligands will substitute for tertiary phosphines in homonuclear Pt(0) trimers.[17] It was of interest to see whether this would occur, or whether the isocyanide would add to $[Pt_3(\mu_3\text{-}CO)(P\{OMe\}_3)(\mu\text{-}dppm)_3]^{2+}$ to give a new 46 electron cluster.

FIGURE 5.8: Space Filling Diagram of 2b

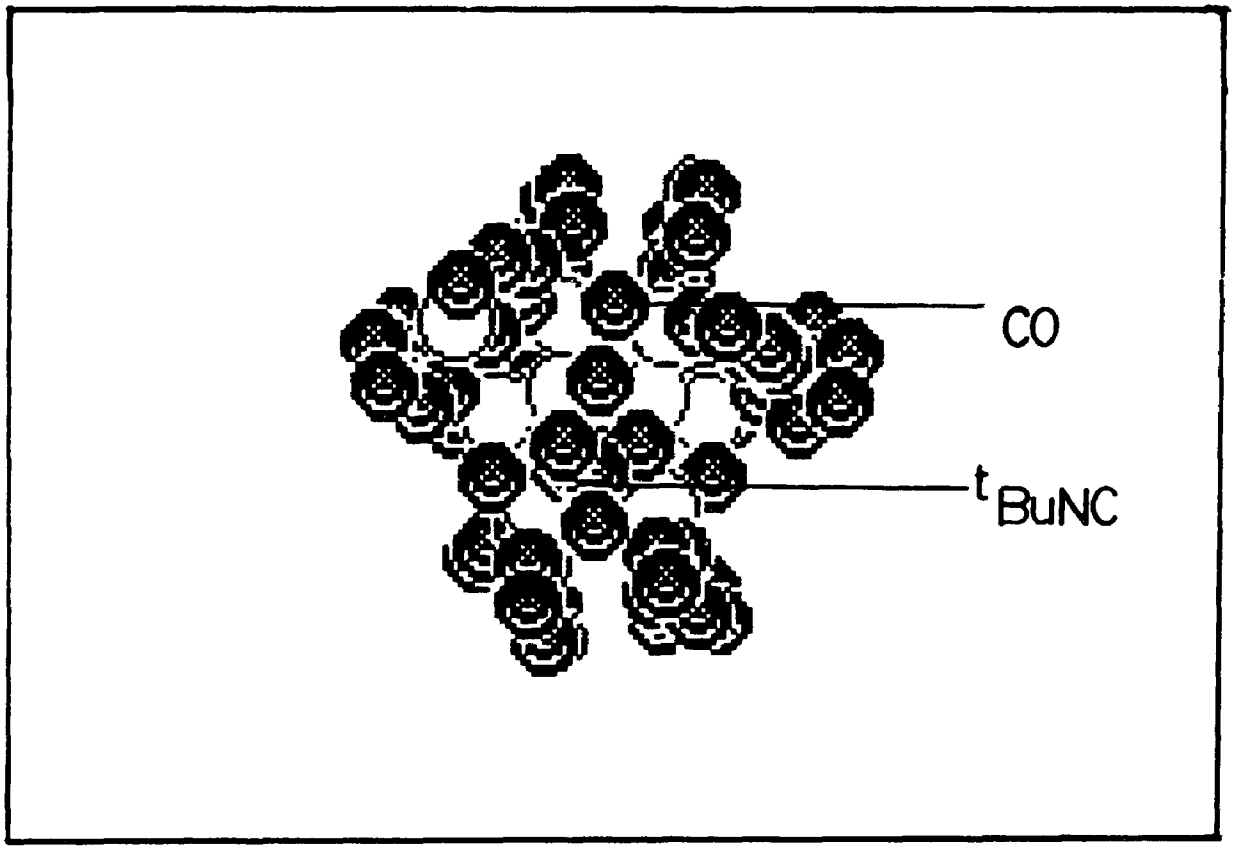

The $^{31}P\{^{1}H\}$ NMR spectrum of the reaction revealed that the isocyanide displaced the $P(OMe)_3$ from the cluster to form complex 3a. The NMR results also indicated that some fragmentation of the cluster had also occurred. This, coupled with the observation of platinum satellites associated with the $P(OMe)_3$ resonance suggests the formation of monomeric platinum-trimethylphosphite complexes. These complexes could not be characterized because they could not be isolated. The reaction is most likely to occur by a dissociative mechanism whereby the $P(OMe)_3$ dissociates from $[Pt_3(\mu_3\text{-}CO)(P\{OMe\}_3)(\mu\text{-}dppm)_3]^{2+}$ and cyclohexyl isocyanide adds to the vacant coordination site.

5.2.8 The Reaction of $[Pt_3(\mu_3\text{-}CO)(2,6\text{-}Me_2C_6H_3NC)(\mu\text{-}dppm)_3]^{2+}$ with Excess CO

The reaction of complex 3c with excess CO was also studied. The $^{31}P\{^{1}H\}$ NMR spectrum obtained when complex 3c was placed under an atmosphere of carbon monoxide displayed six sets of phosphorus resonances indicating the presence of a cluster species with no plane of symmetry (Table 5.8). No definitive assignments of phosphorus resonances could be made.

TABLE 5.8: $^{31}P\{^{1}H\}$ NMR Data for Complex 9

δ P (ppm)	$^{1}J(PtP)$ (Hz)	$^{3}J(PP)$ (Hz)
-16.5	3500	160
-21.1	3460	168
-35.9	3500	160
-46.1	4130	168
-47.9	3120	168
-61.6	3360	160

The ^{13}C NMR spectrum revealed two sets of carbonyl resonances: one due to a doubly-bridging carbonyl [δ = 209.0 ppm, $^{1}J(Pt(1)C)$ = 800 Hz, $^{1}J(Pt(2)C)$ = 954 Hz, $^{2}J(PtC)$ = 117 Hz] and the other due to a terminal carbonyl [δ = 177.4 ppm, $^{1}J(PtC)$ = 1170 Hz]. The $^{13}C\{^{1}H\}$ NMR spectra show that complex 9 contains an asymmetric μ_2-CO which displays greater coupling to the platinum atom with the terminal isocyanide than to the platinum atom with the terminal carbonyl. This can be explained by the fact that isocyanide is a better σ-donor than carbonyl and increases the electron density on the corresponding platinum more than the one to which the CO is bound. This enhances the π backbonding between the bridging carbonyl and this platinum atom.

Low temperature 2D NMR spectra were also run on this system in order to get more information about the structure. These spectra revealed the existence of coupling between the doubly bridging and terminal carbonyls. The spectral information is consistent with the structure shown below.

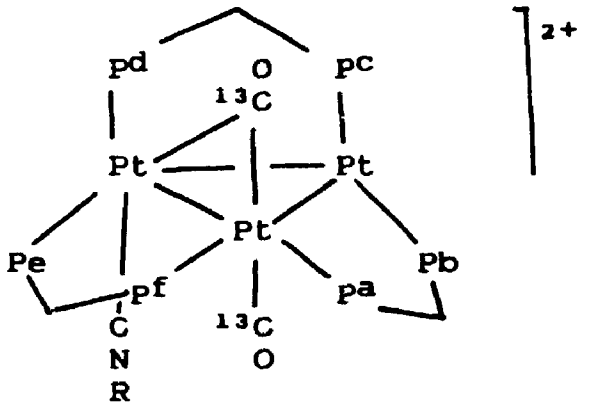

9

This structure is similar to that deduced for the cluster $[Pt_3(\mu_2\text{-}CO)(CO)_2(\mu\text{-}dppm)_3]^{2+}$ which has been previously reported.

Complex 9 was stable up to -50°C after which time the extra CO (terminal) dissociated resulting in the formation of complex 3. Complex 9 also displays fluxionality at -50°C as is evidenced by a broadening of the resonances observed in the $^{31}P\{^1H\}$ NMR spectrum. This fluxionality involves the migration of the μ_2-carbonyl about the top face, and of the CO and CNR ligands about the bottom face of the cluster. The energy difference between μ_3, μ_2 and terminal CO groups as well as terminal and μ_2

isocyanide groups is low. Therefore these ligands migrate over the surface by interactions between each of these bonding modes.

5.3 DISCUSSION

For catalysis by clusters it is necessary to design coordinatively unsaturated clusters that are stable to fragmentation. Complex **1**, which is stabilized by μ-dppm ligands, is one such cluster. The stability is demonstrated by the addition of isocyanide and carbonyl without fragmentation. In order to obtain useful catalysis by clusters it is desirable that two ligands (which may or may not be different) add to adjacent metal centres, then combine and dissociate to give the product and regenerate the catalyst. The addition of both CO and isocyanide shows that the first step in this sequence is possible. This double ligand addition has also been previously observed with two carbonyls adding to complex 1.[35]

5.4 CONCLUSIONS

The reaction of complex **1** with 1 equivalent of isocyanide gives important insight into the reactivity of this cluster with a largely ignored, but important, class of ligands in metal cluster chemistry. The platinum-isocyanide clusters **3a-3c**, reported in this chapter, display rich reactivity. This is particularly true in their reactions with CO to form the novel 46

electron clusters 9. The interconversion between complexes 3 and 9 model several important features of the chemisorption of CO, including the rapidity of addition and the easy interconversion between the bonding modes of CO.

5.5 REFERENCES

1. M.R. Albert and J.J. Yates, Jr., "The Surface Scientist's Guide to Organometallic Chemistry", American Chemical Society, Washington, D.C., (1987).
2. M. Moskovits, Ed., "Metal Clusters", Wiley-Interscience, Toronto, Ontario, (1986).
3. F.A. Cotton and G. Wilkinson, "Advanced Inorganic Chemistry", Wiley-Interscience, New York, New York, (1980), Chapters 25, 26.
4. P.M. Treichel, *Adv. Organomet. Chem.*, (1973), **11**, 21.
5. E. Singleton and H.E. Oostheuizen, *Adv. Organomet. Chem.*, (1983), **21**, 209.
6. D.M.P. Mingos, I.D. Williams and M.J. Watson, *J. Chem. Soc., Dalton Trans.*, (1988), 1509.
7. M. Green, J.A.K. Howard, M. Murray, J.L. Spencer and F.G.A. Stone, *J. Chem. Soc., Dalton Trans.*, (1977), 1509.
8. A. Scrivanti, G. Carturan and V. Belluco, *Inorg. Chim. Acta*, (1976), **20**, 63.
9. M. Ciriano, M. Green, D. Gregson, J.A.K. Howard, J.L. Spencer, F.G.A. Stone and P. Woodri, *J. Chem. Soc., Dalton Trans.*, (1979), 1294.
10. B. Jovanovic and Lj. Manojlovic-Muir, *J. Chem. Soc., Dalton Trans.*, (1972), 1176.
11. C.E. Briant, D.I. Gilmour and D.M.P. Mingos, *J. Organomet. Chem.*, (1986), **308**, 381.
12. B.F.G. Johnson, J. Lewis and D.A. Pippard, *J. Chem.*

Soc., Dalton Trans., (1978), 407.

13. S.J. McKenna and E.L. Meutterties, *Inorg. Chem.*, (1987), **26**, 1296.

14. C.E. Briant, D.I. Gilmour and D.M.P. Mingos, *J. Chem. Soc., Dalton Trans.*, (1986), 835.

15. D.I. Gilmour, M.A. Luke and D.M.P. Mingos, *J. Chem. Soc., Dalton Trans.*, (1987), 335.

16. C.E. Briant, D.I. Gilmour and D.M.P. Mingos, *J. Organomet. Chem.*, (1984), **267**, C52.

17. C.E. Briant, D.I. Gilmour, D.M.P. Mingos and R.W.M. Wardle, *J. Chem. Soc., Dalton Trans.*, (1985), 1693.

18. Y. Yamamoto, H. Yamazaki and J. Sakurai, *J. Am. Chem. Soc.*, (1982), **104**, 2329.

19. Y. Yamamoto, K. Takahashi and H. Yamazaki, *J. Am. Chem. Soc.*, (1986), **108**, 2458.

20. Y. Yamamoto, K. Aoki and H. Yamazaki, *Organometallics*, (1983), **2**, 1377.

21. P. Ewing and L.J. Farrugia, *Organometallics*, (1988), **7**, 871.

22. W.P. Fehlhammer, F. Degel and H. Stolzenberg, *gew. Chem., Int. Ed. Engl.*, (1981), **20**, 214.

23. T. Szilagyi, *Appl. Surf. Sci.*, (1988), **35**, 19.

24. E.L. Meutterties, E. Bard, A. Kokorin, W.R. Pretzer, M.G. Thomas, *Inorg. Chem.*, (1980), **19**, 1377.

25. C.R. Eady, P.D. Gavens, B.F.G. Johnson, J. Lewis, M.C. Molatesta, M.J. Mays, A.G. Orpen, A.V. Rivera

and G.M. Sheldrick, *J. Organomet. Chem.*, (1978), **149**, 243.

26. M.I. Bruce, J.G. Matisens, J.R. Rogers and R.C. Wallis, *J. Chem. Soc., Chem. Commun.*, (1981), 1070.

28. E.O. Fischer and C. Palm, *Chem. Ber.*, (1958), **91**, 1725.

29. Lj. Manojlovic-Muir, K.W. Muir, B.R. Lloyd and R.J. Puddephatt, *J. Chem. Soc., Chem. Commun.*, (1985), 536.

30. G. Ferguson, B.R. Lloyd and R.J. Puddephatt, *Organometallics*, (1986), **5**, 344.

31. A.M. Bradford, G. Douglas, Lj. Manojlovic-Muir, K.W. Muir and R.J. Puddephatt, *Organometallics*, submitted.

32. M.C. Jennings and R.J. Puddephatt, *Inorg. Chem.*, (1988), **27**, 4280.

33. G. Ferguson, B.R. Lloyd, Lj. Manojlovic-Muir, K.W. Muir and R.J. Puddephatt, *Inorg. Chem.*, (1986), **25**, 4190.

34. D.G. Evans, *J. Organomet. Chem.*, (1988), **352**, 397.

35. B.R. Lloyd, A.M. Bradford and R.J. Puddephatt, *Organometallics*, (1987), **6**, 424.

CHAPTER 6

THE REACTIONS OF $[Pt_3(\mu_3\text{-}CO)(\mu\text{-}dppm)_3]^{2+}$ WITH EXCESS ISOCYANIDE

6.1 INTRODUCTION

As was suggested in the previous chapter, the reaction of one molar equivalent of isocyanide with the cluster complex **1** mimics the adsorption of methyl isocyanide on Pt(111) surfaces. It was proposed that the mechanism involved coordination of the methyl isocyanide to **1** on the same face occupied by the μ_3-carbonyl, followed by dissociation of the isocyanide and its addition to the opposite face of the triplatinum cluster.

We were particularly interested in the reactions of excess isocyanide with complex **1**, because of the possibility of the synthesis of an isocyanide-capped cluster. Isocyanides are known to be able to substitute for carbonyls in homonuclear platinum clusters,[1] and there are presently no examples of platinum clusters with isocyanides displaying the μ_3-η^1 capping coordination mode.

In this chapter we report the results of the addition of excess methyl and 2,6-dimethylphenyl isocyanide to complex **1**, as well as the structure of $[Pt_3(2,6\text{-}Me_2C_6H_3NC)_2(\mu\text{-}dppm)_3]^{2+}$, **3**, the product of the

addition of two molar equivalents of 2,6-dimethylphenyl isocyanide to complex 1.

6.2 RESULTS

6.2.1 Synthesis of $[Pt_3(2,6\text{-}Me_2C_6H_3NC_2)(\mu\text{-}dppm)_3]^{2+}$, 5

As monitored by $^{31}P\{^1H\}$ NMR spectroscopy, the addition of a second molar equivalent of $2,6\text{-}Me_2C_6H_3NC$ to $[Pt_3(\mu_3\text{-}CO)(2,6\text{-}Me_2C_6H_3NC)(\mu\text{-}dppm)_3]^{2+}$, complex 3c from the previous chapter, results in the formation of $[Pt_3(2,6\text{-}Me_2C_6H_3NC)_2(\mu\text{-}dppm)_3]^{2+}$, 5, via the intermediate $[Pt_3(\mu\text{-}CO)(2,6\text{-}Me_2C_6H_3NC)_2(\mu\text{-}dppm)_3]^{2+}$, 4 (Scheme 6.1). Dark red crystals of complex 5 were isolated in 85% yield by crystallization from an acetone/pentane mixture.

6.2.2 The Structure of $[Pt_3(2,6\text{-}Me_2C_6H_3NC)_2(\mu\text{-}dppm)_3][PF_6]_2\cdot(CH_3)_2CO$, 5

The structure was solved in collaboration with Dr. N.C. Payne at the University of Western Ontario and consisted of cations, PF_6 anions and a loosely entrapped acetone of solvation. In the cation (Figure 6.1) the platinum atoms form an isosceles triangle with Pt-Pt distances of 2.652(1), 2.647(1) and 2.581(1) Å and Pt-Pt-Pt angles of 58.31(3), 60.74(4) and 60.95(4)[6] (Table 6.1). The Pt-Pt distances are in the expected range for normal Pt-Pt single bonds and the average Pt-Pt distance of 2.627(1) Å is shorter than the average Pt-Pt distance of 2.634(1) Å found for $[Pt_3(\mu_3\text{-}CO)(\mu\text{-}dppm)_3]^{2+}$,[2] 1, of

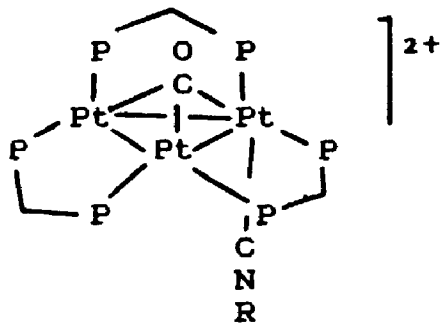

+ $2,6\text{-}Me_2C_6H_3NC$ $\xrightarrow{-92°C}$

$R = 2,6\text{-}Me_2C_6H_3$

3a

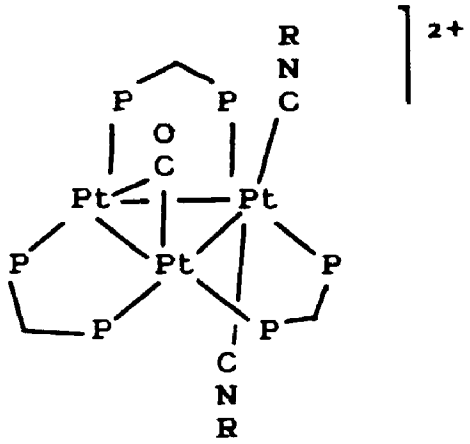

4

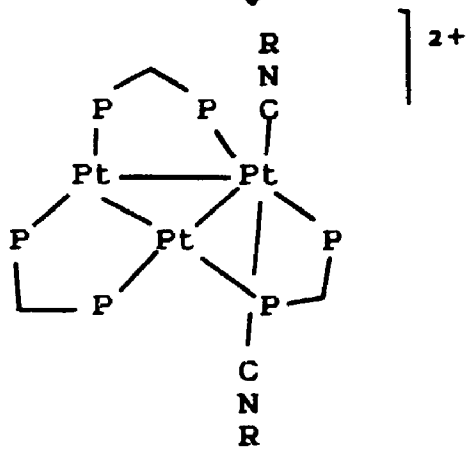

5

Scheme 6.1

2.639(1) Å found for $[Pt_3(\mu_3\text{-}CO)\{P(OPh)_3\}(\mu\text{-}dppm)_3]^{2+}$ [3] and of 2.639(3) Å for $[Pt_3(\mu_3\text{-}CO)(\mu_3\text{-}SnF_3)(\mu\text{-}dppm)_3]^{1+}$ [4] which all have μ_3-carbonyl ligands. Hence the electrons associated with the isocyanide ligands must enter metal-metal bonding orbitals as opposed to nonbonding or antibonding orbitals.

The isocyanides are bound to Pt(1) with Pt(1)-C(9) and Pt(1)-C(19) distances of 1.93(2) and 1.98(2) Å respectively. The Pt(2)-C(9), Pt(2)-C(19), Pt(3)-C(9) and Pt(3)-C(19) distances are 2.95(2), 3.26(2), 2.97(2) and 2.84(2) Å, respectively. These distances are too long to indicate any bonding interaction, however.

The isocyanide ligands are approximately linear with C-N-C angles of 176(3) and 168(3) for C(9) and C(19) respectively. The CN bond lengths are 1.20(2) and 1.14(3) which are in the expected range for C≡N triple bonds. It is interesting to note that the phenyl rings are oriented in such a way that the phenyl ring associated with C(9) is approximately parallel to the Pt(2)-Pt(3) vector while the ring associated with C(19) is approximately perpendicular to it. It is likely that the rings have this orientation to allow the $Pt_3(\mu\text{-}dppm)_3$ core, which contains twelve phenyl rings already, to accommodate the additional two associated with the isocyanide ligands. It is also interesting to note that the isocyanide ligands are not normal to the Pt_3 plane but, that the isocyanide associated with C(19), in particular, is tilted in along the

FIGURE 6.1: ORTEP Diagram of 5 (1)

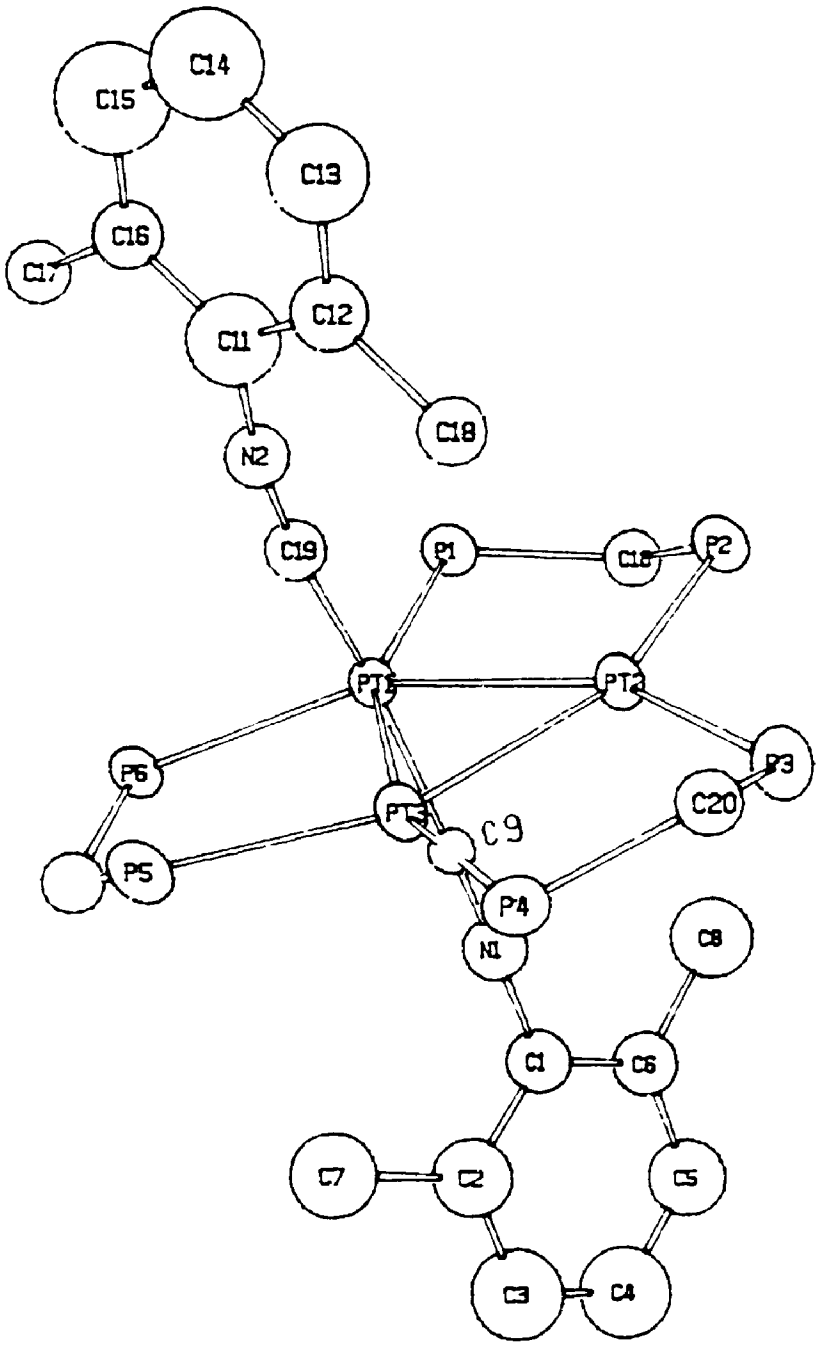

TABLE 6.1: Bond Lengths and Angles for $[Pt_3(2,6\text{-}Me_2C_6H_3NC)_2(\mu\text{-}dppm)_3]^{2+}$

Bond Lengths (Å)		Bond Angles (°)	
Pt(1) - Pt(2)	2.652(1)	Pt(1) - Pt(2) - Pt(3)	60.95(4)
Pt(1) - Pt(3)	2.647(1)	Pt(2) - Pt(1) - Pt(3)	58.31(3)
Pt(2) - Pt(3)	2.581(1)	Pt(2) - Pt(3) - Pt(1)	60.95(4)
Pt(1) - P(1)	2.403(7)	Pt(1) - C(9) - N(1)	173(2)
Pt(1) - P(6)	2.518(7)	Pt(1) - C(19) - N(2)	171(2)
Pt(2) - P(2)	2.246(8)	C(9) - N(1) - C(1)	176(3)
Pt(2) - P(3)	2.162(7)	C(19) - N(2) - C(11)	168(3)
Pt(3) - P(4)	2.202(7)	C(9) - Pt(1) - Pt(2)	78.4(7)
Pt(3) - P(5)	2.411(8)	C(9) - Pt(1) - Pt(3)	79.2(7)
Pt(1) - C(9)	1.93(2)	C(19) - Pt(1) - Pt(2)	88.1(8)
C(9) - N(1)	1.20(3)	C(19) - Pt(1) - Pt(3)	73.9(7)
N(1) - C(1)	1.34(3)	C(19) - Pt(1) - C(9)	153(1)
Pt(1) - C(19)	1.98(2)		
C(19) - N(2)	1.14(3)		
N(2) - C(11)	1.41(3)		
C(9) - Pt(2)	2.95(2)		
C(9) - Pt(3)	2.97(2)		
C(19) - Pt(2)	3.26(2)		
C(19) - Pt(3)	2.84(2)		

Pt(1)-Pt(3) vector (Figure 6.2). The angle C(19)-Pt(1)-C(9) is 153.05(95)°. This "tilt" of the isocyanides probably minimizes steric interactions between the phenyl rings in the cluster.

Each edge of the platinum triangle is bridged by a dppm ligand and the Pt_3P_6 atoms are approximately coplanar. In the Pt_2P_2C rings the two methylene groups closest to Pt(1) lie below the plane of the Pt_3 triangle while the third lies above it. Such a conformation of the $Pt_3P_6C_3$ skeleton serves to direct the majority of dppm phenyl rings above the Pt_3 plane and away from the isocyanide with the phenyl ring parallel to the Pt(2)-Pt(3) vector. The Pt-P distances consisted of three longer [2.518(7), 2.403(7) and 2.411(8) Å] and three shorter distances [2.246(7), 2.202(7) and 2.162(7) Å].

This can be compared with the Pt-P distances observed in the cluster $[Pt_3(\mu_3\text{-}CO)\{P(OPh)_3\}(\mu\text{-}dppm)_3]^{2+}$. In this case the Pt-P bond lengths involving Pt(1), the platinum atom to which the $P(OPh)_3$ ligand is bound were longer [2.341(8) and 2.335(8) Å] than those involving Pt(2) and Pt(3) [2.290(8), 2.323(8), 2.288(8) and 2.300(8) Å]. The tertiary phosphite lies directly beneath Pt(1) and these variations in Pt-P bond distances were thought to arise from a rehybridization of platinum orbitals due to the higher coordination number Pt(1), or from steric congestion around Pt(1). In $[Pt_3(2,6\text{-}Me_2C_6H_3NC)_2(\mu\text{-}dppm)_3]^{2+}$, however, the elongation

FIGURE 6.2: ORTEP Diagram of 5 (2)

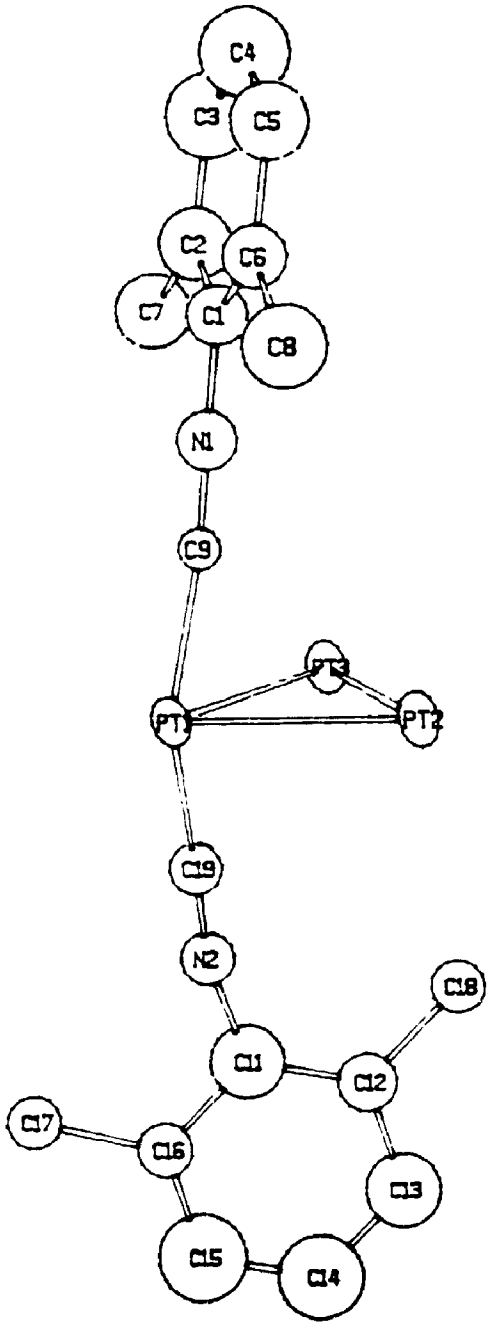

of Pt(3)-P(5), in particular, suggests that steric factors are primarily responsible for these results in that the C(19) isocyanide lies beneath the Pt(1)-Pt(3) bond.

6.2.3 Characterization of $[Pt_3(2,6\text{-}Me_2C_6H_3NC)_2(\mu\text{-}dppm)_3]^{2+}$, 5, by Spectroscopic Methods

The CN stretching frequency of the isocyanide ligands in complex 5 was 2122 cm^{-1} which is indicative of the presence of terminal isocyanides.

Complex 5 was fluxional at room temperature and the NMR spectra had to be run at -92°C to freeze out the fluxionality. At room temperature the resonances due to the dppm phosphorus atoms in the $^{31}P\{^1H\}$ NMR spectrum broaden significantly and begin to coalesce. The observed fluxionality is most likely to involve migration of the isocyanides about both faces of the Pt_3 cluster. It is not possible to tell, however, if ligand migration involves a $Pt_2(\mu_2\text{-}CNR)_2$, or a $Pt_3(\mu_3\text{-}CNR)_2$ transition state, 6 or 7 respectively, but the low activation energy for fluxionality of complex 5 opens up the possibility that stable complexes with such functional groups might be prepared.

The ^1H NMR spectrum of complex 5 at -90°C consisted of a singlet resonance at 2.30 ppm due to the methyl groups of the $2,6\text{-}Me_2C_6H_3NC$ ligands and a broad resonance due to the protons of the methyl groups at 5.82 ppm. Since the x-ray structure shows non-equivalent isocyanide groups, it

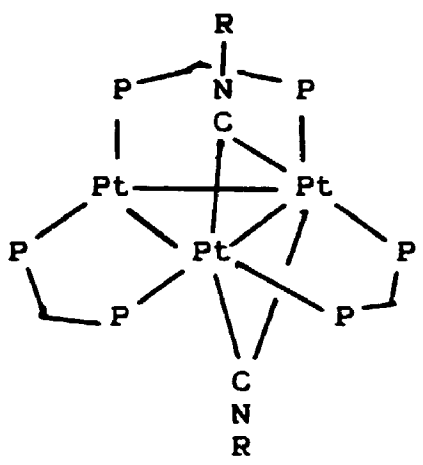

6

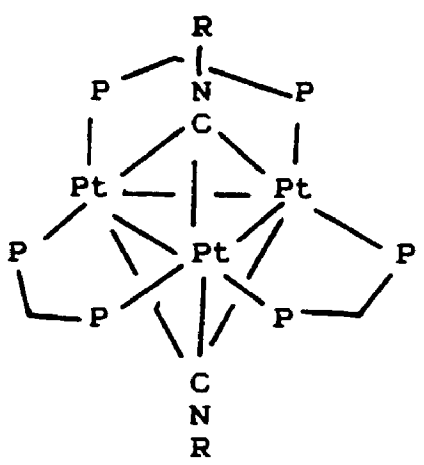

7

seems that rotation of the isocyanides about the Pt-C bonds is possible and leads to equivalence of the methyl groups.

The $^{31}P\{^{1}H\}$ NMR spectrum of complex **5** consisted of two doublet resonances and a singlet resonance all with platinum satellites (Figure 6.3).

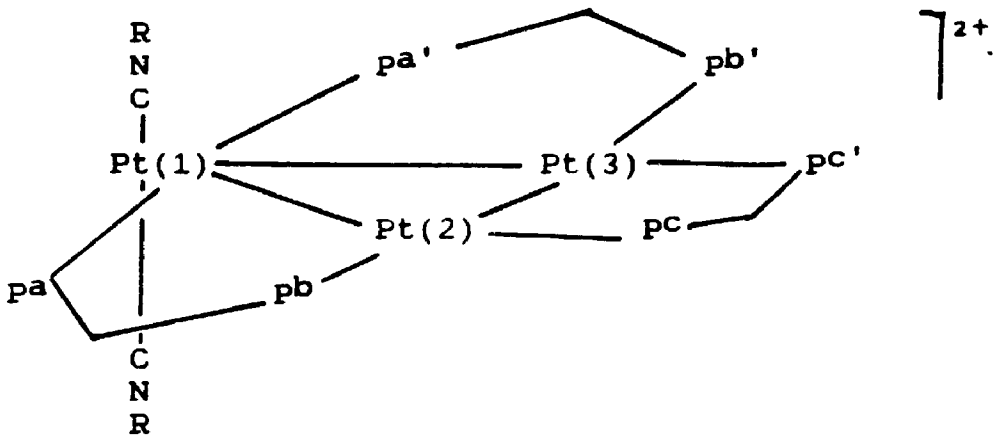

R = 2,6-$Me_2C_6H_3$

5

The doublet resonances are due to the trans-like coupling of P^a and P^c across the Pt-Pt bonds while the singlet

FIGURE 6.3: $^{31}P\{^{1}H\}$ NMR Spectrum of 5

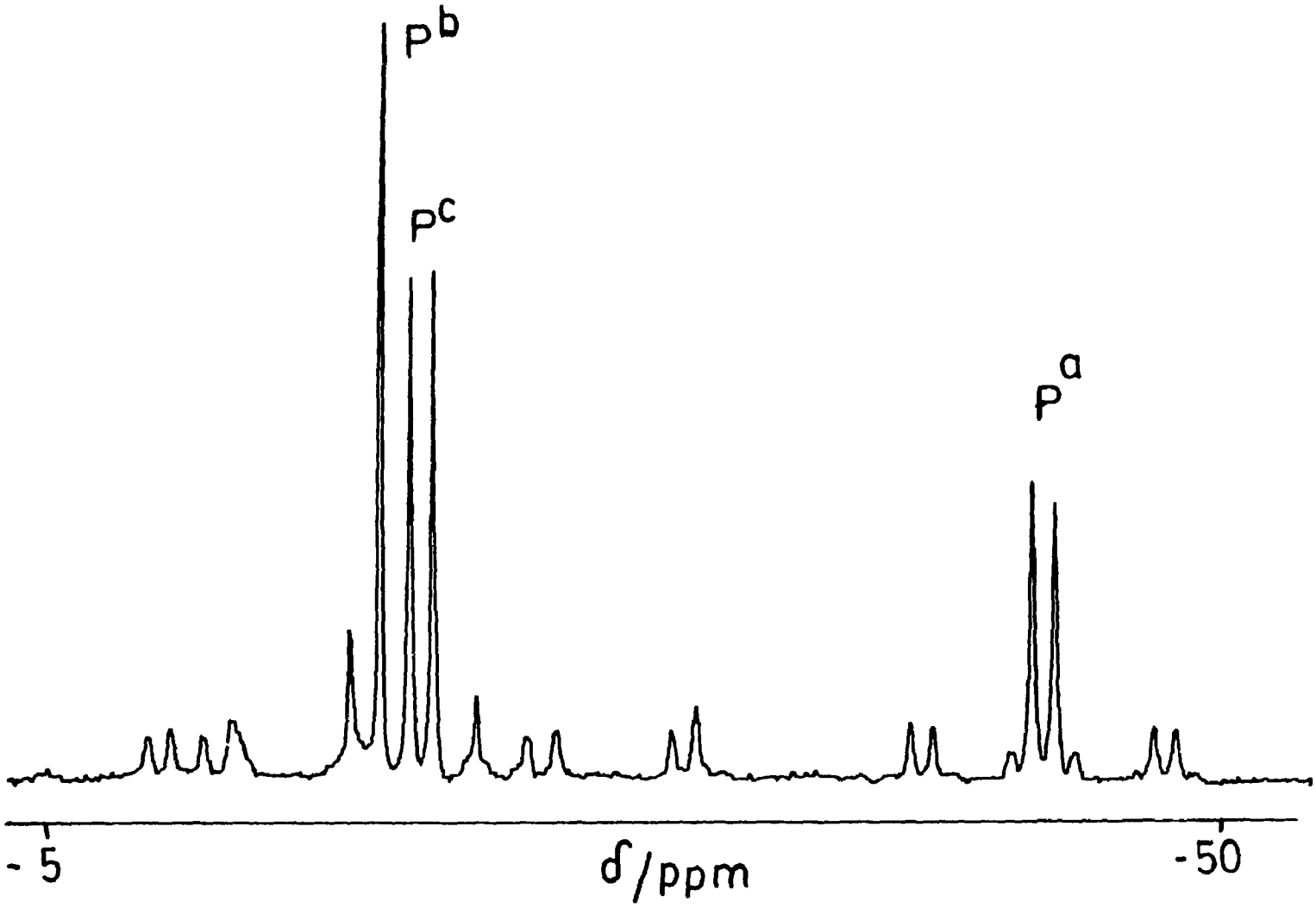

resonance is due to P^b (Table 6.2). The resonances due to P^a and P^c were assigned by correlation of the $^1J(PtP)$ values with the Pt-P bond distances and with the ^{195}Pt NMR data.

The $^{195}Pt\{^1H\}$ NMR spectrum of complex 3 consisted of two sets of resonances (Figure 6.4). The first was a triplet of quintets due to Pt(1) [δ Pt(1) = -3190 ppm, $^1J(Pt(1)P^a)$ = 1776 Hz, $^1J(Pt(1)Pt(2)$ = 900 Hz] and the second was a doublet of doublets due to Pt(2) [δ Pt(2) = -2002 ppm, $^1J(Pt(2)P^b)$ = 2600 Hz, $^1J(Pt(2)P^c)$ = 4200 Hz]. The magnitude of the coupling constant $^1J(Pt(1)Pt(2))$ = 900 Hz verifies the existence of a bonding interaction between these two platinum atoms.

6.2.4 Characterization of the Intermediate, 2

As monitored by $^{31}P\{^1H\}$ NMR, the intermediate appeared at -92°C, immediately upon the addition of a second molar equivalent of isocyanide, and persisted until approximately -20°C after which time the μ_2-CO dissociated to yield complex 3. The intermediate was not fluxional in the above temperature range.

The $^{31}P\{^1H\}$ NMR spectrum of complex 4 consisted of two doublet resonances and a singlet, all with platinum satellites in a 1:1:1 intensity ratio (Table 6.1 and Figure 6.5). In this case, as in complex 5, the multiplicities are due to coupling across metal-metal bonds and indicate that all three metal-metal bonds are intact.

FIGURE 6.4: $^{195}Pt\{^{1}H\}$ NMR Spectrum of 5

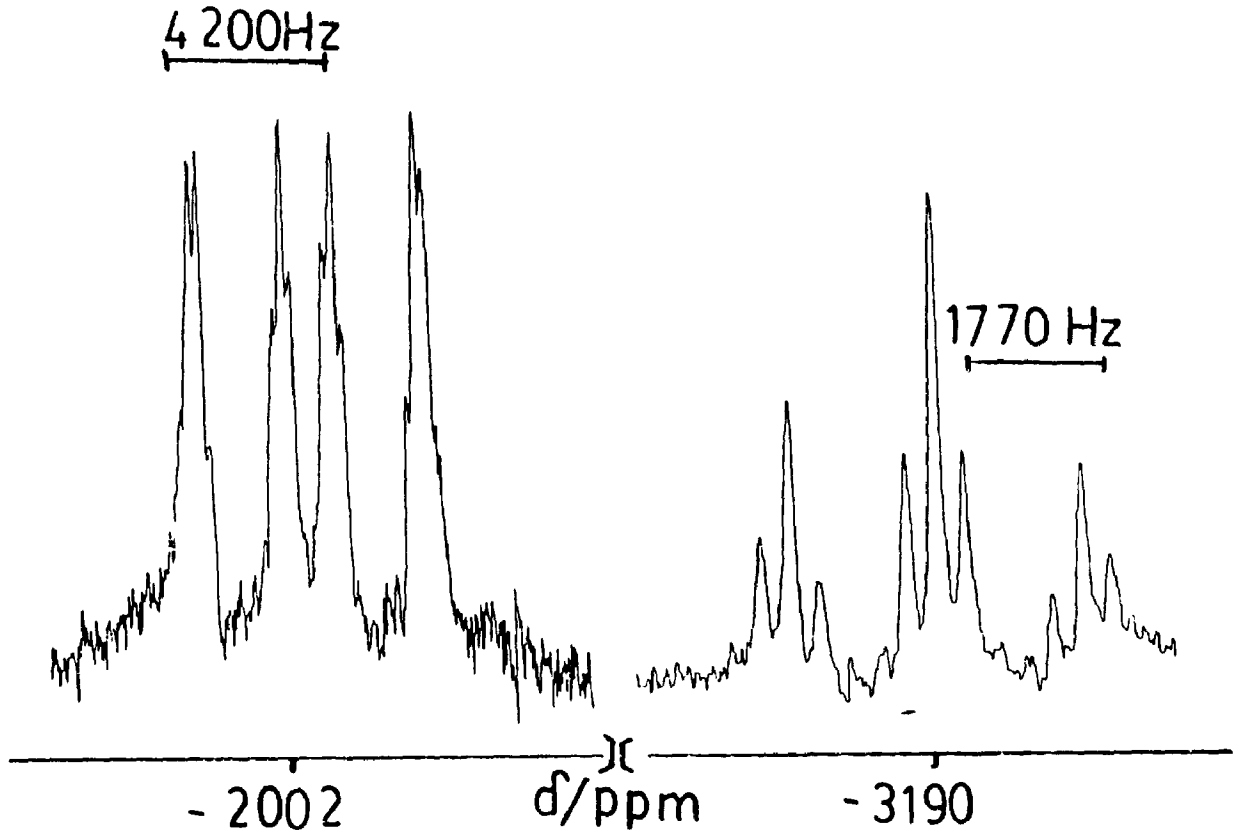

TABLE 6.2: $^{31}P\{^{1}H\}$ NMR Data for Complexes 4 and 5

	4	5
δ P^a/ppm	-41.3	-47.8
$^1J(PtP^a)$/Hz	2200	1760
$^2J(PtP)$/Hz	300	310
$^3J(P^aP^c)$/Hz	200	160
δ P^b/ppm	-63.0	-7.6
$^1J(PtP^b)$/Hz	3090	2440
$^2J(PtP)$/Hz	348	---
$^3J(P^bP^{b'})$/Hz	180	220
δ P^c/ppm	-24.1	-16.7
$^1J(PtP^c)$/Hz	3380	4030
$^3J(P^aP^c)$/Hz	180	160

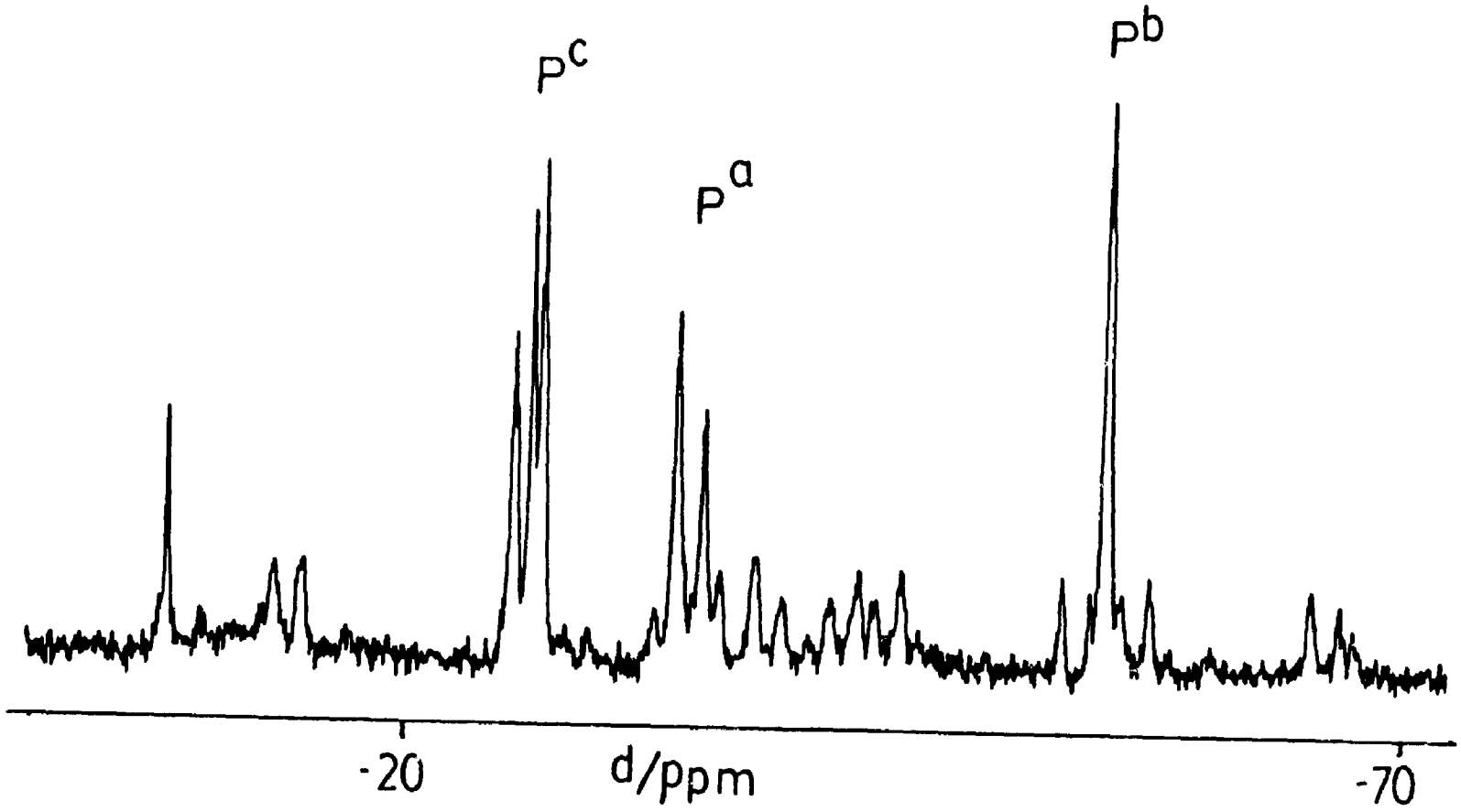

FIGURE 6.5: $^{31}P\{^{1}H\}$ NMR Spectrum of 4

The $^{13}C\{^{1}H\}$NMR spectrum revealed a μ_2-carbonyl at δ = 217.4 ppm, $^{1}J(PtC)$ = 908 Hz (Figure 6.6).

Both the NMR data and the lack of fluxionality allow us to propose the following structure for the intermediate in this case.

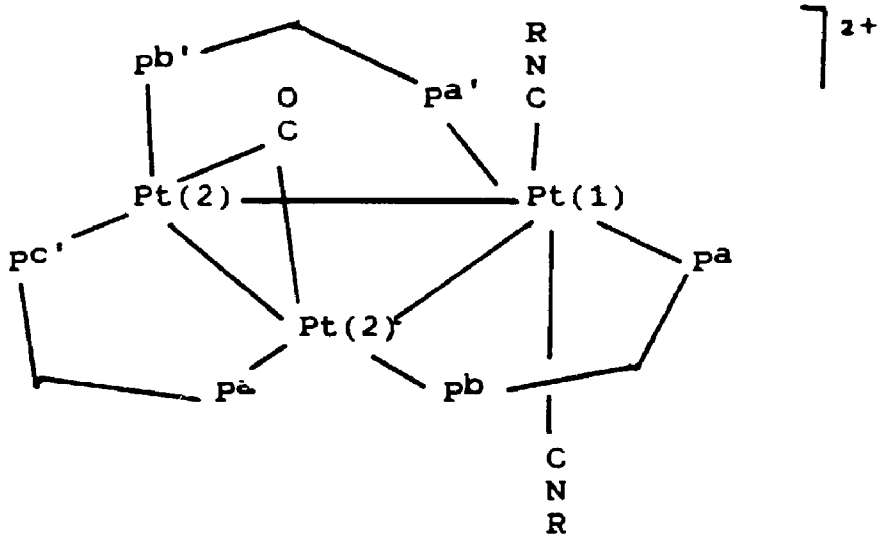

R = 2,6-$Me_2C_6H_3$

4

Complex 4 is formed by the attack of the second molar equivalent of isocyanide on the face of complex 3a which is occupied by the μ_3-carbonyl. This results in the formation of an intermediate species with a μ_2-carbonyl and two terminal isocyanides. The second isocyanide must add on at the face opposite the first terminal isocyanide because addition on the same face would be prohibited by steric factors.

FIGURE 6.6: $^{13}C\{^{1}H\}$ NMR Spectrum of 4

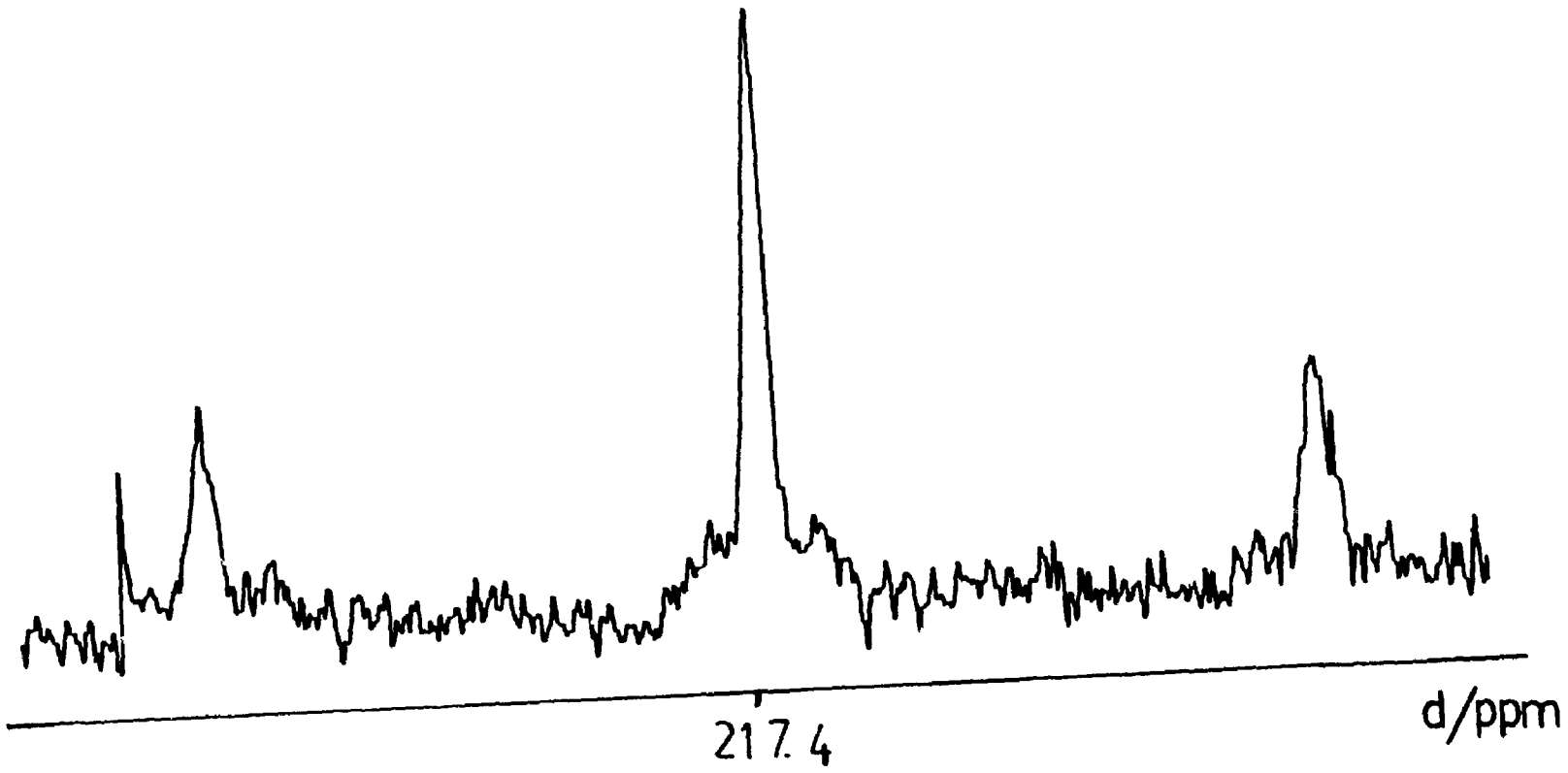

6.2.5 The Addition of Greater than 2 Equivalents of Isocyanide to $[Pt_3(\mu_3\text{-}CO)(\mu\text{-}dppm)_3]^{2+}$, 1

Studies done with $2,6\text{-}Me_2C_6H_3NC$ showed that no reaction occurred after the second molar equivalent of isocyanide was added to complex 1. The steric bulk of this isocyanide probably hinders the addition of greater than two equivalents of isocyanide to the cluster. This is not the case, however, with methyl isocyanide.

The $^{31}P\{^1H\}$ NMR spectrum obtained when a large excess (between 4 and 5 molar equivalents) of methyl isocyanide was added to complex 1 at low temperature, consisted of two singlet resonances with platinum satellites [δ P^a = 10.4 ppm, $^1J(PtP)$ = 3180 Hz, $^2J(PtP)$ = 210 Hz, δ P^b = 7.5 ppm, $^1J(PtP)$ = 3200 Hz, $^2J(PtP)$ = 210 Hz]. The long range coupling observed for each of these resonances indicates the existence of at least one metal-metal bond. No singlet resonances with platinum satellites were observed, therefore no monomeric phosphorus-containing platinum species were formed.

The spectral data is consistent with structure 8 since μ_3-CNMe does not appear to be likely based on our work outlined in both the previous chapter and this one.

Complex 5 is similar to a trinickel cluster recently reported by Kubiak[5] et al except that in Kubiak's cluster the bottom face of the Ni_3 triangle is capped by an iodide ligand. Preliminary reactivity studies indicate that the

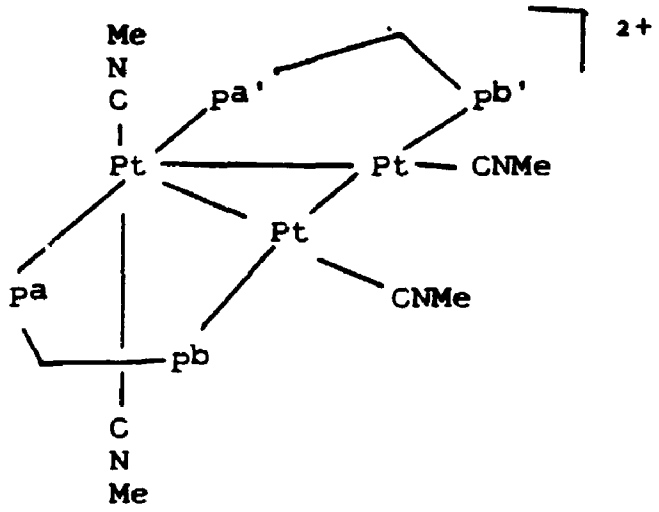

8

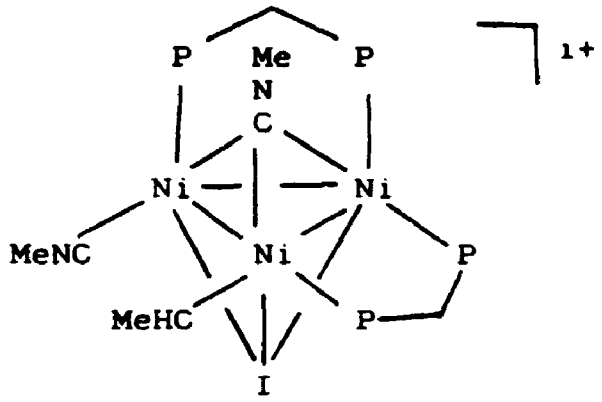

capping iodide is essential to the stability of this cluster.

The resonances due to the platinum-methyl isocyanide species in the $^{31}P\{^{1}H\}$ NMR spectrum are significantly broadened at room temperature and indicate that this species is fluxional at this temperature.

From the results obtained in this study it is possible to say that with the smaller isocyanides, the addition of excess ligand to complex 1 results in the

substitution of isocyanides from dppm. It is logical to postulate that, if this process is taken far enough, cluster degradation will occur. The substitution probably proceeds via a dissociative mechanism since there would not be adequate room to allow additional isocyanides to coordinate before the dppm ligands dissociate.

6.3 DISCUSSION

The results reported in this chapter are important in our group's ongoing study of $Pt_3(\mu\text{-dppm})_3$ clusters,. The structure of $[Pt_3(2,6\text{-}Me_2C_6H_3NC)_2(\mu\text{-dppm})_3]^{2+}$, 5, is novel in that it is the first such cluster with no capping ligand. This is especially surprising considering that Mealli's theoretical study of Pt_3L_6 clusters revealed that bridging ligands tend to stabiiize the a_1' orbital, and that this is an important factor in stabilizing clusters such as $[Pt_3(\mu_3\text{-}CO)(\mu\text{-dppm})_3]$,[6] 1. Theoretical calculations are presently being done on complex 5.

The structure of complex 3 is also interesting from the point of view that both terminal isocyanides bond to Pt(1). $[Pt_3(2,6\text{-}Me_2C_6H_3NC)_2(\mu\text{-dppm})_3]^{2+}$, 5, is a dicationic cluster and, if the 18 electron rule is to be obeyed by this atom, it must be Pt(II) while the other two are Pt(O). This is an apparent violation of the Pauling Electroneutrality principle which says that the 2+ charge should be spread out evenly over the three platinum atoms,

as opposed to being localized on Pt(1). At present we are unsure about why this is the case.

D.G. Evans has predicted,[7] and it has been verified by the experimental results discussed in the previous chapter, that a slip distortion of the capping carbonyl in $[Pt_3(\mu_3\text{-}CO)(\mu\text{-}dppm)_3]^{2+}$ monoisocyanide complexes is observed due to the carbonyl ligand's ability to behave as a π-acceptor ligand. In the bis(isocyanide) case this situation is carried to an extreme in that both isocyanides are now terminal.

6.4 CONCLUSIONS

The addition of excess isocyanide to complex **1** indicates strongly that although much is known about the reactivity of $[Pt_3(\mu_3\text{-}CO)(\mu\text{-}dppm)_3]^{2+}$, **1**, more can still be learned. For example, it would not have been predicted by various theoretical and experimental studies that $[Pt_3(2,6\text{-}Me_2C_6H_3NC)_2(\mu\text{-}dppm)_3]^{2}$, **5**, would contain two terminal isocyanides as it has been shown to by crystallographic and spectral data.[8] Rather, complex **1** continues to be a source of novel structures in the field of platinum cluster chemistry. The ability of complex **1** to react with large excesses of methyl isocyanide demonstrates, yet again, the ability of the bridging dppm ligands to prevent cluster fragmentation.

6.5 REFERENCES

1. C.E. Briant, D.I. Gilmour, D.M.P. Mingos and R.W.M. Wardle, *J. Chem. Soc., Dalton Trans.*, (1985), 1693.
2. G. Ferguson, B.R. Lloyd and R.J. Puddephatt, *Organometallics*, (1986), **5**, 344.
3. A.M. Bradford, G. Douglas, Lj. Manojlovic-Muir, K.W. Muir and R.J. Puddephatt, submitted.
4. Personal correspondence with M.C. Jennings and R.J. Puddephatt.
5. K.S. Ratliff, G.K. Brocker, P.E. Fanwick and C.P. Kubiak, submitted.
6. C. Mealli, *J. Am. Chem. Soc.*, (1985), **107**, 224.
7. D.G. Evans, *J. Organomet. Chem.*, (1988), **352**, 397.
8. A.M. Bradford, N.C. Payne, D.S. Yang and R.J. Puddephatt, manuscript in preparation.

CHAPTER 7

OXIDATIVE ADDITION: THE REACTION OF $[Pt_3(\mu_3\text{-}CO)(\mu\text{-}dppm)_3]^{2+}$ WITH ISOTHIOCYANATES

7.1 INTRODUCTION

Although it has been recognized from as early as 1967 that a close analogy exists between the reactions of unsaturated molecules such as carbon disulphide and the isothiocyanates,[1] RNCS, the C=S bond cleavage of RNCS groups has been much less studied than that of OCS or CS_2.[2-13] Both CS_2 and OCS undergo C=S bond cleavage when more than one metal centre is present in their reactions with low oxidation state platinum complexes. In the case of CS_2, the carbon atom of the coordinated CS_2 ligand is attacked by a nucleophilic Pt(0) molecule as shown in Scheme 7.1, on the following page. This reaction can be reversed to give the recombination of CS_2.[4-6]

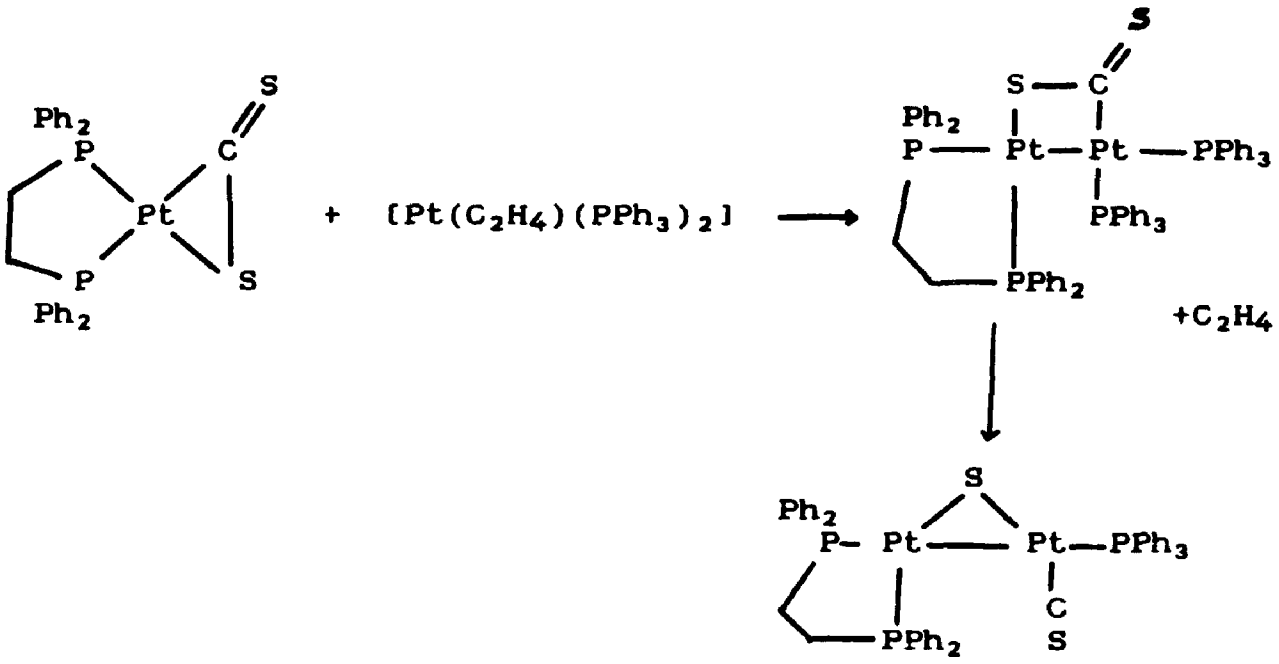

Scheme 7.1

For carbonyl sulphide the reaction occurs according to Scheme 7.2.[7]

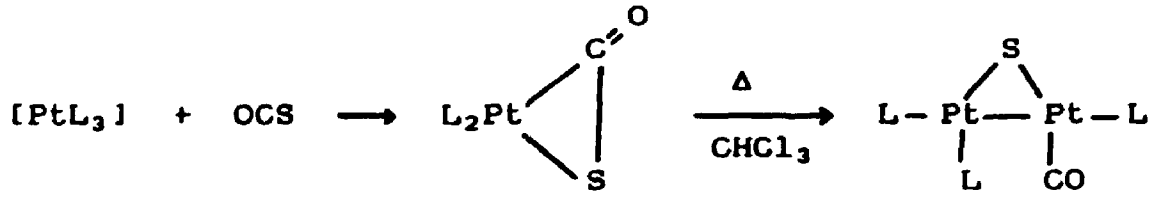

Scheme 7.2

Carbon disulphide causes fragmentation of the trinuclear cluster $[Pt_3(\mu\text{-}CO)_3L_3]$, L = P^tBu_2Ph, to give $[Pt_2(\mu_2\text{-}\eta^3\text{-}CS_2)_2L_2]$ or $[Pt_2(\mu\text{-}S)(CO)_2L_2]$, and adds to the Pt-Pt bond of $[Pt_2Cl_2(\mu\text{-dppm})_2]$ to give $[Pt_2Cl_2(\mu_2\text{-}\eta^2\text{-}CS_2)(\mu\text{-dppm})_2]$.[8-10]

Due to the similarities that exist between the isothiocyanates and OCS and CS_2, it was of interest to extend this chemistry to studies with the locked trinuclear cluster $[Pt_3(\mu_3\text{-}CO)(\mu\text{-}dppm)_3]^{2+}$, 1, which is much more stable to fragmentation than the clusters $[Pt_3(\mu\text{-}CO)_3L_3]$ studied by Farrar and coworkers, in the hope that the mechanism of C=S bond cleavage at a cluster centre might be clearer if the nuclearity could be maintained by bridging ligands.

7.2 RESULTS

7.2.1 Synthesis

The major chemical results are shown in Equation 7.1. As monitored by $^{31}P\{^1H\}$ NMR spectroscopy, reaction of complex 1 with an equimolar amount of RNCS resulted in initial complexation of the added ligand followed by cleavage of the S=C bond to yie'd complex 3, and the displacement of the terminally bound CO by isocyanide to yield complexes 4a-4c. These complexes, 4, were thermally stable and could be isolated in analytically pure form as the hexafluorophosphate salts in about 90% yield. Yellow crystals of complexes 4 were obtained by fractional recrystallization from an acetone/pentane mixture.

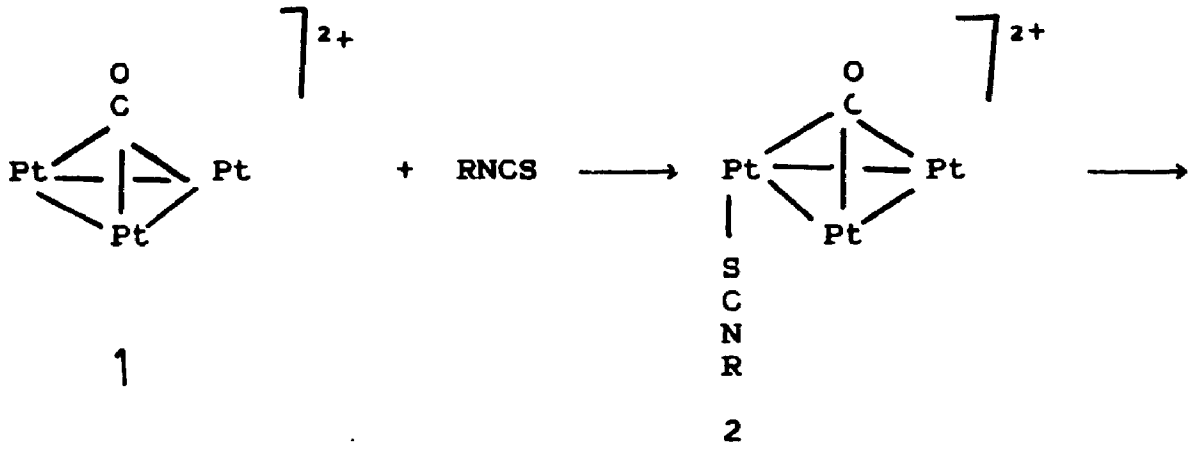

1 2

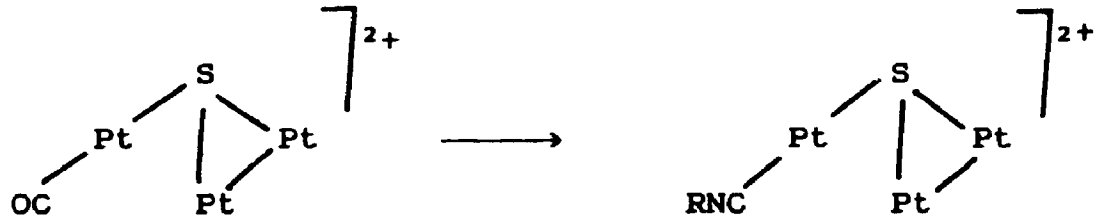

3 4

3a:	R = Me	**4a:**	R = Me
3b:	R = ^{t}Bu	**4b:**	R = ^{t}Bu
3c:	R = Ph	**4c:**	R = Ph

* dppm ligands are omitted for clarity

Equation 7.1

7.2.2 Initial Complexation of the Cluster

The reagents studied form initial complexes with $[Pt_3(\mu_3\text{-}CO)(\mu\text{-}dppm)_3]^{2+}$, **1**, in a similar way to that established earlier for SCN^-.[11]

By analogy with this precedent it is proposed that the complexes have structure **2** with terminal isothiocyanate groups. With all of the ligands studied the $^{31}P\{^1H\}$ NMR spectra of complexes **2** gave only a single resonance even at

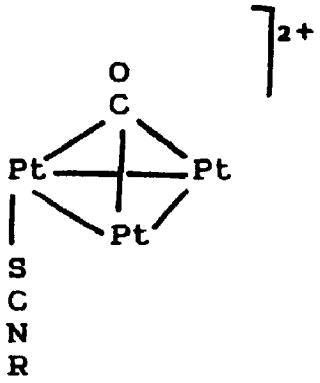

2

low temperature (Table 7.1 and Figure 7.1). The complexes must therefore be fluxional. This fluxionality was previously observed for the thiocyanate complex and involves migration of the RNCS group about the platinum triangle. These adduct clusters were short-lived intermediates which were not isolable; however, the $^{31}P\{^{1}H\}$ NMR parameters are so similar to those of the stable SCN^- adduct that there is little doubt about their structures.

TABLE 7.1: $^{31}P\{^{1}H\}$ NMR Parameters of the Complexes $[Pt_3(\mu_3\text{-}CO)(SCNR)(\mu\text{-}dppm)_3]^{2+}$

Complex	δ (^{31}P)[a]	$^{1}J(PtP)$
4a	-16.7	3714
4b	-16.7	3660
4c	-17.1	3570
5[b]	-17.7	3670

[a] Reference is H_3PO_4.

[b] 5 is $[Pt_3(\mu_3\text{-}CO)(SCN)(\mu\text{-}dppm)_3]^{2+}$

FIGURE 7.1 $^{31}P\{^{1}H\}$ NMR Spectrum of 2

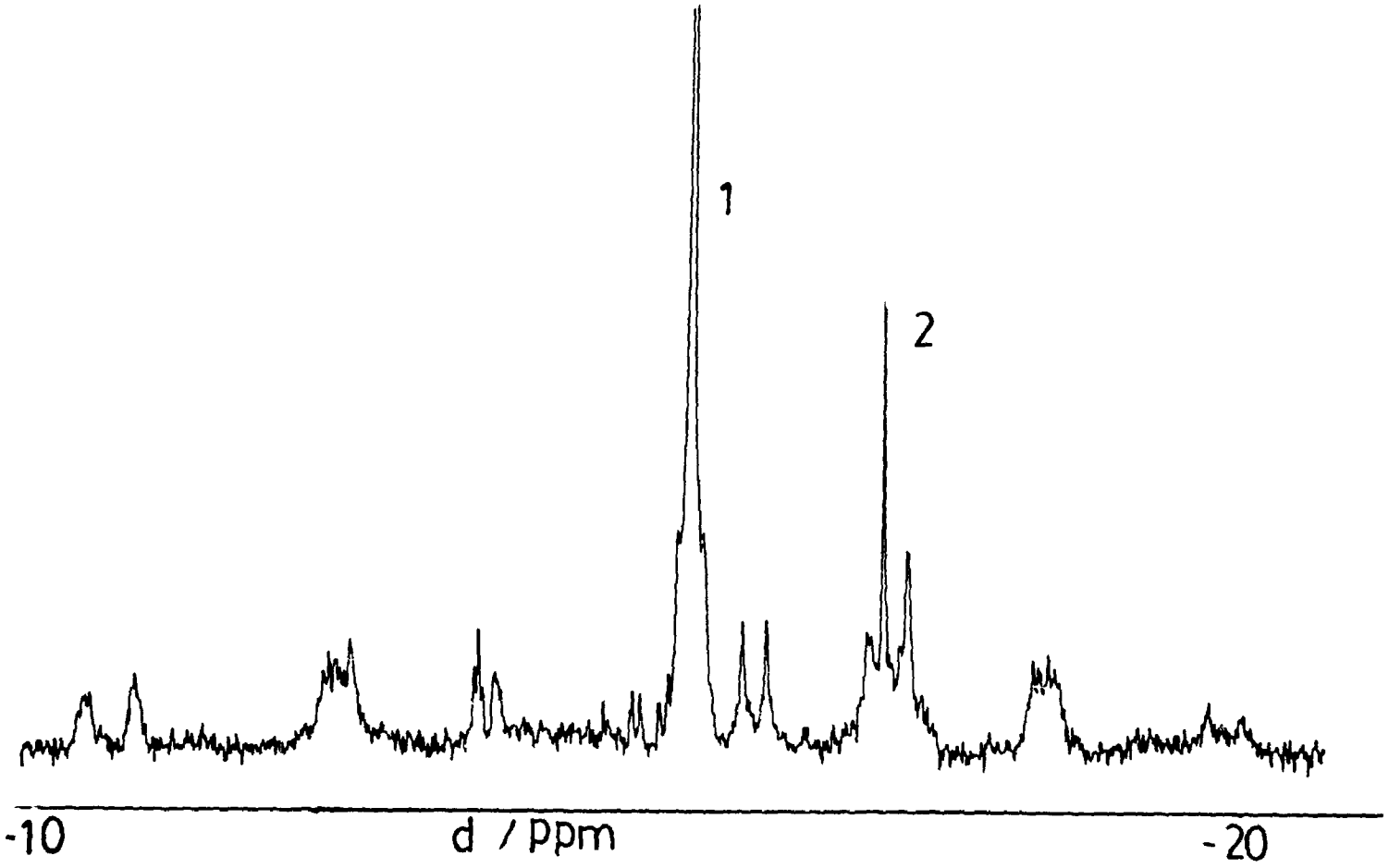

7.2.3 Further Intermediates

The initially formed equilibrium mixture of 1 and 2 reacted further at -40°C to form complex 3 which was characterized as $[Pt_3(\mu_3\text{-}S)(CO)(\mu\text{-}dppm)_3]^{2+}$. The cluster cation consists of an isosceles triangle of platinum atoms linked by dppm ligands and a triply bridging sulphur atom. The terminal carbonyl is located trans to the bridging sulphide.

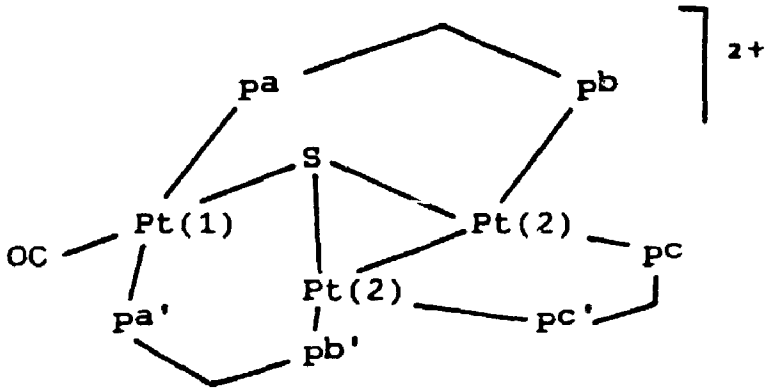

3

The structures of the similar complexes $[Pd_3(\mu_3\text{-}S)(CN)(\mu\text{-}dppm)_2]^{1+}$[11] and $[Pt_3H(\mu_3\text{-}S)(\mu\text{-}dppm)_3]^{1+}$[14] have been determined crystallographically and the spectral properties are characteristic of a structure for 3 with just one Pt-Pt bond.

The $^{31}P\{^1H\}$ NMR spectrum of 3 consisted of three singlet resonances with platinum satellites (Table 7.2 and Figure 7.2). The spectrum is complicated by the presence of spectra due to various isotopomers of the Pt_3 cluster which will be described later in this chapter.

TABLE 7.2: ^{31}P NMR Parameters of the Complexes $[Pt_3(\mu_3\text{-}S)(CNR)(\mu\text{-}dppm)_3]^{2+}$

Complex	δ (P^a)[a]	δ (P^b)	δ (P^c)	$^1J(PtP^a)$	$^1J(PtP^b)$	$^1J(PtP^c)$	$^2J(PtP^b)$	$^3J(P^bP^b)$
4a	15.0	-0.7	-12.4	2410	3020	3980	170	170
4b	15.2	0.9	-12.5	2420	3040	3980	170	160
4c	15.3	0.3	-12.2	2400	3040	3960	170	170

[a] Reference H_3PO_4.

FIGURE 7.2: Variable Temperature $^{31}P\{^{1}H\}$ NMR Spectrum of 3 and 4

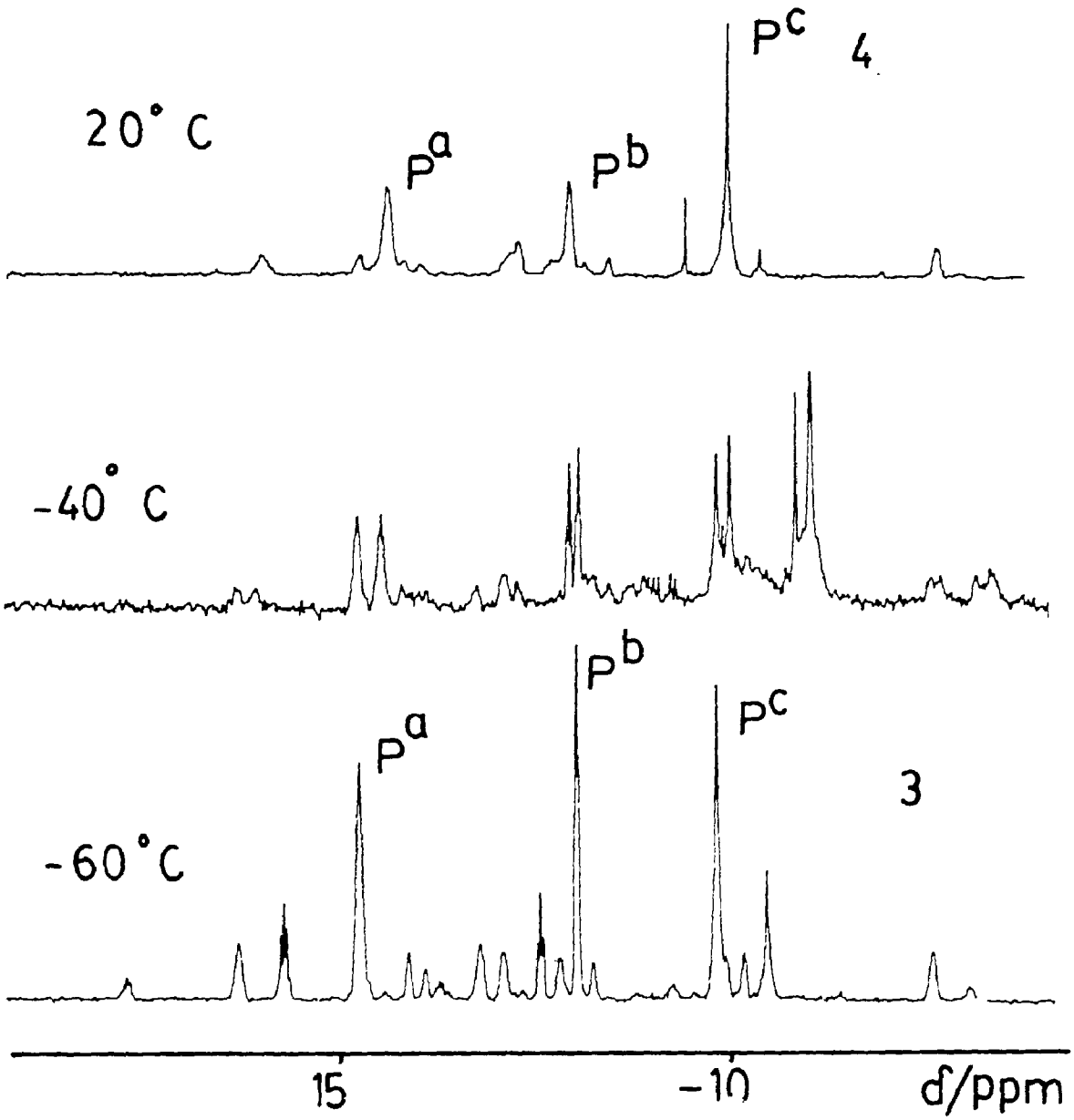

The $^{13}C\{^1H\}$ NMR spectrum of **3** consisted of a triplet resonance with relative intensity 1:4:1 (δ ^{13}CO = 164.45 ppm, $^1J(PtC)$ = 1421 Hz) (Figure 7.3). The multiplicity and relative intensities of this resonance indicate a carbonyl group bound terminally to a platinum atom. This compares favourably with the $^{13}C\{^1H\}$ NMR data obtained for the complex

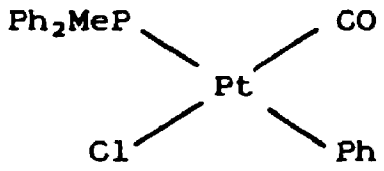

in which the carbonyl is trans to the chloride ligand [δ ^{13}C = 162.1 ppm, $^1J(PtC)$ = 1947 Hz, $^2J(PC)$ = 8 Hz].[15] Since the trans directing ability of the chloride ligand is similar to that of a sulphide group, it is apparent that the chemical shift for the carbonyl and the platinum-carbon coupling constant is in line with the values observed for **3**.

The $^{195}Pt\{^1H\}$ NMR spectrum of **3** consisted of a triplet due to Pt(1), [δ = -2809.1 ppm], and a doublet of doublets due to Pt(2), [δ = -3171 ppm]. The multiplicities are the result of one bond platinum phosphorus couplings. More complex spin systems due to the various isotopomers for the platinum cluster are seen to lead to further fine structure in the Pt(2) resonance. The ^{195}Pt spectrum of **3**, enriched with ^{13}CO, showed the triplet resonance due to

FIGURE 7.3: $^{13}C\{^{1}H\}$ NMR Spectrum of 3

Pt(1) to be split into a triplet of doublets due to coupling to the terminal ^{13}CO group.

7.2.4 Spectral Characterization of the Final Products

On warming complex 3 above -20°C the carbonyl group trans to the triply bridging sulphide exchanges with the isocyanide to give products of the form $[Pt_3(\mu_3\text{-}S)(CNR)(\mu\text{-}dppm)_3]^{2+}$, 4.

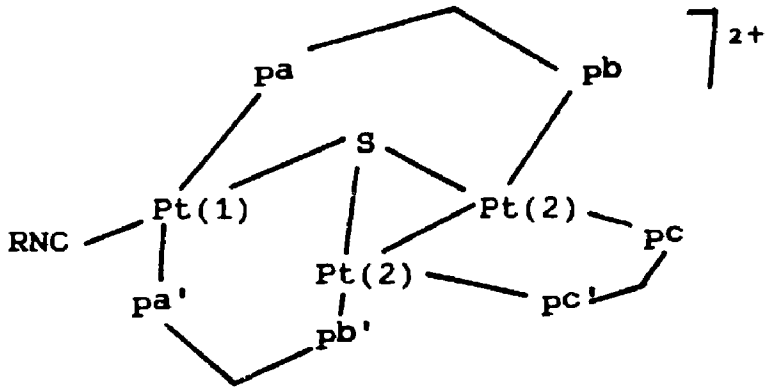

4

The infrared spectra of 4a-4c displayed isocyanide stretching frequencies of 2215 to 2287 cm^{-1}. These values are in the range expected for terminal isocyanide ligands.

The $^{31}P\{^1H\}$ NMR spectra for complexes 4a-4c consisted of three distinct signals due to P^a, P^b and P^c (Figure 7.2). The further complexity of the spectrum is due to the four isotopomers which are present as a result of zero, one, two or three spin active ^{195}Pt nuclei; (I = 1/2, 33.8% natural abundance) in the cluster. There are six possible isotopomers for the three platinum nuclei.

I	II	III	IV	V	VI
Pt1	Pt^*	Pt	Pt^*	Pt	Pt^*
Pt2-Pt2	Pt-Pt	Pt^*-Pt	Pt^*-Pt	Pt^*-Pt^*	Pt^*-Pt^*

Scheme 7.3: $^{195}Pt = Pt^*$

The major resonances are due to isotopomer I which gives three simple signals as a result of the three types of phosphorus nuclei. Superimposed on this spectrum, however, are the spectra due to the other five isotopomers. The coupling between Pt(1) and Pt(2) is negligable as is the coupling between Pt(1) and P^b or P^c. This simplifies the situation somewhat and the spectra can be rationalized in terms of whether the platinum atom (Pt(1) is spin active (II, IV, VI), and whether the Pt(2) - Pt(2) unit contains zero (I, II), one (III, IV), or two (V, VI) spin active nuclei.

There is a coupling between P^a and Pt(1) which manifests itself as a doublet superimposed on the P^a resonance from isotopomers II and IV. In the case of a single spin active Pt(2), (III, IV), both $^1J(P^aPt(2))$ and $^2J(P^bPt(2))$ are resolved and each satellite contains an extra doublet splitting due to $^3J(P^bP^{b'})$. The presence of a single spin active Pt(2) atom makes the two P^b atoms magnetically inequivalent. This observation of long range Pt-P and P-P coupling is characteristic of an almost linear P-Pt-Pt-P unit. The three bond $P^bP^{b'}$ coupling is the

doublet splitting seen in the satellites of the P^b signal while the long range $^2J(Pt(2)P^b)$ coupling is obtained by measuring the distance between the outer lines of the inner satellites and subtracting the $^3J(P^bP^{b'})$ value from this. In cases where both Pt(2) atoms are spin active (V and VI) the spin system is complex.

The $^{195}Pt\{^1H\}$ NMR spectrum of complex **4a** is directly analogous to that for complex **3** with the triplet due to Pt(1) at -2858 ppm and the doublet of doublets due to Pt(2) at -3147 ppm (Figure 7.4).

7.2.5 Sulphur Inversion

Complexes **3** and **4a-4c** undergo a fluxional process in solution which leads to an effective plane of symmetry containing the $Pt_3(PCP)_3$ unit. This is demonstrated in the ^1H NMR spectra by equivalence of the $CH^aH^bP_2$ protons of the dppm ligands in the room temperature ^1H NMR spectra, but by the inequivalence of these same protons at low temperatures. This effect has been observed previously in $[Pt_3(\mu_3\text{-}S)(CN)(\mu\text{-}dppm)_3]^{1+}$[11] and related complexes,[14,16] and is due to inversion at the μ_3-S unit giving a planar $Pt_3(\mu_3\text{-}S)(CNR)$ and $Pt_3(\mu_3\text{-}S)(CO)$ transition state.

7.3 DISCUSSION

This work lends additional evidence to the fact that C=S bond cleavage by oxidative addition to Pt_3 clusters is a general reaction. Although a number of

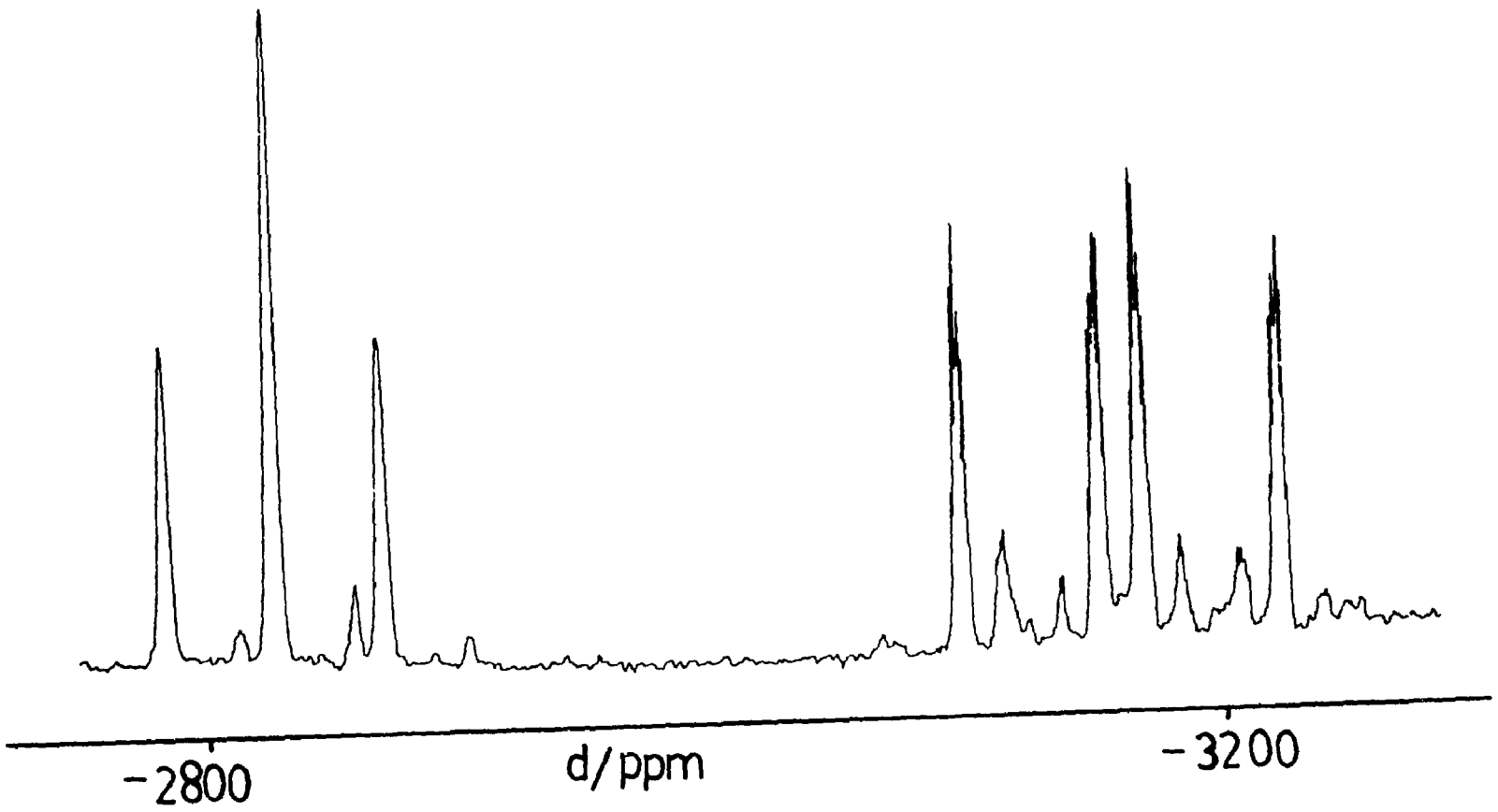

FIGURE 7.4: $^{195}Pt\{^{1}H\}$ NMR Spectrum of 4

intermediates were detected it is difficult, as with most cluster reactions, to determine the detailed mechanism of the reaction. One reasonable sequence is shown in Scheme 7.4. The easy formation of complexes 2a-2c was established by NMR studies and the next detectable intermediate was 3. Complexes 5 and 6 are proposed by analogy with the mechanism of Scheme 7.1 and structure 5 is closely related to the proposed structure of the palladium complex $[Pd_3(\mu\text{-}CS_2)(\mu\text{-}dppm)_3]^{2+}$.[18] All precedents suggest that an η^2-C-S bonded complex should be formed prior to CS bond cleavage.[1-10]

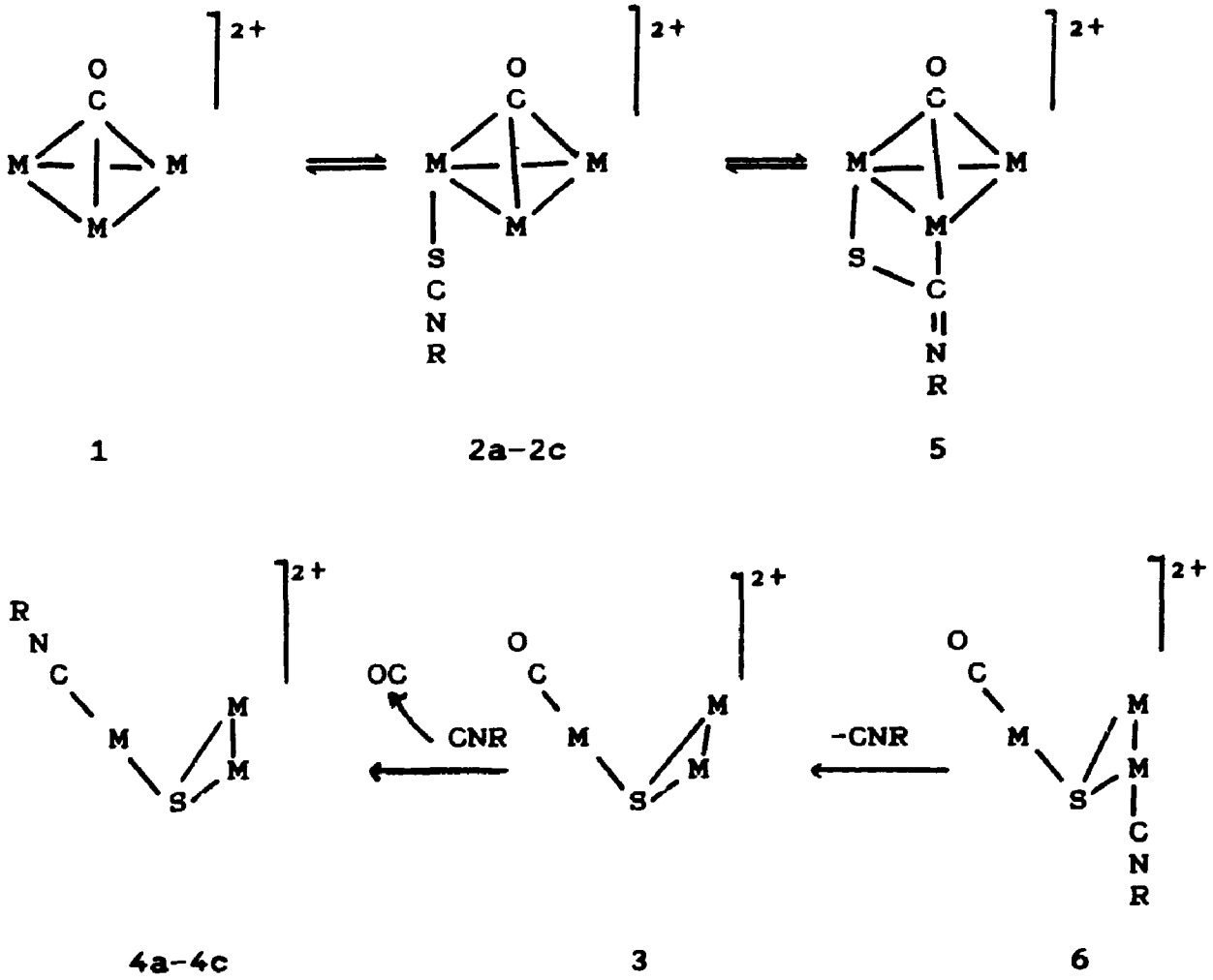

Scheme 7.4

Not all compounds containing C=S double bonds add oxidatively to $[Pt_3(\mu_3\text{-}CO)(\mu\text{-}dppm)_3]^{2+}$, 1. Two such compounds are thiophene and thioacetamide. The $^{31}P\{^1H\}$ NMR spectra obtained when both were added to complex 1 showed that no reaction had occurred. Since complex 1 is an electrophile it may be that these ligands are not strong enough electron donors to allow initial addition to complex 1 to occur.

7.4 CONCLUSIONS

This work gives an overview of how the strong C=S bond of the isothiocyanate ligand can be cleaved under mild conditions by Pt_3 clusters. The strongly bonded μ-dppm ligands a e able to prevent fragmentation of $[Pt_3(\mu_3\text{-}CO)(\mu\text{-}dppm)_3]^{2+}$, 1, to binuclear and mononuclear complexes resulting in a clearer, though incomplete picture, of these reactions.

7.5 REFERENCES

1. M.C. Baird and G. Wilkinson, *J. Chem. Soc.*, (1967), (A), 865.
2. W.H. Howling, A. Walker, M.A. Woitzik, *J. Chem. Soc., Chem. Commun.*, (1983), 4, 1750.
3. M. Ebner, H. Werner, *Chem. Ber.*, (1988), 121, 1449.
4. E. Ma, G. Semelhago, A. Walker, D.H. Farrar and R.R. Gukathasan, *J. Chem. Soc., Dalton Trans.*, (1985), 2595.
5. M. Ebner, H. Otto and H. Werner, *Angew. Chem. Int. Ed. Engl.*, (1985), 24, 518.
6. M. Ebner, M. Otto and H. Werner, *J. Organomet. Chem.*, (1988), 350, 257.
7. A.C. Skapski and P.G.H. Troughton, *J. Chem. Soc.*, (1967), (A), 865.
8. D.H. Farrar, R.R. Gukathasan and S.A. Morris, *Inorg. Chem.*, (1984), 23, 3258.
9. T.S. Cameron, P.A. Gardner and K.A. Grundy, *J. Organomet. Chem.*, (1981), 212, C19.
10. C.S. Browning, D.H. Farrar, R.R. Gukathasan and S.A. Morris, *Organometallics*, (1985), 4, 1750.
11. G. Ferguson, B.R. Lloyd, Lj. Manojlovic-Muir, K.W. Muir and R.J. Puddephatt, *Inorg. Chem.*, (1986), 25, 4190.
12. R.D. Adams and I.T. Horvath, *Inorg. Chem.*, (1985), 33, 127.

13. H. Vahrenkamp, *Sulphur*, A. Muiller, B. Kubs, Eds.; Elsevier: Amsterdam (1984), p. 121-139.

14. M.C. Jennings, N.C. Payne and R.J. Puddephatt, *Inorg. Chem.*, (1987), **26**, 3776.

15. G.K. Anderson and R.J. Cross, *Acc. Chem. Res.*, (1984), **17**, 67.

16. A.M. Bradford, M.C. Jennings and R.J. Puddephatt, *Organometallics*. In press.

17. B.R. Lloyd, Ph.D. Thesis, The University of Western Ontario, 1985.

18. M. C. Jennings, Ph.D. Thesis, The University of Western Ontario, 1989.

CHAPTER 8

SYNTHESIS AND CHARACTERIZATION OF A TETRANUCLEAR PLATINUM CLUSTER

8.1 INTRODUCTION

Up to this point, this thesis has dealt exclusively with the reactions of the trinuclear platinum cluster $[Pt_3(\mu_3\text{-}CO)(\mu\text{-}dppm)_3]^{2+}$, **1**, with various main group reagents. In this chapter we discuss the synthesis of a novel tetranuclear cluster by reaction of **1** with a transition metal reagent.

Triplatinum clusters have electron counts ranging from 42 to 46 electrons. The 42 electron clusters have three metal-metal bonds as do the 44 electron clusters discussed in this thesis. Not all 44 electron clusters have three metal-metal bonds however. The cluster $[Pt_3(\mu\text{-}PPh_2)_3(Ph)(PPh_3)_2]$ is an example of a 44 electron triplatinum cluster with only two M-M bonds.[1,2] The 46 electron clusters are able to have one or three M-M bonds. The number of M-M bonds in the 44 and 46 electron species is determined by whether the extra electrons inhabit M-M antibonding orbitals or not.

The most common electron count for tetraplatinum clusters is 58 and their general formula is $[Pt_4(\mu\text{-}CO)_3L_4]$, L = phosphine.[2-6] These clusters have five M-M bonds

forming a "butterfly" structure of platinum atoms containing two different environments for both phosphine ligands and platinum atoms. One would therefore predict two distinct ^{31}P and ^{195}Pt NMR signals. The $^{31}P\{^{1}H\}$ and $^{195}Pt\{^{1}H\}$ NMR spectra reveal equivalent ^{31}P and ^{195}Pt centres even at low temperature. This is interpreted in terms of a tetrahedral arrangement of platinum atoms. There must therefore be time averaging of all possible isomeric edge opened tetrahedra as shown in Scheme 8.1.

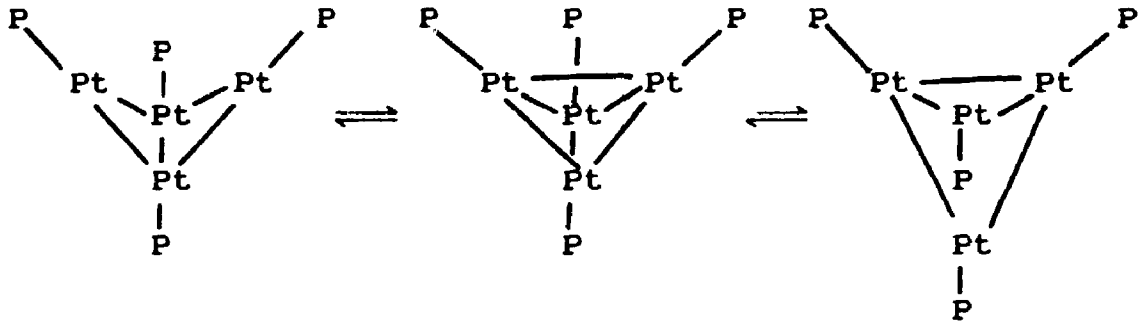

Scheme 8.1

This fluxionality of a butterfly "flapping" its wings is well documented.

A series of 58 electron $Pt_4(\mu\text{-dppm})_3$ clusters have been characterized in this research group. They include $[Pt_4(\mu\text{-H})(\mu\text{-CO})_2(\mu\text{-dppm})_3(\eta^1\text{-dppm})]^{1+}$,[7] 2, which is synthesized from $[Pt(CF_3COO)_2(dppm)]$ under water gas shift reaction conditions (100°C, 60 mL MeOH-H_2O, (2:1 V/V), P(CO) = 110 lb in^{-2}, 3 days) and $[Pt_4(\mu\text{-CO})_2(\mu\text{-Ph}_2PCH_2PPh_2)_3\{Ph_2PCH_2P(:O)Ph_2\}]$[8] synthesized

from the binuclear platinum hydride $[Pt_2H_2(\mu\text{-}H)(\mu\text{-}dppm)_2]^{1+}$ under the same conditions.

Each of these clusters displays a Pt_4 butterfly arrangement of metal atoms, with the μ-dppm ligands bridging three platinum-platinum edges to give a roughly planar Pt_3P_6 unit. They also have η^1-diphosphine ligands bonding to the fourth platinum atom.

The reactivity of complex 2 towards a number of reagents was investigated and it has been found that the dangling phosphorus atom could be readily oxidized to give $[Pt_4(\mu\text{-}H)(\mu\text{-}CO)_2(\mu\text{-}dppm)_3(Ph_2PCH_2P(:O)PPh_2)]^{1+}$. The reaction of complex 2 with MeNC resulted in the isocyanide readily replacing the isolobal carbonyls to give bridging MeNC groups. Complex 2 also reacts with two equivalents of $[Ph_3PAu]^{1+}$ to give $[Pt_4(\mu\text{-}AuPPh_3)(\mu\text{-}CO)_2(\mu\text{-}dppm)_3(Ph_2PCH_2P\{AuPPh_3\}Ph_2)]^{2+}$ in which the first $[Ph_3PAu]^{1+}$ ligand attaches itself to the dangling phosphine and the second replaces the μ_2-H ligand.[9]

Not all tetraplatinum clusters have 58 electrons however. $[Pt_4H_8(P^iPr_2Ph)_4]$ is a 56 electron cluster with an approximately tetrahedral core containing four short and two long Pt-Pt bonds. $[Pt_4H_2(P^tBu_3)_4]^{2+10}$ and $[Pt_4H_2(P^tBu_3)_4]^{11}$ are two very electron deficient clusters which also possess a tetrahedron of platinum atoms. The loss of electrons from 58 electron Pt_4 clusters results in the formation of a sixth M-M bond and a tetrahedral core of metal atoms.

Our interest in Pt_4 clusters stems from the rich reactivity previously exemplified by $Pt_4(\mu\text{-dppm})_3$ clusters. We therefore decided to investigate the ability of complex 1 to act as a precursor for homonuclear Pt_4 clusters, and higher nuclearity clusters, under less forcing conditions than the water gas shift reaction.

8.2 RESULTS

8.2.1 Synthesis of $[Pt_4(\mu\text{-CO})_3(CO)(\mu\text{-dppm})_3]^{2+}$, 3

The reaction of $[Pt_3(\mu_3\text{-CO})(\mu\text{-dppm})_3]^{2+}$, 1, with a 2.7 molar excess of $Pt(DBA)_x$ ($2 \leq x \leq 3$), using a CO bubbler, resulted in the formation of the tetraplatinum cluster $[Pt_4(\mu\text{-CO})_3(CO)(\mu\text{-dppm})_3]^{2+}$, 3. It is likely that the carbon monoxide first reacts with the $Pt(DBA)_x$ ($2 \leq x \leq 3$) forming "$Pt(CO)_2$", which then goes on to react with complex 1. Complex 3 is formed in approximately 70% yield and could not be isolated, but decomposed readily to form complex 1 and a black solid presumed to be metallic platinum. Complex 3 was more stable under a CO atmosphere and therefore all spectra were recorded under approximately 1 atmosphere of CO. The additional carbonyl ligand in complex 3 is thought to be the result of placing the reaction products under the atmosphere of CO.

8.2.2 Characterization of Complex 3 by Spectral Methods and a Study of Its Fluxionality

Complex 3 was characterized by $^{31}P\{^1H\}$, $^{13}C\{^1H\}$ and $^{195}Pt\{^1H\}$ NMR and the results were compared with those obtained for $[Pt_4(\mu\text{-}H)(\mu\text{-}CO)_2(\mu\text{-}dppm)_3(\eta^1\text{-}dppm)]^{1+}$, 2, which has been characterized by x-ray crystallography[7] in addition to spectral methods, and the cluster $[Pt_4(\mu\text{-}CO)_2(PPh_3)(\mu\text{-}dppm)_3]^{2+}$, 4, synthesized by R. Ramachandran of this research group.[12]

The fluxionality of complex 3 is very different from that of the usual butterfly structures.[2,13] However, it can be defined from the variable temperature NMR spectra. The symmetry of complex 3 was determined from the variable temperature $^{31}P\{^1H\}$ NMR spectra. The NMR labelling scheme is depicted in Scheme 8.2.

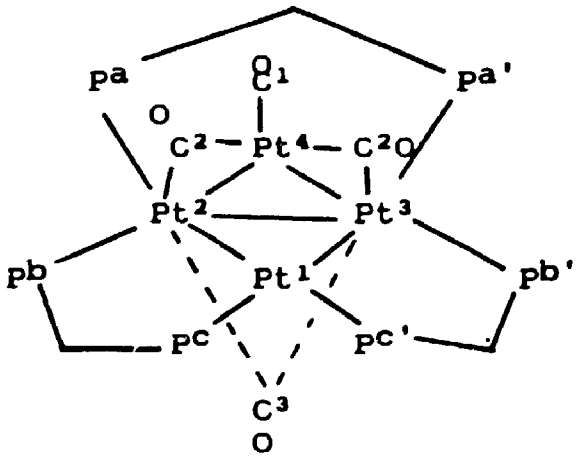

1 2+

3

Scheme 8.2: NMR Labelling Scheme

The room temperature $^{31}P\{^{1}H\}$ NMR spectrum consisted of a sharp singlet resonance at -18.4 ppm with platinum satellites [$^{1}J(Pt^{1,2,3}pa,b,c)$ = 3240 Hz, $^{2}J(Pt^{4}pa,b,c)$ = 12 Hz. This clearly indicates threefold symmetry of the $Pt_3(\mu\text{-dppm})_3$ unit but no fluxionality of the $Pt^{4}(CO)$ ligand of the type observed for the 58 electron clusters $[Pt_4(\mu\text{-CO})_5L_4]$, L = phosphine, due to the fact that the bridging dppm ligands do not make this possible. Spectral parameters compare favourably with those observed for the μ-dppm ^{31}P resonances of complexes 2 and 4 at room temperature (Table 8.1). The $^{3}J(PP)$ value was 160 Hz and was apparent from the satellite spectra. At -92°C the μ-dppm ^{31}P resonance is significantly broadened, but is still a singlet. This is in contrast to complexes 2 and 4 where this same resonance splits into three signals at -40°C. It is therefore apparent that complex 3 is a much more fluxional cluster than are complexes 2 and 4 (Figure 8.1).

The $^{195}Pt\{^{1}H\}$ NMR spectrum at room temperature was very helpful in the elucidation of the strucutre of complex 3 (Figure 8.2). A triplet resonance at -3784 ppm was observed due to Pt^{1}, Pt^{2} and Pt^{3}. The triplet was due to Pt-P coupling [$^{1}J(PtP)$ = 3300 Hz]. The resonance due to Pt^{4} appeared as an overlapping binomial septet, due to $^{1}J(Pt^{4}pa,b,c)$, of 1:12:49:84:49:12:1 septets, due to $^{1}J(Pt^{4}Pt^{1,2,3})$. In the ^{13}CO enriched species the Pt-^{13}C

TABLE 8.1: Room Temperature $^{31}P\{^1H\}$ and $^{195}Pt\{^1H\}$ NMR Data for Complexes 2-4

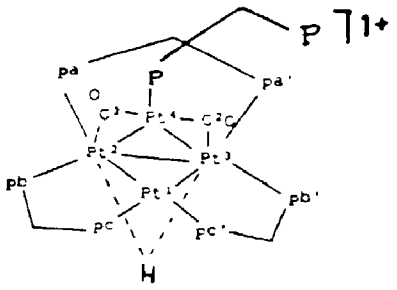

2

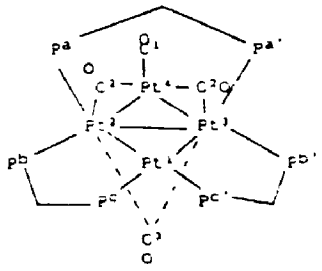

3

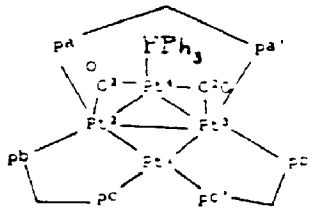

4

Complex	2[9]	3	4[12]
δ (P^{a-c})/ppm	-21.5	-18.8	-17.0
$^1J(Pt^{1-3}P^{a-c})$/Hz	3200	3200	3270
$^3J(P^{a-c}P^{a-c})$/Hz	--	140	150
δ (P^d)/ppm	18.2	--	34.0
$^1J(Pt^4P^d)$/Hz	5400	--	5520
$^2J(Pt^{1-3}P^d)$/Hz	336	--	336
$^3J(P^dP^{a-c})$/Hz	15.0	--	15.0
δ P^e/ppm	-31.4	--	--
$^2J(P^dP^e)$/Hz	73	--	--
$^3J(Pt^4P^e)$/Hz	97	--	--
δ Pt^4/ppm	-3340	-2687	--
$^1J(Pt^4Pt^{2-3})$/Hz	--	165	--
$^1J(Pt^4P^d)$/Hz	5400	--	
$^2J(Pt^4P^{a-c})$/Hz	--	12	--
δ Pt^{1-3}/ppm	--	-3784	--
$^1J(Pt^{1-3}P^{a-c})$/Hz	--	3300	--

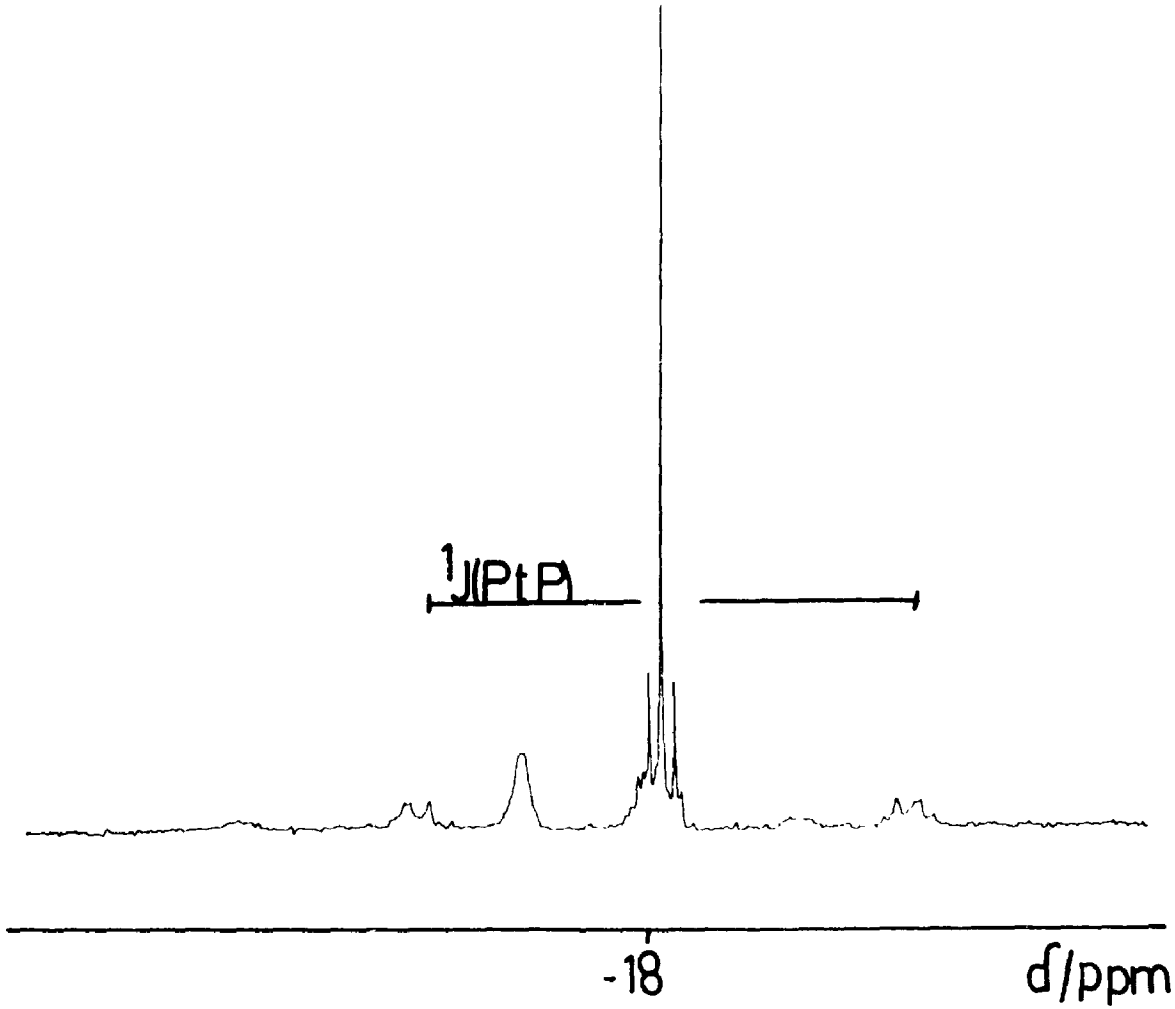

FIGURE 8.1: $^{31}P\{^{1}H\}$ NMR Spectrum of 3

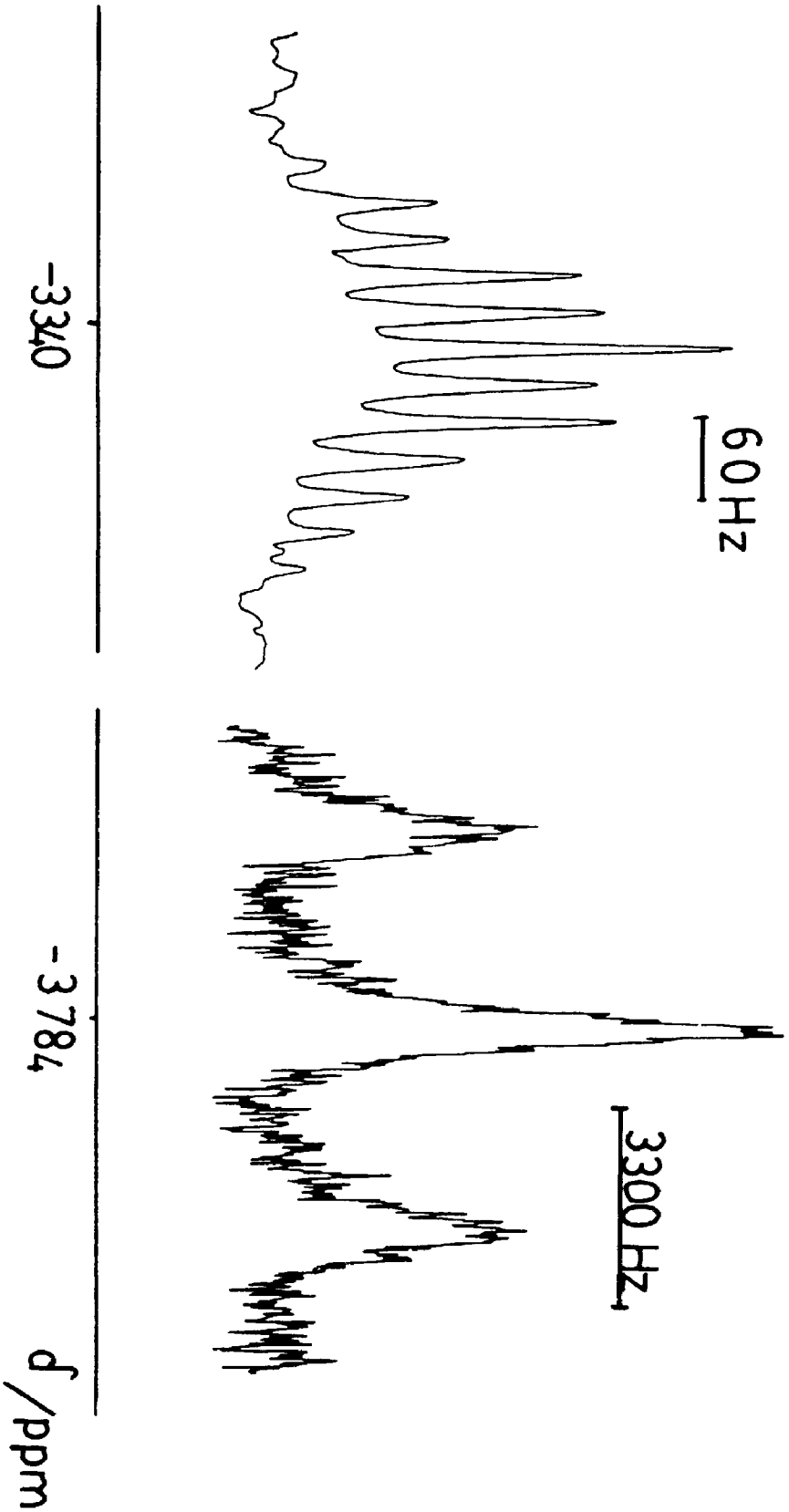

FIGURE 8.2: $^{195}Pt\{^{1}H\}$ NMR Spectrum of 3

couplings obscure the other couplings and broaden the resonance into a featureless hump.

In contrast, the $^{195}Pt\{^{1}H\}$ NMR of complex 2 was not very helpful in the structural determination. Here a broad doublet resonance due to Pt^4 was observed. The doublet was due to a large Pt-P coupling of 5400 Hz which is common for a terminal phosphorus atom on a $Pt(\mu\text{-}CO)Pt_2$ unit.[2] The other three platinum atoms, Pt^1-Pt^3, gave resonances which were too broad to observe even at -40°C.

The room temperature $^{13}C\{^{1}H\}$ NMR spectrum of 3 consists of several sets of resonances (Table 8.2). The first is due to a terminal carbonyl C^1O [δ ^{13}CO = 188.9 ppm, $^{1}J(Pt^4\text{-}C^1)$ = 1176 Hz, $^{2}J(Pt^{1,2,3}C^1)$ = 126 Hz]. This carbonyl does not appear to be fluxional on the basis of the chemical shift and coupling constant values which are typical for a terminal carbonyl group (Figure 8.3). This is somewhat surprising considering the low activation energy barriers that can exist between terminal and μ_2-CO groups. The second resonance is due to a bridging carbonyl, C^2O [δ = 212.2 ppm, $^{1}J(Pt^4C^2)$ = 876 Hz, $^{1}J(Pt^1C^2)$ = $^{1}J(Pt^2C^2)$ = $^{1}J(Pt^3C^2)$ = 138 Hz]. These values compare favourably with those found for complexes 2 and 4 [2: δ ^{13}CO = 246.0 ppm, $^{1}JPt^4C)$ = 816 Hz, $^{1}J(Pt^1C^2)$ = $^{1}J(Pt^2C^2)$ = $^{1}J(Pt^3C^2)$ = 130 Hz; 4: δ ^{13}CO = 221.6 ppm, $^{1}J(Pt^4C^2$ = 1006 Hz, $^{1}J(Pt^1C^2)$ = $^{1}J(Pt^2C^2)$ = $^{1}J(Pt^3C_2)$ = 112 Hz]. The ^{13}CO resonances for complexes 2 and 4 at -40°C contained quarter intensity satellites due to $^{1}J(Pt^4C^2$ = 820 and

TABLE 8.2: $^{13}C\{^{1}H\}$ NMR Data for Complexes 2, 3 and 4

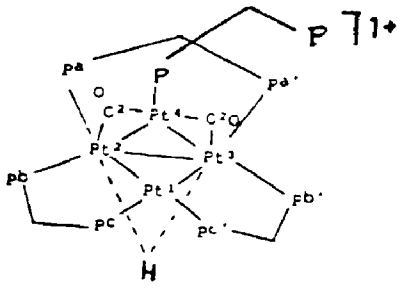

2

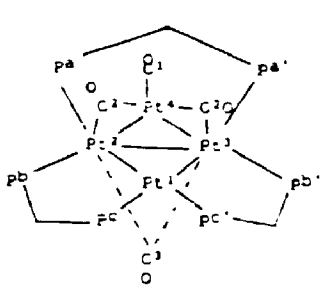

3

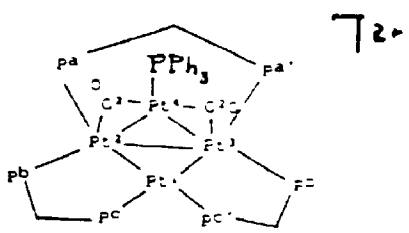

4

Complex	2[9]	3	4[12]
δ $C^{1}O$/ppm	--	188.9	--
$^{1}J(Pt^{4}C^{1})$/Hz	--	1176	--
$^{2}J(Pt^{2,3}C^{1})$/Hz	--	126	--
δ $C^{2}O$/ppm	246.0	212.2	221.6
$^{1}J(Pt^{4}C^{2})$/Hz	820	876	1006
$^{1}J(Pt^{1-3}C^{2})$/Hz	130	138 Hz	112
δ $C^{3}O$/ppm	--	201.1	--
$^{1}J(Pt^{1-3}C^{3})$/Hz	--	376	--
$^{2}J(PC^{3})$/Hz	--	12.0	--

FIGURE 8.3: $^{13}C\{^{1}H\}$ NMR Spectrum of 3

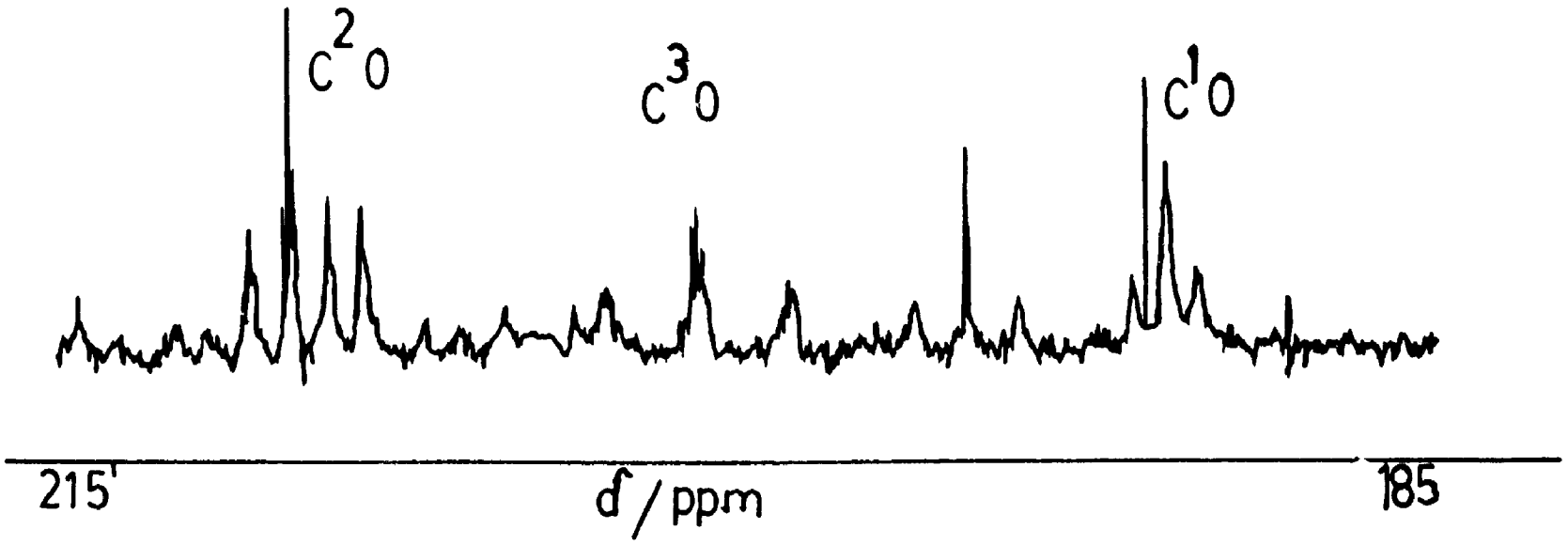

990 Hz and $^1J(Pt^2C^2)$ = 392 Hz and 333 Hz, respectively. These data indicate that, in these complexes at room temperature, the carbonyl is fluxional with respect to the $Pt^1Pt^2Pt^3$ triangle while remaining bound to Pt^4. The room temperature $^{13}C\{^1H\}$ NMR results for complex 3 indicate that the C^2-carbonyls undergo the same fluxionality as those in complexes 2 and 4 and that by analogy with complexes 2 and 4, the $^1J(Pt^4C^2)$ value for the static structure of complex 3 should be 138 x 3 = 414 Hz.[7,9,12]

There is also a third resonance in the $^{13}C\{^1H\}$ NMR spectrum of complex 3. It is due to a bridging carbonyl at δ = 201.1 ppm and $^1J(PtC)$ = 376 Hz. From the magnitude of J(PtC) it is possible to say that the carbonyl is fluxional. It is not possible however, from the spectral data alone, to unambiguously assign the resonance to a μ_2- or a μ_3-carbonyl. By analogy with complex 2 which contains a μ_2-H ligand, we propose a μ_2-carbonyl, C^3O. It is interesting to note that in the ^1H NMR spectrum at room temperature for complex 2, the PtH resonance appeared as a 1:12:49:84:49:12:1 septet due to equal coupling to Pt^1, Pt^2 and Pt^3. Thus the hydride appears to be triply bridging with an observed Pt-H coupling of 508 Hz. At -40°C a more complex resonance is observed with $^1J(Pt^2H) = {}^1J(Pt^3H)$ = 670 Hz (1:8:18:8:1) and $^2J(Pt^1H)$ = 168 Hz (1:4:1) as expected for the static structure. The average J(PtH) is expected to be 1/3 [(2 x 670) + 168] = 503 Hz which is in agreement with the observed value if the hydride is

fluxional with respect to the $Pt^1Pt^2Pt^3$ triangle. On the basis of the spectral data outlined for complexes 2 and 3 it is therefore proposed that the μ_2-carbonyl, C^3O, is fluxional with respect to the $Pt^1Pt^2Pt^3$ triangle.

Together all of the NMR data describe a fluxionality that is different from the usual "flying butterfly" mechanism. Our mechanism involves an edge to edge migration of the μ-CO groups on opposite faces of the $Pt_3(\mu\text{-dppm})_3$ triangle (Scheme 8.3). Complete equivalence requires six of these 60° steps. The time-averaged structure apears to contain a μ_3-CO group, C^3O, below and a rapidly spinning μ_3-$Pt^4(\mu\text{-CO})_2(CO)$ group above the Pt_3dppm_3 unit.

8.3 DISCUSSION

The cluster $[Pt_4(\mu\text{-CO})_3(CO)(\mu\text{-dppm})_3]^{2+}$, 3, is much less stable than the previously characterized $Pt_3(\mu\text{-dppm})_3$ 58 electron clusters. Each of these previously characterized clusters contains a tertiary phosphine ligand (either mono- or bidentate) bound to Pt^4. Complex 3, on the other hand, contains a terminal carbonyl bound to Pt_4. Since it is known that tertiary phosphine ligands are better electron donors than is CO, it may be that the instability of complex 3 is due to electronic factors in that these 58 electron $Pt_4(\mu\text{-dppm})_3$ clusters may require a good σ-donor ligand, like the tertiary phosphines, to bind to Pt^4 for stability. This would make the Pt^4 centre more

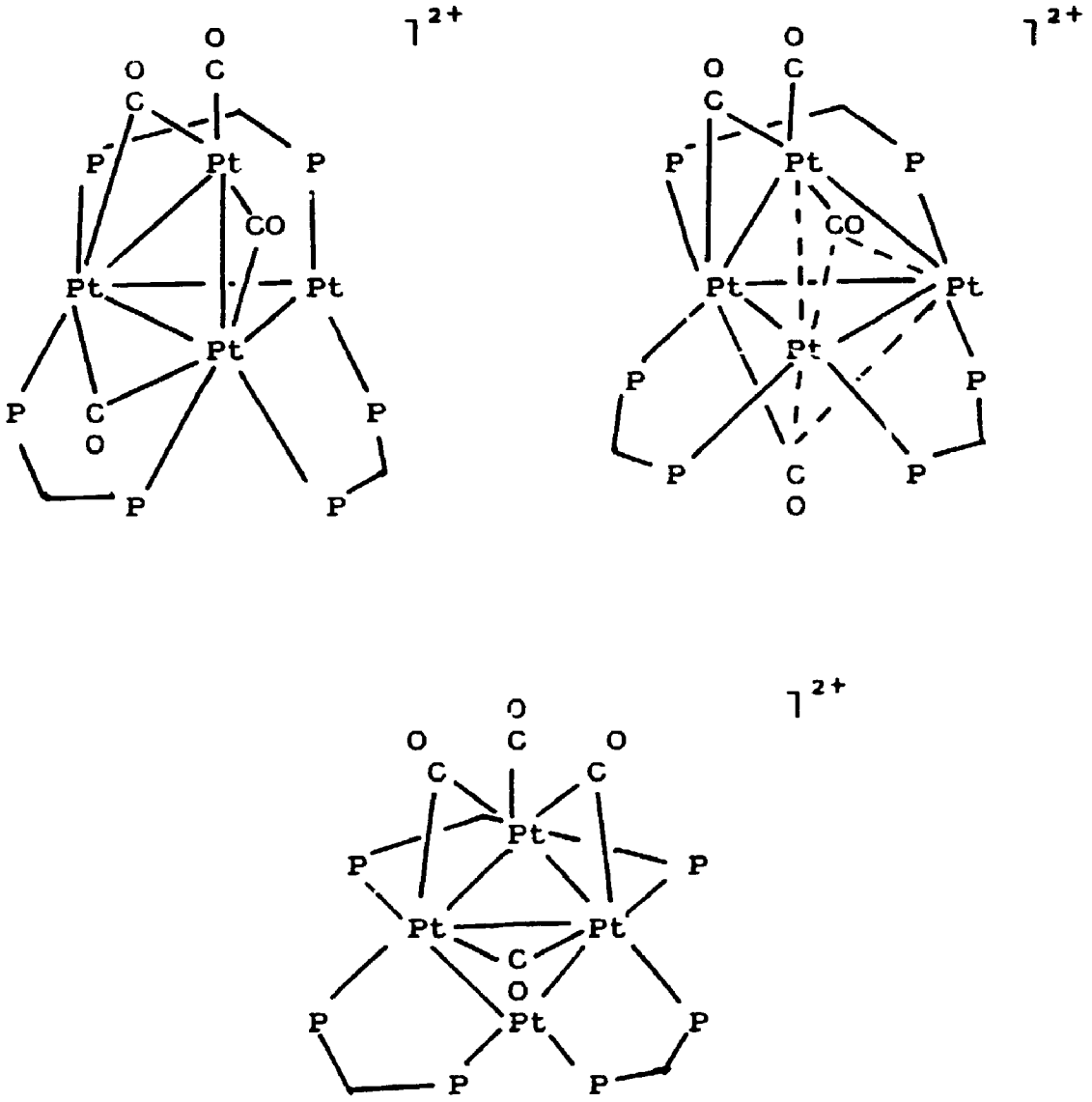

Scheme 8.3

electron rich and therefore a better Lewis base. Complex 3 is also more fluxional than the other known $Pt_4(\mu\text{-dppm})_3$ clusters in that the fluxionality of the cluster core could not be frozen out at -92°C.

The synthesis of a heteronuclear cluster was attempted by reacting $CpRh(CO)_2$, Cp = C_5H_5, with complex 1. The $^{31}P\{^1H\}$ NMR spectrum indicated however that no reaction occurred. This is most likely due to the large steric bulk of the Rh complex inhibiting the reaction with the platinum centres of complex 1. Since the reaction of complex 1 with $Pt(CO)_2$ can be considered to be a ligand addition reaction, $Pt(CO)_2$ is the first and only example in this thesis of a ligand that adds in a μ_2-bridging fashion to complex 1. With this example we complete the spectrum of ligands which add to $[Pt_3(\mu_3\text{-CO})(\mu\text{-dppm})_3]^{2+}$, 1, in terminal, μ_2-bridging and μ_3-capping modes.

8.4 CONCLUSIONS

The previous chapters have demonstrated that $[Pt_3(\mu_3\text{-CO})(\mu\text{-dppm})_3]^{2+}$, 1, displays a rich reactivity towards main group ligands. The reaction of complex 1 with $Pt(CO)_2$ also suggests that it may have a rich reactivity with other metal centres. Insights obtained on factors which influence the stability of $Pt_4(\mu\text{-dppm})_3$ clusters indicate that complex 1 is a useful precursor for stable higher nuclearity clusters (both homonulcear and hetero-nuclear) with the right combinations of ancilliary ligands.

8.5 REFERENCES

1. N.J. Taylor, P.C. Chich and A.J. Carty, *J. Chem. Soc., Chem. Commun.*, (1975), 448.
2. D.M.P. Mingos and R.W.M. Wardle, *Transition Met. Chem.*, (1985), **10**, 441.
3. N.K. Eremenko, E.G. Medrikov, S.S. Kurasov, *Russ. Chem. Rev.*, (1985), **54**, 394.
4. R.G. Vranka, L.F. Dahl, P. Chini and J. Chatt, *J. Am. Chem. Soc.*, (1969), **91**, 157.
5. D.G. Evans, M.F. Hallam, D.M.P. Mingos and R.W.M. Wardle, *J. Chem. Soc., Dalton Trans.*, (1987), 1889.
6. J. Chatt and P. Chini, *J. Chenm. Soc.*, (A), (1970), 1538.
7. G. Douglas, Lj. Manojlovic-Muir, K.W. Muir, M.C. Jennings, B.R. Lloyd, M. Rashidi and R.J. Puddephatt, *J. Chem. Soc., Chem. Commun.*, (1988), 149.
8. A.A. Frew, R.H. Hill, Lj. Manojlovic-Muir, K.W. Muir and R.J. Puddephatt, *J. Chem. Soc., Chem. Commumn.*, (1982), 198.
9. M.C. Jennings, Ph.D. Thesis, University of Western Ontario, (1989).
10. P.W. Frost, J.A.K. Howard, J.L. Spencer and D.G. Turner, *J. Chem. Soc., Chem. Commun.*, (1981), 1104.

11. R.J. Goodfellow, E.M. Hamon, J.A.K. Howard, J.L. Spencer and D.G. Turner, *J. Chem. Soc., Chem. Commun.*, (1984), 1604.

12. R. Ravindranath and R.J. Puddephatt, Personal Commun.

13. A. Moor, P.S. Pregosin, L.M. Venanzi and A.J. Welch, *Inorg. Chim. Acta*, (1984), **85**, 103.

CHAPTER 9

SUMMARY

This thesis documents the reactivity of the cluster cation $[Pt_3(\mu_3\text{-}CO)(\mu\text{-}dppm)_3]^{2+}$, **1**, towards various main group and transition metal reagents. The cluster is coordinatively unsaturated in that it is electron deficient and possesses vacant sites of coordination at the cluster core. It should therefore be able to mimic the reactions that occur on metal surfaces.

Although a wide variety of analytical techniques exist, the structure and stereochemistry of chemisorbed species cannot be established precisely apart from simple cases such as CO and NO. The structure and stereochemistry of molecular metal clusters however can be determined very readily, and the comparison of the spectroscopic data obtained for the latter can be used to provide information on the structure of the former. This in turn aids in the efforts to delineate the electronic and structural factors that significantly influence catalytic activity as the nuclearity of the metal framework increases.

Another interesting feature of metal clusters is the possibility of performing unique catalytic reactions due to the unusual stereoselectivity or chemoselectivity possible because of the participation of more than one

metal centre. This also includes the cluster catalysis of reactions that either cannot occur, or occur with difficulty, at single metal atom centres. A critical need, if this is to be accomplished, is a more detailed understanding of basic types of cluster reactions such as ligand substitution, oxidative addition, reductive elimination and ligand addition. Such a study is documented in this thesis.

In Chapter 2 the results of the reactions of complex 1 with the halide ions Cl^-, Br^- and I^- were outlined and insights into the coordinative nature of these ligands at the vacant site opposite the carbonyl bridge position on the dicationic cluster were developed with regard to preference for site occupancy. Attempts were also made to qualitatively investigate the bonding in these systems with respect to the degree of ionic or covalent character in the $Pt_3(\mu_3\text{-}X)$ bonds. The presence of a weak covalent bonding interaction between complex 1 and the monoanionic halide ligands have profound effects on the chemistry of these trinuclear systems. The high stability constants for halide addition together with the lability of the coordinated halide is very unusual and suggests that other ligands may be capable of coordination at the μ_3-site.

In Chapter 3 the results of the reactions of complex 1 with various tertiary phosphine and phosphite ligands were outlined. These ligands add to complex 1 in a terminal fashion and this leads to a slippage of the

μ_3-carbonyl towards the platinum atom to which the phosphine and phosphite ligands are bound. This confirms suggestions made by Evans that the μ_3-carbonyl behaves primarily as a π-acceptor ligand. The phosphine and phosphite ligands display a unique fluxionality not previously observed in cluster chemistry and this work also demonstrated the feasibility of the synthesis of both $Pt_3(\mu_3\text{-}PF_3)$ and $M_3(\mu_3\text{-}PF_3)$ groups which have not been seen before. Finally, the interaction of PH_3 and PF_3 on Pt(111) and Ni(111) surfaces was successfully modelled.

Chapter 4 documents the results of the reactions of complex 1 with phosphorus and sulphur-containing bidentate ligands. Ligand addition occurs to adjacent metal centres to give stable 46 electron clusters with all three metal-metal bonds intact. A new form of fluxionality was observed for the dppm ligand which involved migration around the triangular face of the cluster. The fluxionality may be facilitated by the formation of asymmetric μ_3-CO and μ_2-CO groups upon ligand addition.

In Chapter 5 the results of the addition of one molar equivalent of isocyanide ligand to complex 1 is reported. A novel mechanism was observed in which some isocyanide ligands added to complex 1 via the formation of an intermediate which is believed to have the isocyanide on the same face of the cluster as the carbonyl ligand. This is followed by the dissociation of the isocyanide and coordination to the opposite face of the triplatinum

cluster. A greater "slip distortion" of the μ_3-carbonyl was observed for these Pt_3-isocyanide clusters than was observed for the Pt_3-tertiary phosphine phosphite clusters reported in Chapter 3 and the isocyanide is fluxional at room temperature about the triangular face of the cluster. It was also demonstrated that these Pt_3-isocyanide clusters can add excess CO reversibly. This is important in that, if useful catalysis by metal clusters is to be obtained, it is desirable that two ligands add to adjacent metal centres, then combine and dissociate to give the product and regenerate the catalyst. The addition of both CO and isocyanide to complex 1 shows that the first step in this sequence is possible.

The reactions of complex 1 with excess isocyanide are documented in Chapter 6. In particular we report the structure of $[Pt_3(2,6\text{-}Me_2C_6H_3NC)_2(\mu\text{-dppm})_3]^{2+}$, the first $Pt_3(\mu\text{-dppm})_3$ cluster with no cappping ligand. This cluster is interesting in that its structure does not agree with the results of theoretical calculations performed on similar systems. The way the charge is distributed among the metal atoms also appears to violate the Pauling Electroneutrality Principle.

Chapter 7 outlines the mechanism of the oxidative addition reaction which occurs when various isothiocyanates are reacted with complex 1. The strong C=S bond of the isothiocyanate ligand is cleaved under mild conditions by Pt_3 clusters and the strongly bonded μ-dppm ligands are

able to prevent the fragmentation of complex 1 to binuclear and mononuclear complexes. This has resulted in a clearer, though incomplete picture of these reactions.

Finally, Chapter 8 outlines the results of the reaction of complex 1 with the platinum (0) species $Pt(CO)_2$ under a CO atmosphere. The formation of $[Pt_4(\mu\text{-}CO)_3(CO)(\mu\text{-}dppm)_3]^{2+}$ indicates that complex 1 is a useful precursor for higher nuclearity clusters.

In conclusion, ligand addition, oxidative addition and ligand substitution reactions of $[Pt_3(\mu_3\text{-}CO)(\mu\text{-}dppm)_3]^{2+}$, 1, have been studied. The coordinative unsaturation of this cluster species has resulted in a rich reactivity which has not only allowed the successful modelling of the chemisorption of several main group reagents on Pt(111) surfaces, but has also served to show that the chemistry of this species is interesting in its own right.

CHAPTER 10

EXPERIMENTAL DETAILS

10.1 INSTRUMENTATION

10.1.1 Nuclear Magnetic Resonance Spectroscopy

^{1}H NMR spectra were recorded using a Varian XL-200 spectrometer. Non-proton spectra ($^{19}F\{^{1}H\}$, $^{31}P\{^{1}H\}$, $^{13}C\{^{1}H\}$ and $^{195}Pt\{^{1}H\}$) were recorded on a Varian XL-300 spectrometer. ^{1}H and $^{13}C\{^{1}H\}$ chemical shifts were measured relative to Me_4Si; $^{31}P\{^{1}H\}$, $^{195}Pt\{^{1}H\}$ and $^{19}F\{^{1}H\}$ chemical shifts were measured relative to 85% H_3PO_4, aqueous K_2PtCl_4 and $CFCl_3$. The solvent used in all cases was acetone-d_6 unless otherwise noted.

10.1.2 Infrared Spectroscopy

Infrared spectra were recorded on a Bruker IR/32 FT-IR spectrometer equipped with an IBM 9000 computer. Solid samples were run as Nujol mulls between NaCl plates.

10.1.3 Mass Spectrometry

The FAB mass spectra were recorded using a Finnigan MAT 8230 mass spectrometer on samples prepared as mulls in oxalic acid/3-mercapto-1,2-propanediol.

10.1.4 UV-Visible Spectroscopy

Ultraviolet and visible spectra were recorded on a Varian Cary 2290 spectrophotometer.

10.1.5 Glove Box

A Vacuum Atmospheres Company HE-43-2 DRI-LAB was used to handle various air sensitive reagents.

10.1.6 Melting Point Apparatus

The melting points of new compounds were determined using a Fisher Scientific Electrothermal Melting Point Apparatus.

10.1.7 Elemental Analysis

Elemental analyses were performed by Guelph Chemical Laboratories Ltd., Guelph, Ontario, Canada.

10.1.8 Preparation of Known Compounds

$[Pt_3(\mu_3\text{-}CO)(\mu\text{-}dppm)_3][PF_6]_2$, **1**, was prepared as previously described.[1] The aforementioned clusters were prepared using a PARR 300 mL, high pressure mini reactor equipped with a magnetic drive and an automatic temperature control.

10.1.9 Enrichment of $[Pt_3(\mu_3\text{-}CO)(\mu\text{-}dppm)_3][PF_6]_2$, 1, with ^{13}CO

Complex 1 (40 mg) was dissolved in acetone-d_6 (10 mL) in a 5 mL round bottom flask equipped with a stir bar. The flask was attached, via rubber bands, to a bridge on the vacuum line. A flask cantaining ^{13}CO was attached to the other side of the bridge. After degassing the solvent and evacuating the air from the bridge, ^{13}CO was condensed into the round bottom flask. The contents of the flask were left to stir for 24 hours under an atmosphere of ^{13}CO.

10.1.10 Sources of Chemicals

Starting materials such as K_2PtCl_4 and bis(diphenylphosphino)methane were obtained from Strem Chemicals and Aldrich. Solvents were obtained from Fisher, Aldrich or BDH and were used without further purification. All deuterated solvents were obtained from MSD isotopes. Gases and some low boiling liquids were obtained from the Matheson Gas Company except ^{13}CO which was obtained from MSD isotopes. All reactions were performed at room temperature unless otherwise stated.

10.2 EXPERIMENTAL FOR CHAPTER 2

10.2.1 $[Pt_3(\mu_3\text{-}CO)(\mu_3\text{-}Cl)(\mu\text{-}dppm)_3][PF_6]$, 2a

KCl (2.9 mg) was added to complex 1 (40 mg) dissolved in methanol (10 mL). This corresponds to a 2:1 excess of KCl to cluster. The solution was allowed to stir

for 2 hours after which time the methanol was removed by reduced pressure distillation. The orange solid was washed with three 1 mL aliquots of distilled water to remove excess salts. The orange solid was them dried under high vacuum. The product was obtained in 98% yield. Anal. Calcd. for $C_{76}H_{66}Pt_3OClP_7F_6$: C, 46.9; H, 3.4. Found: C, 47.3; H, 3.8%.

10.2.2 $[Pt_3(\mu_3\text{-}CO)(\mu_3\text{-}Br)(\mu\text{-}dppm)_3][PF_6]$, 2b

KBr (4.6 mg) was added to complex 1 (40 mg) dissolved in methanol (10 mL). This corresponds to a 2:1 excess of KBr to cluster. The solution was allowed to stir for 2 hours after which time the methanol was removed by reduced pressure distillation. The orange solid was washed with three 1 mL aliquots of distilled water to remove excess salts. The orange solid was then dried under high vacuum. The product was obtained in 97% yield. Anal. Calcd. for $C_{76}H_{66}Pt_3OBrP_7F_6$: C, 45.9; H 3.3. Found: C, 45.1; H, 3.5%.

10.2.3 $[Pt_3(\mu_3\text{-}CO)(\mu_3\text{-}I)(\mu\text{-}dppm)_3][PF_6]$, 2c

KI (6.5 mg) was added to complex 1 (40 mg) dissolved in methanol (10 mL). This corresponds to a 2:1 excess of KI to cluster. The solution was allowed to stir for 2 hours after which time the methanol was removed by reduced pressure distillation. The orange solid was washed with three 1 mL aliquots of distilled water to remove

excess salts. The orange solid was then dried under high vacuum. The product was obtained in 96% yield. Anal. Calcd. for $C_{76}H_{66}Pt_3OIP_7F_6$: C, 44.8; H, 3.3. Found: C, 43.5; H, 3.9%.

10.3 EXPERIMENTAL FOR CHAPTER 3

10.3.1 $[Pt_3(\mu_3\text{-}CO)(\mu\text{-}dppm)_3(P(OMe)_3)][PF_6]_2$, 2a

$P(OMe)_3$ (3.22 μL) was added by syringe to a solution of complex **1** (40 mg) in acetone (10 mL). The solvent was evaporated under vacuum to give the product **2a** which could be crystallized from acetone/pentane or CH_2Cl_2/pentane as orange crystals. The reaction was essentially quantitative and the isolated yield was 85%. Anal. Calcd. for $C_{79}H_{75}F_{12}O_4P_9Pt_3$: C, 43.5; H, 3.5. Found: C,43.2; H, 3.5%. IR: ν(CO) = 1780 cm^{-1}.

10.3.2 $[Pt_3(\mu_3\text{-}CO)(\mu\text{-}dppm)_3P(OEt)_3][PF_6]_2$, 2b

$P(OEt)_3$ (3.33 μL) was added to a solution of complex **1** (40 mg) in acetone (10 mL). The solvent was evaporated under vacuum to give the product **2b** which could be crystallized from acetone/pentane or CH_2Cl_2/pentane as orange crystals. The isolated yield was 87%. Anal. Calcd. for $C_{82}H_{81}F_{12}O_4P_9Pt_3$: C, 44.3; H, 3.7. Found: C, 44.4; H, 3.5%. IR: ν(CO) = 1779 cm^{-1}.

10.3.3 $[Pt_3(\mu_3\text{-}CO)(\mu\text{-}dppm)_3P(OPh)_3][PF_6]_2$, 2c

$P(OPh)_3$ (μL) was added to a solution of complex 1 (40 mg) in acetone (10 mL). The solvent was evaporated under vacuum to give the product **2c** which could be crystallized from acetone/pentane or CH_2Cl_2/pentane as orange crystals. The isolated yield was 90%. Anal. Calcd. for $C_{94}H_{81}F_{12}O_4P_9Pt_3$: C, 47.7; H, 3.5. Found: C, 45.8; H, 3.7%. IR: ν(CO) = 1779 cm^{-1}.

10.3.4 $[Pt_3(\mu_3\text{-}CO)(\mu\text{-}dppm)_3(PMe_2Ph)][PF_6]_2$, 2d

PMe_2Ph (2.77 μL) was added to a solution of complex **1** (40 mL) in acetone (10 mL). The solvent was evaporated under vacuum to give the product **2d** which could be crystallized from acetone/pentane or CH_2Cl_2/pentane as orange crystals. The isolated yield was 83%. Anal. Calcd. for $C_{84}H_{77}F_{12}OP_9Pt_3$: C, 46.0; H, 3.5. Found: C,46.4; H, 4.0. IR: ν(CO) = 1774 cm^{-1}.

10.3.5 $[Pt_3(\mu_3\text{-}CO)(\mu\text{-}dppm)_3(PMePh_2)][PF_6]_2$, 2e

A twofold excess of $PMePh_2$ (3.62 μL) was added to complex 1 (40 mg) dissolved in acetone-d_6 (0.5 mL). NMR spectra were then run on this sample. The product could not be isolated due to the existence of an equilibrium between complex 2e, complex 1 and free phosphine.

10.3.6 $[Pt_3(\mu_3\text{-}CO)(\mu\text{-}dppm)_3(PPh_3)][PF_6]_2$, 2f

To a solution of complex 1 (40 mg) in acetone-d_6 (0.50 mL) in an NMR tube was added PPh_3 (5.1 mg). NMR spectra were then run on this sample from which pure 2f could not be isolated due to the existence of an equilibrium between complex 2f, complex 1 and free phosphine. Integration of $^{31}P\{^1H\}$ NMR signals allowed the equilibrium constant to be determined over the range -83 to -92°C. At higher temperatures the signals were too broad to be useful. Typical values of K/L mol^{-1} = 7.8 at 190K, 22.4 at 183K and 28.6 at 181K.

10.3.7 $[Pt_3(\mu_3\text{-}CO)(\mu\text{-}dppm)_3(PF_3)][PF_6]_2$, 2g

Excess PF_3 was added to an NMR tube fitted with a teflon tap containing a solution of complex 1 (40 mg) in CD_2Cl_2 (0.5 mL) at liquid N_2 temperature. The tube was sealed and then allowed to warm to -78°C after which time it was shaken to mix the contents thoroughly. Most of the excess PF_3 was then removed by pumping at -78°C. The tube was sealed again and NMR spectra were recorded. A mixture of complexes 2g and 1 were obtained, as shown by $^{31}P\{^1H\}$ NMR spectroscopy after the solvent was evaporated from the sample.

10.4 EXPERIMENTAL FOR CHAPTER 4

10.4.1 $[Pt_3(\mu_3\text{-}CO)(\mu\text{-}dppm)_3(\mu_2\text{-}S_2CNMe_2)][PF_6]$, 3a

$(CH_3)_2NCS_2Na\cdot 2H_2O$ (3.5 mg) was added to complex 1 (40 mg) dissolved in acetone (10 mL). The mixture was allowed to stir until all of the ligand had dissolved in solution. The solvent was removed by reduced pressure distillation and the solid was washed three times with 10 mL portions of distilled water to remove the $NaPF_6$ which formed. The water was then removed by reduced pressure distillation and the product dried in vacuo. Anal. Calcd. for $C_{79}H_{72}NOS_2F_6P_7Pt_3.4H_2O$: C, 45.1; H, 3.8; N, 0.7. Found: C, 44.7; H, 3.4; N, 0.6. ^1H NMR: δ 3.83 [s, CH_3]; 5.24, 5.70 [AB, CH_2P_2].

10.4.2 $[Pt_3(\mu_3\text{-}CO)(\mu\text{-}dppm)_3(\mu\text{-}S_2CN(CH_2CH_3)_2)][PF_6]$, 3b

$(C_2H_5)_2NCS_2Na\cdot 3H_2O$ (4.4 mg) was added to complex 1 (40 mg) dissolved in acetone (10 mL). The mixture was stirred until all of the ligand had gone into solution. The solvent was removed by reduced pressure distillation and the solid washed three times with distilled water. The water was them removed by reduced pressure distillation and the product was dried in vacuo. Anal. Calcd. for $C_{81}H_{76}NOS_2F_6P_7Pt_3.4H_2O$: C, 45.6; H, 4.0; N, 0.7. Found: C, 45.2; H, 3.8; N, 0.9. ^1H NMR: δ 1.61 [q, $^3J(HH)$ = 8 Hz, CH_2CH_3]; 4.32 [t, CH_2CH_3]; 5.23, 5.70 [AB, $^2J(HH)$ = 16 Hz].

10.4.3 $[Pt_3(\mu_3\text{-}CO)(\mu\text{-}dppm)_3(\mu\text{-}S_2CP(C_2H_5)_3][PF_6]_2$,[2] 3c

$(C_2H_5)_3PCS_2$ (3.8 mg) was added to a solution of complex 1 (40 mg) in acetone (10 mL). Reaction occurred instantly. The solvent was removed by reduced pressure distillation and the product dried in vacuo. Anal. Calcd. for $C_{83}H_8OS_2F_{12}P_9Pt_3$: C, 44.3; H, 3.6. Found: C, 44.6; H, 3.8. ^1H NMR: δ 2.73 [d/q, $^2J(PH)$ = 14 Hz, CH_2CH_3P]; 1.17 [d/t, $^3J(PH)$ = 18 Hz, $^3J(HH)$ = 14 Hz]; 5.38 [br, CH_2P_2].

10.4.4 $[Pt_3(\mu_3\text{-}CO)(\mu\text{-}dppm)_3(\mu\text{-}S_2CP(C_6H_{11})_3][PF_6]_2$,[2] 3d

$(C_6H_{11})_3PCS_2$ (7 mg) was added to a solution of complex 1 (40 mg) in acetone (10 mL). Reaction occurred instantly. The solvent was removed by reduced pressure distillation and the product was dried in vacuo. Anal. Calcd. for $C_{95}H_{99}OS_2F_{12}P_9Pt_3$: C, 47.3; H, 4.1. Found: C, 47.7; H, 4.4.

10.4.5 $[Pt_3(\mu\text{-}CO)(\mu\text{-}dppm)_3(\mu\text{-}dmpm)][PF_6]_2$, 3e

Dmpm (3.6 μL) was added to a solution of complex 1 (40 mg) in acetone (10 mL) in a Vacuum Atmospheres Company HE-43-2 Dri Lab. Reaction was instantaneous with the solution changing from orange-red to red-black in colour. The product was removed from the Dri Lab and the solvent was removed by reduced pressure distillation. The sample was then dried in vacuo. Anal. Calcd. for

$C_{81}H_{80}OF_{12}P_{10}Pt_3$: C, 43.5; H, 3.7. Found: C, 43.5; H, 4.1.. ^1H NMR: δ 4.85, 2.27 [br, CH_2P_2].

10.4.6 $[Pt_3(\mu\text{-}CO)(\mu\text{-}dppm)_4][PF_6]_2$, 3f

Dppm (15 mg) was added to complex 1 (40 mg)in acetone (10 mL). This corresponds to a twofold excess of ligand to cluster. Reaction occurred immediately and pure 3f was isolated by cooling the solution to 0°C to allow crystallization to occur. The black crystals of 3f were then separated by hand from the red crystals of 1 which also formed. The product was dried in vacuo. Anal. Calcd. for $C_{101}H_{88}OF_{12}P_{10}Pt_3$: C, 49.7; H, 3.6. Found: C, 49.7; H, 3.8. ^1H NMR: δ 6.26, 5.68 [AB, CH_2P_2].

10.4.7 Preparation of NMR Sample of Complex 3f for ^{31}P NMR at -124°C

Complex 3f (20 mg) and acetone-d_6 (0.5 mL) were added to an MNR tube fitted with a teflon tap. $CHCl_2F$ (1 mL) was condensed into a 5 mL round bottom flask using a vacuum line and liquid N_2. The $CHCl_2F$ was allowed to melt and the approximately 0.25 mL were transferred to the NMR tube which was then tightly sealed.

10.5 EXPERIMENTAL FOR CHAPTER 5

10.5.1 Synthesis of $[Pt_3(\mu_3\text{-}CO)(CNC_6H_{11})(\mu\text{-}dppm)_3][PF_6]_2$, 3a

$C_6H_{11}NC$ (2.2 μL) was added to complex 1 (40 mg) in acetone (10 mL). The solution was allowed to stir for 5 minutes after which time the solvent was removed by reduced pressure distillation. Orange-red crystals of **3a** were isolated by crystallization from an acetone/pentane mixture in 95% yield. Anal. Calcd. for $C_{83}H_{77}NOF_{12}P_8Pt_3$: C, 46.0; H, 3.6; N, 0.6. Found: ^{1}H NMR: δ 1.2-2.6 ppm [m, C_6H_{11}], δ 4.36 ppm [m, δ $C_2H_2P_2$], δ 5.24 [m, $C_2H_2P_2$] (T = -92°C).

10.5.2 Synthesis of $[Pt_3(\mu_3\text{-}CO)(CNC(CH_3)_3)(\mu\text{-}dppm)_3][PF_6]_2$, 3b

$(CH_3)_3CNC$ (1.2 μL) was added to complex 1 (40 mg) in acetone (10 mL). The solution was allowed to stir for 5 minutes after which time the solvent was removed by reduced pressure distillation. Orange-red crystals of **3b** were isolated by crystallization from an acetone/pentane mixture in 90% yield. Anal. Calcd. for $C_{81}H_{75}NOF_{12}P_8Pt_3$: C, 45.4; H, 3.5; N, 0.6.

10.5.3 Synthesis of $[Pt_3(\mu_3\text{-}CO)(2,6\text{-}Me_2C_6H_3NC)(\mu\text{-}dppm)_3][PF_6]_2$, 3c

$2,6\text{-}Me_2C_6H_3NC$ (2.6 mg) was added to complex 1 (40 mg) in acetone (10 mL). The solution was allowed to

stir for 5 minutes after which time the solvent was removed by reduced pressure distillation. Orange-red crystals of 3c were isolated by crystallization from an acetone/pentane mixture in 96% yield. Anal. Calcd. for $C_{85}H_{75}NOF_{12}P_8Pt_3$: C, 47.4; H, 3.8; N, 0.6. Found: C, 47.5; H, 3.9; N, 0.7. ^1H NMR: δ 2.70 ppm [s, CH_3], δ 6.0 ppm [br, CH_2P_2].

10.5.4 Preparation of Samples for Spectral Characterization of Intermediates, 2a and 2b

Complex 1 (40 mg) was dissolved in acetone-d_6 (0.5 mL) in an NMR tube and the solution was cooled to dry ice temperature. One molar equivalent of cyclohexyl and ^{t}butyl isocyanide were added to the cooled solution and the samples were immediately placed in an NMR probe cooled to -92°C. The temperature was raised by increments (between 20° and 40°C) and the $^{31}P\{^1H\}$ NMR spectra were monitored.

10.6 EXPERIMENTAL FOR CHAPTER 6

10.6.1 Synthesis of $[Pt_3(2,6\text{-}Me_2(C_6H_3NC)_2(\mu\text{-}dppm)_3][PF_6]_2$, 5

2,6-$Me_2C_6H_3HC$ (2.4 mg) was added to $[Pt_3(\mu_3\text{-}CO)(2,6\text{-}Me_2C_6H_3NC)(\mu\text{-}dppm)_3][PF_6]_2$ (complex 3a from the previous chapter) (40 mg) in acetone (10 mL). The solution was stirred for 10 minutes at room temperature after which time the solvent was removed by reduced pressure distillation. Dark red crystals of complex 3 were isolated by crystallization from an acetone/pentane

mixture. Anal. Calcd. for $C_{96}H_{90}F_{12}N_2P_8$: C, 49.1; H, 3.5; N, 1.2. Found: C, 49.3; H, 3.7; N, 1.2. IR: ν(CNR) = 2122 cm^{-1}. ^1H NMR: δ 2.30 [s, CH_3], 5.82 [br, $P_2C_2H_2$].

10.6.2 Preparation of Sample for Detection of Intermediate Complex 4

$[Pt_3(\mu_3\text{-}CO)(2,6\text{-}Me_2C_6H_3NC)(\mu\text{-}dppm)_3][PF_6]_2$ (40 mg) was dissolved in acetone-d_6 (0.5 mL). The solution was transferred to an NMR tube (0.5 mm:d) and the tube and its contents were cooled using dry ice. $2,6\text{-}Me_2C_6H_3NC$ (2.4 mg) was added to the contents of the NMR tube which was then placed in the probe of the NMR spectrometer which had been previously cooled to -92°C. The $^{31}P\{^1H\}$ NMR spectra of the reaction species were monitored by raising the temperature in 40° increments up to 20°C.

10.6.3 Synthesis of the Cluster-Methyl Isocyanide Species Complex 8

MeNC (0.6 mL of a 1 μL MeNC/mL acetone standard solution) was added to a solution of $[Pt_3(\mu_3\text{-}CO)(\mu\text{-}dppm)_3]^{2+}$, 1 (25 mg), in acetone-$d_6$ (0.5 mL) in an NMR tube. Teflon tape was wrapped around the top of the NMR tube to prevent loss of MeNC and the contents of the NMR tube were shaken vigorously. The sample was then sent for NMR analysis by $^{31}P\{^1H\}$ NMR.

10.7 EXPERIMENTAL FOR CHAPTER 7

10.7.1 $[Pt_3(\mu_3\text{-}S)(MeNC)(\mu\text{-}dppm)_3][PF_6]_2$, 4a

To a solution of $[Pt_3(\mu_3\text{-}CO)(\mu\text{-}dppm)_3][PF_6]_2$, 1 (40 mg), was added MeNCS (1.33 μL). The solution was stirred at room temperature for 1 hour and the product was isolated by evaporation of the solvent under vacuum and purified by precipitation using n-pentane. Yield 97%. m.p. 208-210°C. Anal. Calcd. for $C_{77}M_{69}F_{12}NP_8Pt_3S$: C, 44.0; M, 3.3; N, 0.7. Found: C, 44.4; H, 3.4; N, 0.7%. IR: ν(C≡N) 2240 cm^{-1}. ^1H NMR: δ 4.45 ppm [m, CH_2P_2], δ 2.71 [s, $J_{(PtH)}$ = 16 Hz, CH_3, NC] (T = 20°C), δ 4.93, 4.75 [AB, $^2J(H^aH^b)$ = 14 Hz, $CH^aH^bP_2$], δ 2.89 [S, CH_3NC] (T = -80°C).

10.7.2 $[Pt_3(\mu_3\text{-}S)(^tBuNC)(\mu\text{-}dppm)_3][PF_6]_2$, 4b

To a solution of $[Pt_3(\mu_3\text{-}CO)(\mu\text{-}dppm)_3][PF_6]_2$, 1 (40 mg), in acetone (20 mL) was added ^{t}BuNC (2.5 μL). This corresponds to a 1:1 ratio of cluster to ligand. The solution was stirred at room temperature for 1 hour and the product was isolated by evaporation of the solvent under vacuum and purified by precipitation using n-pentane. Yield 95%. m.p. 180-183°C. Anal. Calcd. for $C_{80}H_{75}F_{12}NP_8Pt_3S$: C, 44.8; H, 3.5; N, 0.7%. Found: C, 45.0; H. 3.7; N, 0.6%. IR: ν(C≡N) 2215 cm^{-1}. ^1H NMR: δ 4.45 [m, CH_2P_2], δ 0.82 [s, $(CH_3)_3CNC$] (T = 20°C); δ 4.30 [m, CH_2P_2]; δ 4.97 [AB, $^2J(H^aH^b)$ = 16 Hz, $CH^aH^bP_2$], δ 0.58 [s, $(CH_3)_3CNC$] (T = -80°C).

10.7.3 $[Pt_3(\mu_3\text{-}S)(PhNC)(\mu\text{-}dppm)_3][PF_6]_2$, 4c

To a solution of $[Pt_3(\mu_3\text{-}CO)(\mu\text{-}dppm)_3][PF_6]_2$, 1 (40 mg), in acetone (20 mL), was added PhNCS (2.3 μL). The solution was stirred at room temperature for 1 hour and the product was isolated by evaporation of the solvent under vacuum and purifed by precipitation using n-pentane. Yield 97%. m.p. 265°C (decomp). Anal. Calcd. for $C_{82}H_{71}F_{12}NP_8Pt_3S$: C, 45.5; H, 3.3; N, 0.6%. Found: C, 45.8; H, 3.5; N, 0.6%. IR: ν(C≡N) 2187 cm^{-1}.

10.8 EXPERIMENTAL FOR CHAPTER 8

10.8.1 Synthesis of $[Pt_4(\mu\text{-}CO)_3(CO)(\mu\text{-}dppm)_3][PF_6]_2$, 2

Platinum dibenzylidene acetone,[3] was added to $[Pt_3(\mu_3\text{-}CO)(\mu\text{-}dppm)_3]^{2+}$, 1 (30 mg) in acetone (10 mL). CO was bubbled through the solution until the acetone evaporated to dryness after which time acetone-d_6 (0.5 mL) was added to the sample for NMR spectral analysis. The Pt_4 cluster was highly unstable and decomposed to give Pt(0) and complex 12 in solution in less than 24 hours even under a CO atmosphere.

10.8.2 Sample Preparation for ^{13}C NMR for Complex 2

Complex 2 was prepared as described above. After the acetone was evaporated to dryness using CO, acetone-d_6 (0.5 mL) was added to the sample which was then transferred to an NMR tube fitted with a teflon tap. The air was removed from the tube using a vacuum line and ^{13}CO was

condensed into it. The tube and its contents were shaken vigorously for 2 minutes after which time the solution was degassed. ^{13}CO was again condensed into the NMR tube, the contents vigorously shaken and the sample stored at 0°C for 12 hours to ensure that complete exchange had taken place before the $^{13}C\{^{1}H\}$ NMR spectrum was run.

10.9 REFERENCES

1. B.R. Lloyd, "Trinuclear Clusters of Palladium and Platinum", Ph.D. Thesis, The University of Western Ontario, 1985.

2. Ligands made by the synthesis devised by W. Davies, *J. Chem. Soc.*, (1933), 1043.

3. Sample obtained from Dr. R. Kumar, formerly of this research group.

APPENDIX I

CALCULATION OF FRACTIONS OF ISOTOPOMERS OF A TRIPLATINUM CLUSTER

Platinum-195 is 33.8% abundant and thus the remaining platinum fraction (0.662) is not ^{195}Pt. To determine the fraction present of a given isotopomer of a triplatinum cluster (containing a mirror plane bisecting Pt^1 and the Pt^2-Pt^2 bond), one determines the fraction of each platinum atom present, multiplies them together and then multiplies by the number of perturbations possible.

$^{195}Pt = {}^{*}Pt$

Pt^1 Pt^2 Pt^2	1 x .662 x .662 x .662 = .290	29.0%
$^{*}Pt^1$ Pt^2 Pt^2	1 x .338 x .662 x .662 = .148	14.8%
Pt^1 $^{*}Pt^2$ Pt^2	2 x .662 x .338 x .662 = .296	29.6%
$^{*}Pt^1$ $^{*}Pt^2$ Pt^2	2 x .338 x .338 x .662 = .151	15.1%
Pt^1 $^{*}Pt^2$ $^{*}Pt^2$	1 x .662 x .338 x .338 = .076	7.6%
$^{*}Pt^1$ $^{*}Pt^2$ $^{*}Pt^2$	1 x .338 x .338 x .338 = .039	3.9%
		100.0%

APPENDIX II

CALCULATION OF PLATINUM SATELLITE SPECTRA FOR BRIDGING LIGANDS OR GROUPS EQUALLY BOUND TO PLATINUM ATOMS

a) Biplatinum Centre (*Pt = ^{195}Pt)

active platinum	isotopomer(i) fraction	multiplicity	intensity
Pt Pt	.4382	singlet (1)	.4382
*Pt Pt	.4475	doublet (1:1)	.2238 : .2238
*Pt*Pt	.1142	triplet (1:2:1)	.0285 : .057 : .0285

(i) isotopomer fraction calculated in Appedix I

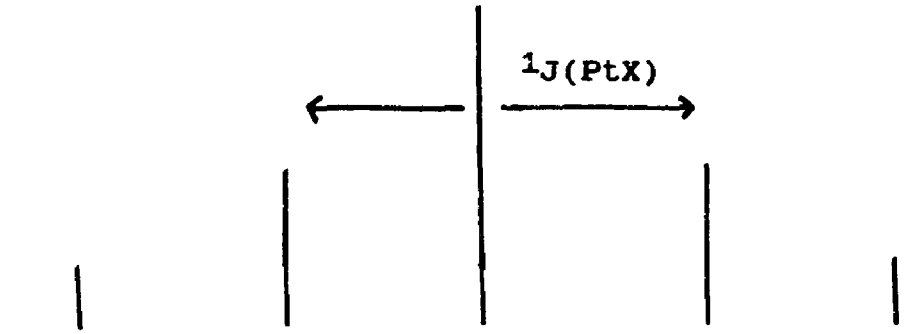

.4382

.2238 .2238

.0285 .057 .0285

.0285 :	.2238 :	.4952 :	.2238 :	.0285	sum
8 :	7.8 :	17.3 :	7.8 :	1	
1 :	8 :	18 :	8 :	1	

b) Triplatinum Centre

active platinum	isotopomer(i) fraction	multiplicity	intensity
Pt Pt Pt	.290	s (1)	.290
*Pt Pt Pt	.444	d (1:1)	.222 : .222
*Pt*Pt Pt	.227	t (1:2:1)	.057 : .114 : .057
*Pt*Pt*Pt	.0386	q (1:3:3:1)	.005:.0144 :. 0144:.005

(i) isotopomer fraction calculated in Appedix II

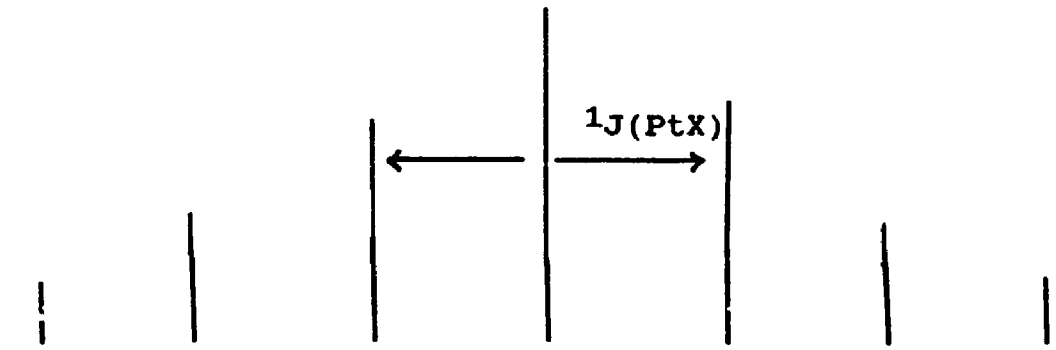

.290

.222 .222

.057 .114 .057

.005 .0144 .0144 .005

.005	.057	.236	.404	.236	.057	.005	sum
1	11.8	49.0	83.5	49.0	11.8	1	
1	12	49	84	49	12	1	

APPENDIX III

THE CALCULATION OF ΔG, ΔH AND ΔS FOR TEMPERATURE DEPENDENT EQUILIBRIA USING VARIABLE TEMPERATURE NMR

In order to calculate the thermodynamic parameters for temperature dependent equilibria the reactant and product concentrations in the mixture must be determined at several temperatures. $K_{equilibrium}$ can then be found using the equation

$$K_{equilibrium} = \frac{[\ Products\ ]}{[\ Reactants\ ]} \ .$$

$$\text{It is known that } \ln K_{equilibrium} = \frac{-\Delta H}{RT} + \frac{\Delta S}{R} \ .$$

A plot of $\ln K_{equilibrium}$ <u>vs.</u> $1/T$ should therefore yield a straight line of which the slope is $-\Delta H/R$ and the intercept is $\Delta S/R$. ΔG is calculated from the equation $\Delta G = \Delta H - T\Delta S$.